THE DEVELOPMENT OF REAL TIME DNA PIEZOELECTRIC BIOSENSOR FOR THE DETECTION OF *MYCOBACTERIUM TUBERCULOSIS*

A THESIS

BY

THONGCHAI KAEWPHINIT

Presented in Partial Fulfillment of the Requirements for the

Doctor of Philosophy in Molecular Biology

at Srinakharinwirot University

March 2010

THE DEVELOPMENT OF REAL TIME DNA PIEZOELECTRIC BIOSENSOR FOR THE DETECTION OF *MYCOBACTERIUM TUBERCULOSIS*

A THESIS

BY

THONGCHAI KAEWPHINIT

Presented in Partial Fulfillment of the Requirements for the

Doctor of Philosophy in Molecular Biology

at Srinakharinwirot University

March 2010

การพัฒนาดีเอ็นเอไพโซอิเล็กตริกไบโอเซนเซอร์ชนิดเรียลไทม์ สำหรับการตรวจเชื้อ *ไมโคแบคทีเรียม ทุเบอร์คูโลสิส*

บทคัดย่อ

ของ

ธงชัย แก้วพินิจ

เสนอต่อบัณฑิตวิทยาลัย มหาวิทยาลัยศรีนครินทรวิโรฒ เพื่อเป็นส่วนหนึ่งของการศึกษา
ตามหลักสูตรปริญญาดุษฎีบัณฑิต สาขาวิชาอณูชีววิทยา
กุมภาพันธ์ 2553

ธงชัย แก้วพินิจ. (2553). *การพัฒนาดีเอ็นเอไพโซอิเล็กตริกไบโอเซนเซอร์ชนิดเรียลไทม์ สำหรับการตรวจเชื้อ ไมโคแบคทีเรียม ทุเบอร์คูโลสิส.* ปริญญานิพนธ์ ปร.ด. (อณูชีววิทยา). กรุงเทพฯ: บัณฑิตวิทยาลัย มหาวิทยาลัยศรีนครินทรวิโรฒ คณะกรรมการควบคุม: รองศาสตราจารย์ ดร. โกสุม จันทร์ศิริ, รองศาสตราจารย์ สมชาย สันติวัฒนกุล, ผู้ช่วยศาสตราจารย์ ดร. นำคุณ ศรีสนิท

วัณโรคเป็นโรคที่มีสาเหตุมาจากเชื้อแบคทีเรีย ชนิด *ไมโครแบคทีเรียม ทูเบอร์คูโลสิส* เป็นสาเหตุการตายอันดับหนึ่งในสิบของการตายจากโรคติดเชื้อทั่วโลก และเป็นโรคหนึ่งที่เป็นปัญหาทางสาธารณสุขของไทยด้วย การพัฒนาดีเอ็นเอไพโซอิเล็กตริกไบโอเซนเซอร์ชนิด เรียลไทม์ในการตรวจตัวอย่างเชื้อวัณโรคชนิด *ไมโครแบคทีเรียม ทูเบอร์คูโลสิส* การพัฒนาเครื่องมือดังกล่าวสามารถอ่านค่าความถี่ได้ถึง 20 เมกกะเฮิร์ต ในสภาวะที่มีของเหลว โดยใช้ควอทซ์ คริสตัลเป็นอิเล็กโทรด อาศัยการเกิดปฏิกิริยาระหว่างดีเอ็นเอโพรบ (ไบโอติน, ไทอัล-6-เมอร์แคปโตเฮกซะนอล, และไทอัล) ที่จำเพาะต่อดีเอ็นเอเป้าหมาย ตรึงลงบนผิวควอทซ์ คริสตัล โดยใช้อัตราการไหลของปั๊มเท่ากับ 30 µL/min การลดลงของความถี่ ควอทซ์ คริสตัล บ่งตัวบ่งชี้การเกิดปฏิกิริยา ความเข้มข้นของดีเอ็นเอมีความเหมาะสมในการทำปฏิกิริยาสูงสุดของ ไบโอติน, ไทอัล-6-เมอร์แคปโตเฮกซะนอล, และไทอัล คือ 1.0, 1.5, และ 1.0 µM ตามลำดับ ซึ่งมีความไวในการเกิดปฏิกิริยาต่อดีเอ็นเอเป้าหมายสังเคราะห์ อยู่ที่ 0.25 µM ความไวในการตรวจวัด สามารถตรวจวัดปริมาณ ดีเอ็นเอเป้าหมายของเชื้อได้น้อยที่สุดคือ 0.5 µg/ml ซึ่งสามารถเพิ่มความไวในการตรวจวัดได้ดีที่สุด เมื่อใช้แอฟวิดิน/อนุภาคนาโนของทอง 25 %(v/v) เชื่อมต่อที่ปลาย 3’ ของสายดีเอ็นเอเป้าหมาย ซึ่งสามารถวัดปริมาณเชื้อได้ 1.5×10^{3} CFU/mL ส่วนการทดสอบความจำเพาะพบว่าไม่ปฏิกิริยาต่อเชื้อ *ไมโคแบคทีเรียม เอเวียม* และ แบคทีเรียชนิดอื่น ควอทซ์ คริสตัล ในระบบเซนเซอร์นี้สามารถนำกลับมาใช้ใหม่ในชิ้นงานเดิมได้มากกว่า 10 ครั้งและการเตรียมพื้นผิวที่มีดีเอ็นเอเก็บไว้ได้ไม่น้อยกว่า 4 เดือน ที่อุณหภูมิ 4 องศาเซลเซียส โดยปฏิกิริยาไม่ลดลง เครื่องมือชนิดมีความสามารถในการวัดค่าถูกต้องและแม่นยำสูง การตรวจวัดกับตัวอย่างเสมหะจำนวน 200 ตัวอย่าง (150 ตัวอย่างให้ผลบวกและ 50 ตัวอย่างให้ผลลบ) การตรวจวัดด้วยไบโอเซนเซอร์ชนิดนี้ พบว่า มีความสัมพันธ์ที่ดี เมื่อเปรียบเทียบกับค่าที่ได้ในห้องปฏิบัติด้วยวิธี พีซีอาร์ นอกจากนี้ยังเป็นเครื่องมือตรวจวัดราคาถูกแบบพกพา อีกทางเลือกหนึ่งที่จะนำไปสู่การวินิจฉัยเชื้อวัณโรคได้

THE DEVELOPMENT OF REAL TIME DNA PIEZOELECTRIC BIOSENSOR FOR THE DETECTION OF *MYCOBACTERIUM TUBERCULOSIS*

AN ABSTRACT

BY

THONGCHAI KAEWPHINIT

Presented in Partial Fulfillment of the Requirements for the

Doctor of Philosophy in Molecular Biology

at Srinakharinwirot University

February 2010

Thongchai Kaewphinit. (2010). *The development of real time DNA piezoelectric biosensor for the detection of Mycobacterium tuberculosis*. Dissertation, Ph.D. (Molecular Biology). Bangkok: Graduate School, Srinakharinwirot University. Advisor Committee: Assoc. Prof. Dr.Kosum Chansiri, Assoc. Prof. Dr.Somchai Santiwatanakul, Asst. Prof. Dr.Namkhun Srisanit

Tuberculosis is a disease caused by bacteria called *Mycobacterium tuberculosis*. It is among the top ten causes of global mortality and morbidity which makes it become the important public health problem among developing countries. Real time DNA piezoelectric biosensor has been developed for detection of *Mycobacterium tuberculosis* in clinical specimens. The resonant frequency responsibility of this biosensor device was up to 20 MHz in aqueous phase. The biotin-modified oligonucleotide probe, thiol-modified oligonucleotide probe/mercaptohexanol (MCH), and thiol-modified oligonucleotide probe were immobilized on gold surfaced electrode of quartz crystal by using flow rate at 30 µL/min. Downward shift of resonant frequency was monitored as an indicator of DNA hybridization. The data revealed that biotin-modified oligonucleotide probe, thiol-modified oligonucleotide probe/MCH, and thiol-modified oligonucleotide probe showed highest maximum concentration for detection at 1.0, 1.5, and 1.0 µM, respectively. The sensitivity of DNA detection was 0.25 µM synthetic targets, 1 µg/ml of DNA target sequence. This biosensor can be detected limit as 1.5×10^{3} CFU/mL. The sensitivity can be increased by using avidin/gold nanoparticle at 25 %(v/v) for signal enhancement at 3' end of DNA target sequence. The probe showed no cross hybridization to *Mycobacterium avium* and other microorganisms. Quartz crystal can be reused up to 10 times and kept at 4 °C up to 4 months without losing activity. This device demonstrated high precision and accuracy. Direct detection of 200 clinical specimens (150 positive samples and 50 negative samples) using real time DNA piezoelectric biosensor was corresponded to PCR technique. The tool could be beneficial for further development as portable device for low cost routine diagnosis.

Acknowledgements

I wish to express my deep gratitude to Associate Professor Dr. Kosum Chansiri, my chair, Associate Professor Dr. Somchai Santiwatanakul and, Assistant Professor Dr. Namkhun Srisanit, my co-advisor, and Assistance Professor Dr. Chamras Promptmas, my readers, for their kind guidance, valuable comments and encouragement.

I would like to thank Associate Professor Dr. Surangrat Srisurapanon, my readers, for her valuable suggestions.

I also would like to extend my thanks to the informants of this study for their cooperation. A special thank goes to all my friends for their kind assistance and encouragement.

Finally, I am indebted to my parents, brothers, sister, and cousins for their love and encouragement during my study.

Thongchai Kaewphinit

TABLE OF CONTENTS

Chapters **Pages**

TABLE OF CONTENTS (Continued)

Chapters **Pages**

TABLE OF CONTENTS (Continued)

Chapters **Pages**

LIST OF TABLE

Tables **Pages**

LIST OF TABLE (Continued)

Tables **Pages**

LIST OF ILLUSTRATIONS AND FIGURES

Figures **Pages**

LIST OF ILLUSTRATIONS AND FIGURES (Continued)

Figures **Pages**

ABBREVIATIONS

TB	=	Tuberculosis
HIV	=	Human immunodeficiency virus
LJ	=	Lowenstein-Jensen
ZN	=	Ziehl Neelsen
HPLC	=	High performance liquid chromatography
DNA	=	Deoxyribonucleic acid
RNA	=	Ribonucleic acid
RFLP	=	Restriction fragment length polymorphism
PCR	=	Polymerase chain reaction
MTB	=	*Mycobacterium tuberculosis*
IS*6110*	=	Insertion sequences 6110
dsDNA	=	Double-stranded DNA
PZ	=	Piezoelectric quartz crystal
ΔF	=	Measured frequency shift (Hz)
f_0^2	=	The fundamental resonant frequency of the crystal (Hz)
Δm	=	Mass change (g)
A	=	Area of electrode surface (cm^2)
μ_q	=	Shear modules of quartz crystal = 2.947×10^{11} $g/cm^2 \times s^2$
ρ_q	=	Density of quartz crystal = 2.648 g/cm^3
ρ_L	=	Density of liquid in contact with the quartz crystal
η_L	=	Viscosity of liquid in contact with the quartz crystal
QCM	=	Quartz crystal microbalance
SAM	=	Self assembly monolayer
bp	=	base pair
RMTB	=	Reverse primer
FMTB	=	Forward primer
CFU/mL	=	Colony-forming units per milliliter
*Bst*DSI	=	*Bst*DSI restriction enzyme
mM	=	Milimolar
µL	=	microliter

ABBREVIATIONS (Continued)

°C	=	Degree celsius
TBE	=	Tris/Borate/EDTA buffer
PBS	=	Phosphate buffer saline
M	=	Molar
nm	=	nanometer
˚A	=	Angstrom
MCH	=	6-mercaptohexanol
EDC	=	1-ethyl-3(3-dimethylaminopropil) carbodiimide ethanolic
NHS	=	*N*-hydroxysuccinimide
mg/mL	=	Miligram per milliliter
µL/min	=	Microliter per minute
Hz	=	Hertz
v/v	=	Volume per volume
TEM	=	Transmission electron microscope
KV	=	Kilovolt
SEM	=	Scan electron microscope image
AFM	=	Atomic force microscope
dT	=	Poly T
HSV	=	Herpes simplex virus

Acknowledgements

I wish to express my deep gratitude to Associate Professor Dr. Kosum Chansiri, my chair, Associate Professor Dr. Somchai Santiwatanakul and, Assistant Professor Dr. Namkhun Srisanit, my co-advisor, and Assistance Professor Dr. Chamras Promptmas, my readers, for their kind guidance, valuable comments and encouragement.

I would like to thank Associate Professor Dr. Surangrat Srisurapanon, my readers, for her valuable suggestions.

I also would like to extend my thanks to the informants of this study for their cooperation. A special thank goes to all my friends for their kind assistance and encouragement.

Finally, I am indebted to my parents, brothers, sister, and cousins for their love and encouragement during my study.

Thongchai Kaewphinit

TABLE OF CONTENTS

Chapters **Pages**

TABLE OF CONTENTS (Continued)

Chapters **Pages**

TABLE OF CONTENTS (Continued)

Chapters **Pages**

LIST OF TABLE

Tables **Pages**

LIST OF TABLE (Continued)

Tables **Pages**

LIST OF ILLUSTRATIONS AND FIGURES

Figures **Pages**

LIST OF ILLUSTRATIONS AND FIGURES (Continued)

Figures **Pages**

ABBREVIATIONS

TB	=	Tuberculosis
HIV	=	Human immunodeficiency virus
LJ	=	Lowenstein-Jensen
ZN	=	Ziehl Neelsen
HPLC	=	High performance liquid chromatography
DNA	=	Deoxyribonucleic acid
RNA	=	Ribonucleic acid
RFLP	=	Restriction fragment length polymorphism
PCR	=	Polymerase chain reaction
MTB	=	*Mycobacterium tuberculosis*
IS*6110*	=	Insertion sequences 6110
dsDNA	=	Double-stranded DNA
PZ	=	Piezoelectric quartz crystal
ΔF	=	Measured frequency shift (Hz)
f_0^2	=	The fundamental resonant frequency of the crystal (Hz)
Δm	=	Mass change (g)
A	=	Area of electrode surface (cm^2)
μ_q	=	Shear modules of quartz crystal = 2.947×10^{11} $g/cm^2 \times s^2$
ρ_q	=	Density of quartz crystal = 2.648 g/cm^3
ρ_L	=	Density of liquid in contact with the quartz crystal
η_L	=	Viscosity of liquid in contact with the quartz crystal
QCM	=	Quartz crystal microbalance
SAM	=	Self assembly monolayer
bp	=	base pair
RMTB	=	Reverse primer
FMTB	=	Forward primer
CFU/mL	=	Colony-forming units per milliliter
*Bst*DSI	=	*Bst*DSI restriction enzyme
mM	=	Milimolar
µL	=	microliter

ABBREVIATIONS (Continued)

°C	=	Degree celsius
TBE	=	Tris/Borate/EDTA buffer
PBS	=	Phosphate buffer saline
M	=	Molar
nm	=	nanometer
˚A	=	Angstrom
MCH	=	6-mercaptohexanol
EDC	=	1-ethyl-3(3-dimethylaminopropil) carbodiimide ethanolic
NHS	=	*N*-hydroxysuccinimide
mg/mL	=	Miligram per milliliter
µL/min	=	Microliter per minute
Hz	=	Hertz
v/v	=	Volume per volume
TEM	=	Transmission electron microscope
KV	=	Kilovolt
SEM	=	Scan electron microscope image
AFM	=	Atomic force microscope
dT	=	Poly T
HSV	=	Herpes simplex virus

CHAPTER 1

INTRODUCTION

Tuberculosis (TB) is a disease caused by bacteria called *Mycobacterium tuberculosis*. It can spread through the air from one person to other person by coughing, sneezing, or talking and breathing. Although it can attack any part of human body, it prefers to attack the lungs [1]. *M. tuberculosis* is a slow-growing bacterium which needs 1-2 months to grow in a culture. WHO estimates that 9.27 million new cases of TB occurred in 2007, an estimated 44% or 4.1 million were new smear positive cases [2]. Tuberculosis is among the top ten causes of global mortality and morbidity which makes it becomes the important public health problem in Thailand. In 2008, the Ministry of Public Health reported that approximately 55,252 persons developed the disease and 28,788 persons smear positive [3]. The standard method of laboratory diagnosis is based on cultivation which considered the most accurate test due to high sensitivity and specificity, is labor-intensive and slow but clinical laboratories hold cultures 2 to 4 weeks to achieve maximum sensitivity [4,5]. The acid fast stain or AFB for direct specimen examination is also conventional diagnostic tools but lack of sensitivity [6]. Polymerase chain reaction (PCR) technique [7-11] is sensitive for detection of TB by using specific primers but involves in the use of ethidium bromide staining which is carcinogenic agent in gel electrophoresis [12,13]. The analysis of restriction fragment length polymorphism (RFLP) of PCR product is an alternative DNA detection system and it has been successfully applied to species differentiation [14,15]. DNA piezoelectric biosensor applications detection in gas phase are advantageous in that the frequency signal can, in some cases, be interpreted through the use of the Sauerbrey relation; although, the method is sensitive to errors due to hydration, humidity, and solvent retention. The time consuming and tedious nature of the analysis scheme suggest the dip and dry method (gas phase) is not likely to ever become a routinely used analytical procedure that it is not particularly reliable due to the complexity of sample composition, handling, and lack of automated and continuous operation [16,17].

Recently, there has been an increasing interest real time piezoelectric biosensor technology. The first attempt to use an acoustic devise as a liquid phase sensor was by Konash and Bastiaans in 1980 [18]. The real-time data analysis can be conducted and the system can be configured for on-line analysis. The system using a piezoelectric biosensor in a flow cell might be developed for automated or continuous operation. The relationship

between the oscillation frequency change of a quartz resonator in contact with liquid and accumulated mass had first realized by Kanazawa and Gordon in 1985 [19,20] that derived a relationship by expressing the change in oscillation frequency of a quartz crystal in contact with a fluid. The possibility to perform the piezoelectric biosensor assay in flow-injection mode makes the method more attractive for rapid identification of the biological analytes. DNA based biosensor technology is rapid and sensitive detection among them, especially piezoelectric biosensor by using oligonucleotide hybridization detection method. This biosensor has its own advantages that the detection method is label-free from radioactive or fluorescent tags [21,22]. The piezoelectric biosensor is one of the candidate devices of biosensor technology for detection of DNA hybridization. DNA piezoelectric biosensor is the measurement of frequency change between the frequency of the oligonucleotides probe immobilized on quartz crystal and the frequency after the hybridization of DNA target [23]. There are many reports about the development of piezoelectric quartz crystal specific DNA-based biosensor for detection many pathogenic bacteria in real time such as *Staphylococcus epidermidis* [24], *Escherichia coli* [25], and *Pseudomonas aeruginosa* [26]. The drawback of these studies is the using of PCR for the preparation of bacterial target DNA in DNA probe and target hybridization step.

This objective was focused on development of the DNA-piezoelectric biosensor for direct detection of *M. tuberculosis* in real time. This method consists of the quartz crystal which was immobilized by using three probes as thiol-modified oligonucleotides probe, thiol-modified oligonucleotides probe/MCH, and biotin-modified oligonucleotides that were designed from IS*6110* sequence element specific for *M. tuberculosis*. All probes were immobilized on quartz crystal surface by using the self-assembled monolayer (SAM) method. This biosensor was used for detecting the target DNA by measuring the frequency shift. The development of sensitivity can be using mass enhancement such as avidin, gold nanoparticle, and avidin/gold nanoparticle. The oscillation counting device was used for measuring the resonant frequency of the quartz crystal in all of experiments in this study. The advantage of this study is using a non-amplified genomic bacterial DNA target in real time analysis continuous operation. This target DNA preparation without amplification will reduce time consuming, costs, and the tedious step of amplification. Finally, this study can be extended to develop the new method which is high sensitivity, specificity, cheap, easy to use, and rapid for detection of *M. tuberculosis* in many fields of work in clinical diagnosis.

CHAPTER 2

LITERATURE REVIEW

Tuberculosis

Case and transmission

The name tuberculosis was probably first used by Shonlein in 1939. Its name is an older epithets including *phthisis* and *consumption* of which allude the marked wasting characteristic of advanced disease. Non-pulmonary manifestations particularly cervical lymphadenitis was known as *scrofula* [27].

Tuberculosis (TB) is a disease cause by bacteria called *Mycobacterium tuberculosis* whose principal reservoir is man, and also other mycobacteria belonging to the *Mycobacterium tuberculosis* complex [28] such as *M. bovis* or *M. africaum*. It is the most frequently affected to the lung but the disease has been termed *Morbud percorpus* stressing that it may involve virtually any organ or system of the body. Tuberculosis may ,therefore, mimic many other diseases and often present a serious diagnostic challenge, especially in countries where the disease is now rare and often overlooked.

The infection is acquired by inhalation of droplet nuclei that contain tubercle bacilli from an infected person. An individual's risk of infection depends on the extent of exposure to droplet nuclei and his susceptibility to infection [29]. Once infected with *M. tuberculosis*, only a small proportion of individuals (about 10-12%) will develop the disease [29,30]. The incubation period of tuberculosis is highly variable and ranges from few weeks to many decades. The risk of developing the disease declines steeply with time after infection. Primary tuberculosis appears within a short period after infection and secondary tuberculosis disease due to reactivation or re-infection normally appears after 5 years [31]. Tuberculosis is spreaded mainly by patients with infectious pulmonary tuberculosis when they cough or sneeze [29]. The disease usually affects the lungs although any organ and tissue may be affected. In absence of treatment, tuberculosis has a high case fatality rate, ranging from 60 to 70 percent for smear-positive pulmonary tuberculosis and 40 to 50 percent for other forms of tuberculosis, depending on the site of the disease [29,31].

Epidemiology

TB remains the leading cause of mortality due to a bacterial pathogen, *M. tuberculosis*. The interruption of centuries of decline in case rates of TB occurred, in most cases, was in the late 1980s and involved the US and some European countries due to increased poverty in urban settings and the immigration from TB high-burden countries.

The World Health Organization (WHO) estimates that approximately one-third of the global community is infected with *M. tuberculosis* [32]. Tuberculosis is among the top ten causes of global mortality and morbidity [33]. The 196 countries reporting to WHO in 2008 notified 5.6 million new and relapse cases in 2007, of which 2.6 million (46%) were new smear-positive cases [2] (figure 1).

After human immunodeficiency virus (HIV)/AIDS, TB is the second most common cause of death due to an infectious disease, and current trends suggest that TB will still be among the 10 leading causes of global disease burden in the year 2020 [34].

The global distribution of TB cases is skewed heavily toward low-income and emerging economies. The highest prevalence of cases is in Asia, where China, India, Bangladesh, Indonesia, and Pakistan collectively make up over 50% of the global burden. Africa, and more specifically sub-Saharan Africa, has the highest incidence rate of TB, with approximately 83 and 290 per 100,000, respectively. TB cases occur predominantly (approximately 6 million of the 8 million) in the economically most productive 15- to 49-year-old age group [32]. Our understanding of TB epidemiology and the efficacy of control activities have been complicated by the emergence of drug-resistant bacilli and by the synergism of TB with HIV coinfection.

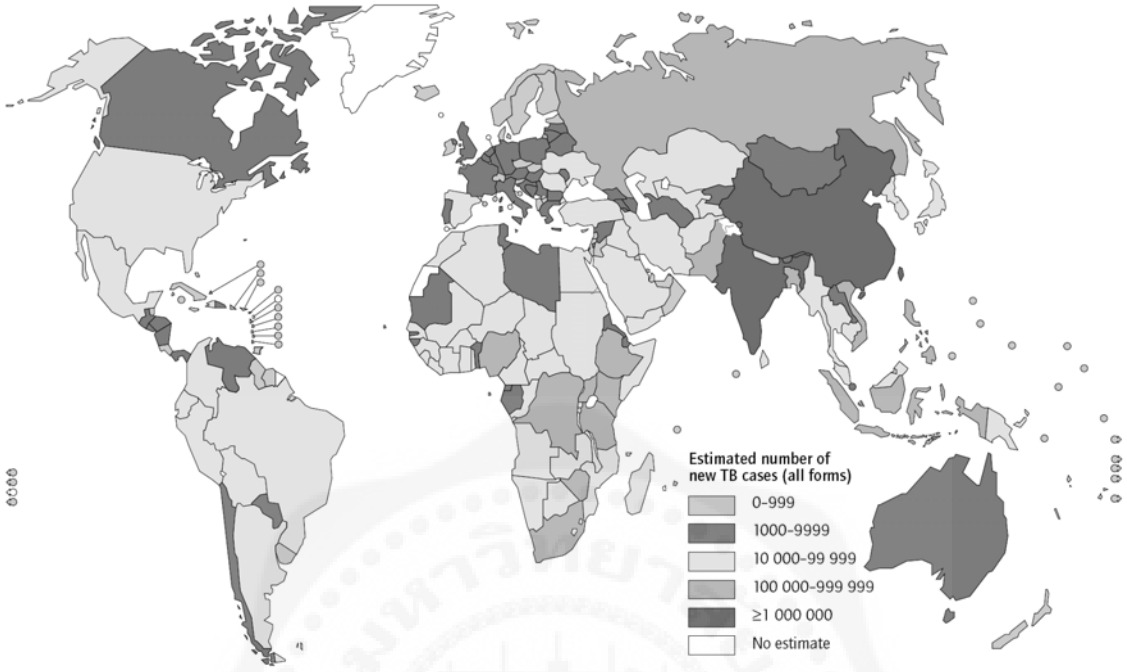

Figure 1 Estimated number of new TB cases in the world, 2007 [2].

Taxonomy

Tuberculosis is classified in [35]

Phylum *Actinobacteria*

Subclass *Actinobacteridae*

Order *Actinomycetales*

Suborder *Corynebacterineae*

Family *Mycobacteriaceae*

Genus *Mycobacterium*

Species *Mycobacterium tuberculosis complex*

(*M. tuberculosis, M. africanum, M. bovis, M. microti*)

Morphology

The mycobacteria are rod-shaped organisms, slim, and 0.2 to 0.4x2 to 10 um in size (figure 2, 3). They are nonmotile and do not form spores. The unusual cell wall (figure 4)

contains *N*-glycolylmuramic acid instead of the *N*-acetylmuramic acid present in the murein sac of most bacteria. The cytoplasmic membrane is encapsulated by a layer of peptidoglycan. The peptidoglycan backbone is attached to arabinolactan through an unusual disaccharide phosphate linker region. The arabinogalactan is a branched – chain polysaccharide consisting of a proximal galactose chain linked to a distal arabinose chain. The hexaarbinofuranosyl termini of arabinogalactan are esterified to mycolic acids. The mycolic acid chains are shown perpendicular to the cytoplasmic membrane with the exposed chains interacting with the mycolic chains of the trehalose dimycolate. Another major component non-covalently associated to the mycobacterial cell wall is the immunogenic lipoarabinomannan, which is attach to the cytoplasmic membrane by a phosphatidylinositol anchor. Small and hydrophilic solutes diffuse through water-filled protein channels, points, whereas hydrophobic compounds use the lipid pathway. Proteins are represented by solid oval bodies [36-39].

Mycobacterium tuberculosis is a slim, strongly acid-alcohol-fast rod. It frequently shows irregular beading in its staining, appearing as connected series of acid-fast granules. It grows at 37°C, and requires enriched or complex media for primary growth from clinical specimens. Growth is enhanced by 5 to 10% carbon dioxide, but is still very slow, with a mean generation time of 12 to 24 hours [40].

Figure 2 The colony morphology of *M. tuberculosis* [38].

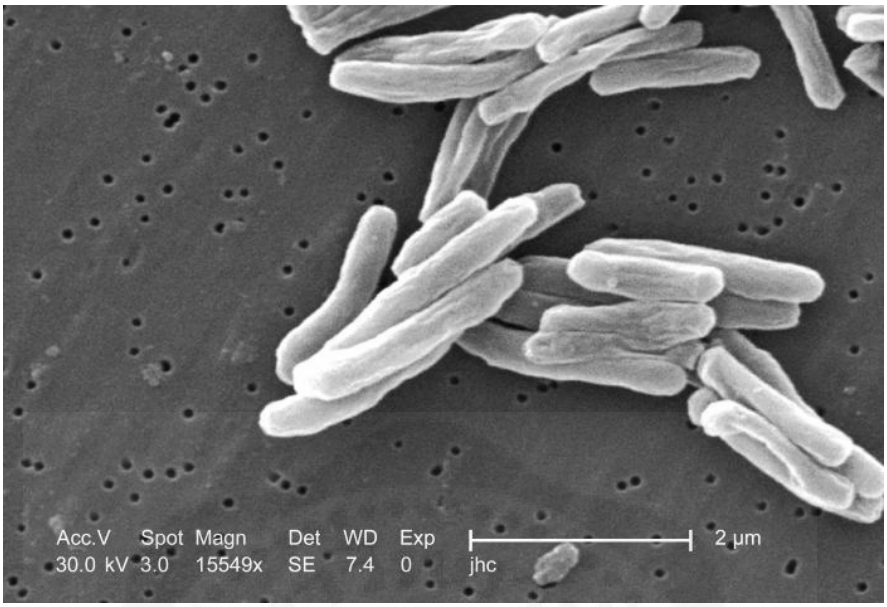

Figure 3 Mycobacterium tuberculosis, the bacterium that causes TB infection, as seen through scanning electron microscope [39].

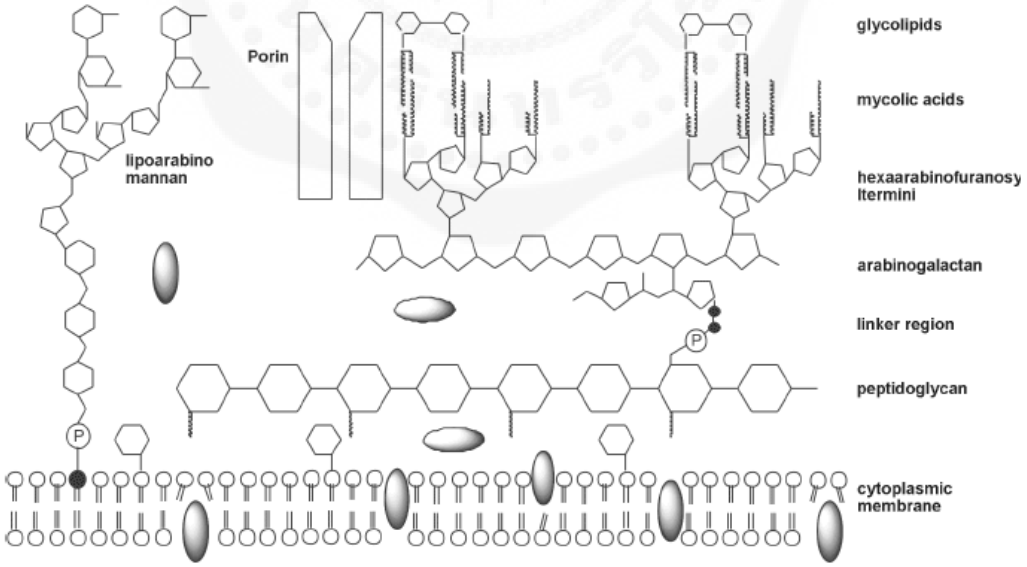

Figure 4 Schematic representation of the mycobacterial cell wall [36].

Pathophysiology

Tuberculosis is spreaded by airborne droplet nuclei, which are particles of 1-5 um in diameter that contain *Mycobacterium tuberculosis*. Because of their small size, the particles can remain airborne for minutes to hours after expectoration by people with pulmonary or laryngeal tuberculosis during coughing, sneezing, singing, or talking [41-43]. The infectious droplet nuclei are inhaled and lodged in the alveoli in the distal airways. *M. tuberculosis* is then taken up by alveolar macrophage. This initiates a cascade of events that results in either successful containment of the infection or progression to active disease (primary progressive tuberculosis). The risk of development of active disease for a newly infected young child is 10%, with roughly half of that risk occurring in the first 2 years after infection [44,45].

After being ingested by alveolar macrophages, *M. tuberculosis* replicates slowly but continuously and spreads via the lymphatic system to the hilar lymph nodes. In most infected individuals, cell-mediated immunity develops 2-8 weeks after infection. Activated T lymphocytes and macrophages form granulomas that limit further replication and spread of the organism. *M. tuberculosis* is in the centre of the characteristically necrotic (caseating or cheese-like) granulomas, but it is usually not viable. Unless there is a subsequent defect in cell-mediated immunity, the infection generally exists and active disease may occur [46].

Tuberculosis in Thailand

TB is expected to be eradicated by the end of this century. However, an increasing incidence of tuberculosis in many parts of the world has led to renewed interest in the disease. The pandemic of HIV infection has changed TB, an endemic disease, to an epidemic worldwide. In Thailand, tuberculosis cases and deaths reduced year after year, until 1992 when the cases began to increase as a result of HIV infection. The annual risk of infection in 1997 was estimated at 1.4%, with approximately 100,000 new TB cases developing each year. Fifteen per cent of tuberculosis patients are seropositive for HIV infection. Increasing antituberculosis drug resistance has been correlated with the high prevalence of HIV infection in some parts of the country. In 1995, cure rate of this disease was approximately 50% and, since 1996, in order to cope with the worsening situation. Despite the current economic turmoil of the country, the programme has now been expanded to cover over 400 of the 810 districts of Thailand. Also, the economic effects of tuberculosis at the household level in Thailand are

recently studied. Tuberculosis is a chronic disease that commonly affects the lower socioeconomic classes. Some patients are unable to follow the treatment regimens because of the financial burden. The low case detection and treatment completion rates are, in part, due to the inability of poor patients to cope with the expenditure [47].

The reported distribution of TB cases by age suggests that TB transmission in Thailand has fallen in recent decades, but there is no other evidence to confirm this. Relatively high rates (for Asia) of HIV infection among TB patients underline the question of whether TB incidence is now falling. It is not known how much money is spent on TB control in Thailand because following decentralization of the information on budgets and expenditures is incomplete. The morbidity and mortality populations of pulmonary TB cases were reported from the Ministry of Public Health in 2001-2008 [3] (figure 5).

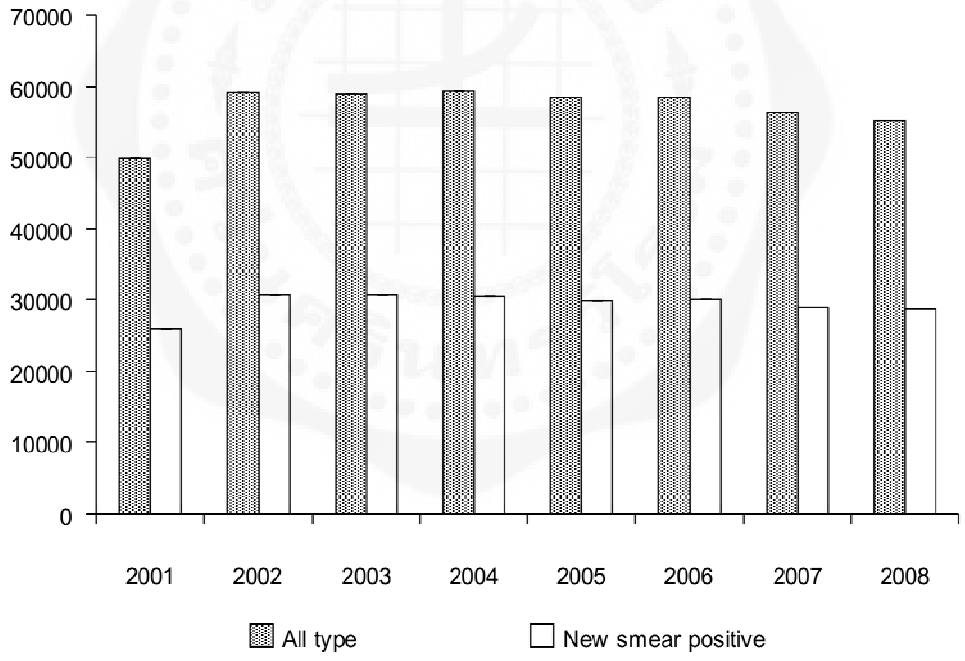

Figure 5 TB case notifications in Thailand during 2001-2008 [3].

Diagnosis *M. tuberculosis*

Cultivation

Culture of *Mycobacterium tuberculosis* from clinical material is the ”Gold standard” for diagnosis of TB which normally requires 3-8 weeks. It is, therefore, not commonly used as a method for diagnosis of TB that detection of tubercle bacilli on the egg-based medium Lowenstein-Jensen (LJ) but it is slow and needs special safety procedures in the laboratory. Clinical laboratories hold cultures to achieve maximum sensitivity [13, 48].

Ziehl Neelsen stain

The Ziehl Neelsen (ZN) stain was the simplest, cheapest, and fastest diagnostic method for detection of tuberculosis. A method of staining used in bacteriology in which a smear on a slide is treated with carbol-fuchsin stain, decolorized with acid alcohol, and counterstained with methylene blue to identify acid-fast bacilli bacteria. Acid-fast organisms resist decolorization and appear red against a blue background when viewed under a light microscope. The stain may be performed on any clinical specimen but is most commonly used in examining sputum for *Mycobacterium tuberculosis* and *Mycobacterium* spp [6].

Fluorochrome stain

The fluorochrome stain is the screening procedure recommended for laboratories that possess a fluorescent microscope. The fluorochrome dye such as auramine-rhodamine stain complex to the mycolic acids in acid-fast cell wall in the clinical specimen. The detection of fluorescing cells is enhanced by the brightness against a dark background [49].

BACTEC radiometry

The basis of the BACTEC radiometric procedure is that when mycobacteria are grown in a medium such as Middlebrook 7H12 supplemented with [^{14}C] palmitic acid, growth is detected by measuring the release of [^{14}C] CO_2 which is produced by the catabolism of labeled palmitic acid. The BACTEC instrument automatically measures [^{14}C] CO_2. The actual production of [^{14}C] CO_2 is expressed by the instrument as ‘growth index’. The δ-napthyl-p-acetylamino β-hydroxy amino propriophenone (NAP) test is very reliable for differentiating *M.*

tuberculosis from all the other mycobacteria and this test has been combined with BACTEC radiometry successfully. Combining the BACTEC system for detecting mycobacterial growth with the Gen-Probe system for identification has been increasingly reported to be of great use in recent years [50,51].

High performance liquid chromatography (HPLC)

HPLC is a reliable and easy to perform technique. It is less costly than some of the other identification methods. The procedure consists of saponification of the cells followed by derivatisation and conversion of the fatty acids to their p-bromophenacyl esters using specific catalysis. The extraction procedures are specific for mycolic acids which are high-molecular weight δ-branched, β-hydroxy fatty acids found in *Corynebacterium*, *Mycobacterium*, *Nocardia*, and *Rhodococcus.* The number of carbon atoms making up the mycolic acid varies from C_{20} to C_{36} in *Corynebacterium* and C_{60} to C_{90} in *Mycobacterium.*

This simple, rapid, and direct method for the detection of specific mycolic acid patterns has proved to be very useful in the species identification of mycobacteria. Standardised protocols are now available for both slow growing and rapid growing mycobacteria. Commercially available pattern recognition software is also now available and it has been shown to have a very high degree of accuracy for 24 species of mycobacteria including *M. tuberculosis, M. avium* complex, and *M. gordonae* [52,53].

Nucleic acid probes for the identification of mycobacteria

In the original Gen-Probe system, the DNA probes homologous to mycobacterial rRNA are labeled with ^{125}I and required physical separation of hybridised and unhybridised probes before detection in a gamma counter. Now chemiluminescent nonradioactive labels are used, and hybridised and unhybridised probes are separated by the addition of chemical ‘selection’ agent. Therefore, the current assays have a more rapid and homogeneous format and allow detection of DNA:RNA hybrids in an illuminometer rather than a gamma counter. Chemiluminescent procedures require only about 45 minutes performing and the acridinium ester label is stable for extending the shelf life of the probe reagent considerably to about 6 months [14].

Restriction fragment length polymorphism (RFLP) and polymerase chain reaction (PCR)

This technique is based on the principle that if a single base difference between two otherwise identical pieces of double stranded DNA lies within the recognition site of a restriction enzyme, then digestion of both the samples with that restriction enzyme will produce different products which can be resolved by electrophoresis. Different banding patterns or genomic fingerprints for the 2 DNA samples are obtained. These differences in banding patterns can be refined as RFLPs which can be used to type different isolates *of M. tuberculosis* and have proved useful for species identification and for subdividing species into different RFLP types [14]. *M. tuberculosis* by using PCR was developed by Van Embden et al [54]. The first detection of *M. tuberculosis* based on PCR used a probe developed from the gene encoding for the 38 kDa protein antigen b of *M. tuberculosis* [55]. Later, the insertion sequence IS*6110*/IS*986* was found in the genome of most of the members of the *M. tuberculosis* complex with multiple copies in *M. tuberculosis* and only a few copies in *M. bovis,* and protocols were developed by using PCR for DNA fingerprinting of clinical isolates of *M. tuberculosis* based on this insertion sequence [56].

Biosensors

Biosensors are a new nano-technology which are used in many detection. For example, the biosensor which is construction of antibody-based piezoelectric crystals is capable of detecting mycobacterial antigens in diluted cultures of attenuated *M. tuberculosis,* in an immunologically specific manner [57]. The other example is an electrochemical biosensor for the determination of short sequences from *Mycobacterium tuberculosis* (MTB) DNA. The sensor relies on the modification of the carbon-paste transducer with 27 or 36 mer oligonucleotide probes [58].

Identification of *Mycobacterium tuberculosis*

IS*6110* Insertion sequences (IS) are small mobile genetic elements, usually less than 2.5 kb in size, that are widely distributed in most bacterial genomes. IS elements are commonly defined as carrying only the genetic information related to their transposition and regulation, unlike transpositions, which can also carry genes that encode phenotypic markers (e.g.,

antibiotic resistance). Transposition of IS elements often causes gene disruptions that can have strong polar effects and in other cases can lead to the activation or alteration of expression of adjacent genes due to the regulatory sequences, including promoters and protein-binding sequences [59]. From an evolutionary perspective, there are at least two distinct hypotheses explaining the role of IS elements in genomes. One regards the elements as genomic parasites that, on balance, harm their hosts (i.e., bacteria) [60]. In contrast, others postulate that IS elements are important to their hosts for adaptive evolution, which is maintained by selection of occasional advantageous IS-derived mutations [61].

IS elements in bacterial species are present in varying numbers of copies: IS*1* in *Escherichia coli* strains is present in 2 to 17 copies, whereas the *Shigella* species contain from 2 to 40 copies. Thierry et al. first described IS*6110*, a 1,355 bp member of the IS3 family that, when intact, is unique to the *M. tuberculosis* complex [62]. IS*6110* has an imperfect 28 bp inverted repeat at its ends and generates a 3 to 4 bp target duplication on insertion. Although "hot spots" have been noted (regions in the *M. tuberculosis* chromosome where IS*6110* seems to preferentially insert), IS*6110* elements are more or less randomly distributed throughout the genome, with copy numbers ranging from rare clones lacking any IS*6110* elements to those with 26 copies [63,64]. In 1993, van Embden and colleagues proposed a standardized method for performing IS*6110*-based Southern blot hybridization analysis [55].

Various genes have been targeted in many PCR assays designed to differentiate between *M. tuberculosis* and *M. bovis*. Unfortunately, most of the assays have been invalidated due to lack of specificity [65]. The 16S rRNA genes sequence has been used for identification of genus-specific mycobacteria [66]. Moreover, the multiplex PCR assay employed selective amplification by targeting the 16S and 23S rDNA, *oxy*R, and IS*6110* (insertion sequences) genes are also used for identification of *M. tuberculosis*. Despite differences in the fragment length and in GC content of selected primer pairs, Kurabachew M. et al [65] were able to optimize the PCR condition in such a way that specific bands were produced successfully under the same PCR conditions. Although the 23S rDNA always presenting a single copy is the least explored, this gene seems to be an interesting target for differentiate *M. tuberculosis* complex from Mycobacteria. The IS*6110* is a member of the IS*3* family which is the most widely spread group of bacterial ISs and found in more than 24 different gram-positive and gram-negative genera. A multiplex PCR-based assay targeting insertion sequence IS*6110* could also

be used to differentiate member in *M. tuberculosis complex* to be specific species. The most strains of *M. tuberculosis* have IS*6110* between 8 and 15 copies [67] result in a good target for amplification [13]. The *oxy*R gene presenting only as a single copy is as primers to distinguish *M. bovis* from *M. tuberculosis* [65].

Biosensor technology

The biosensor technology was first developed many decades ago. The first biosensor was described by Clark and Lyons in 1962 [68] for the determination of glucose. Biosensor is an analytical device made by attaching the biological substances to a suitable transducer, which converts the biological response into electrical signal as shown in figure 6. A biosensor consists of a biological sensing element with a transducer to produce the signal proportional to target analyses.

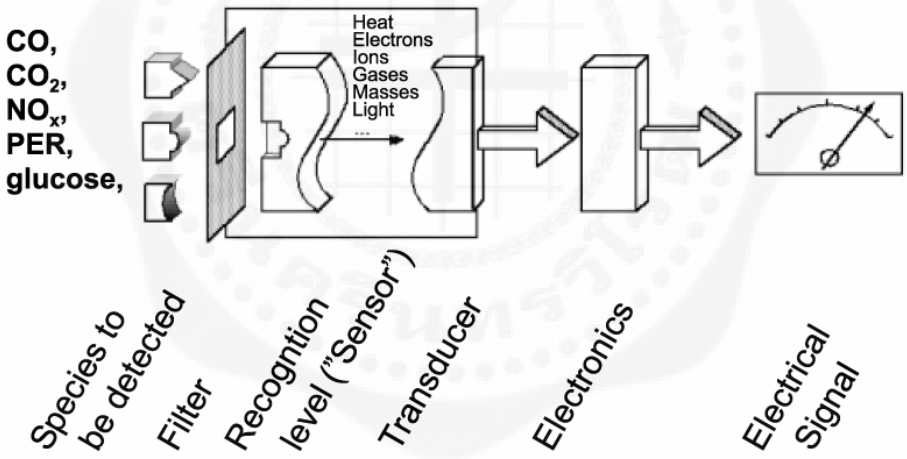

Figure 6 General figuration of biosensor [69].

When biological molecules interact with target analyses, there is a change in one or more physical-chemical parameter that associated with the interaction such as the generation of ions, gases, electrons, heat, or mass. The quantities of these indicating signals are converted into the electrical signals by suitable transducer. The transducer is used to convert the biological recognition into the measurable signal that can be detected and displayed [70]. The most important characteristic of biosensor is the selectivity of bioreceptor for the specific

target analytes. Therefore, the specificity of biosensor depends on the properties of the biological component which providing the selectivity and specificity for target analytes. But the sensitivity depends on both the biological components and the transducer. The significance of reaction is related to the biological substances, target analytes, and high efficiency of transducer [66].

The molecular recognition then corresponds to the association of the biological element and its target molecule (analyte) through an association such as: enzyme-substrate, antibody-antigen, receptor-hormone, and complementary DNA sequencing, etc. These associations maximise the capacity of the biomolecules to recognise a unique substance among various substances [58].

The combinations of recognition-transducer systems are numerous and this explains many definitions and nomenclatures of these types of sensors. The main methods of transduction that are the most current and well developed from both a fundamental and experimental point of view are: electrochemical [71], optical [72], and piezoelectric [73].

The types of transducer have been used in biosensor. These are the measurement of the change in electrochemical (potentiometry, amperometry or conductimetry), mass (piezoelectric crystal or acoustic wave), heat (colorimetry) and optical change (luminescence, fluorescence, reflective index, surface Plasmon resonance and waveguide) [66].

DNA based biosensor

DNA has an important role in clinical diagnostics. DNA is arguably the most important of all biomolecules. The unique complementary structure of DNA between the base parts adenine/thymine and cytosine/guanine has been the basis for genetic analysis over the last few decades. The DNA techniques, including hybridization, amplification, and recombination, are all based on the double helix structure of the DNA. DNA is coiled to form a double helix (double-stranded DNA, dsDNA) composed of two strands held together by hydrogen bonds as shown in figure 7 [74] that can be broken by heat or high pH. The single-stranded DNA is relatively stable, but on removal of the heat source or pH extreme, the ssDNA will reanneal into the double-stranded configuration. Reannealing between the ssDNA from different sources is called hybridization [75]. The reannealing of the dsDNA is possible because nucleotide bases will re-

form hydrogen bonds only with specific complementary bases: adenine pairs with thymine, and cytosine pairs with guanine.

The stability of the hybridization depends on the nucleotides sequences of both strands. A perfect match in the sequence of nucleotides produces very stable dsDNA, whereas one or more base mismatch can increase instability that can lead to weak hybridization of strand.

Molecular detection has shown a great potential for rapid identification of diseases and for food and environmental monitoring. After the recent successes in sequencing the human genome, the detection of specific DNA sequences in biological samples has been playing a fundamental role in genetic diagnostic and in the detection of pathogens in cells [76].

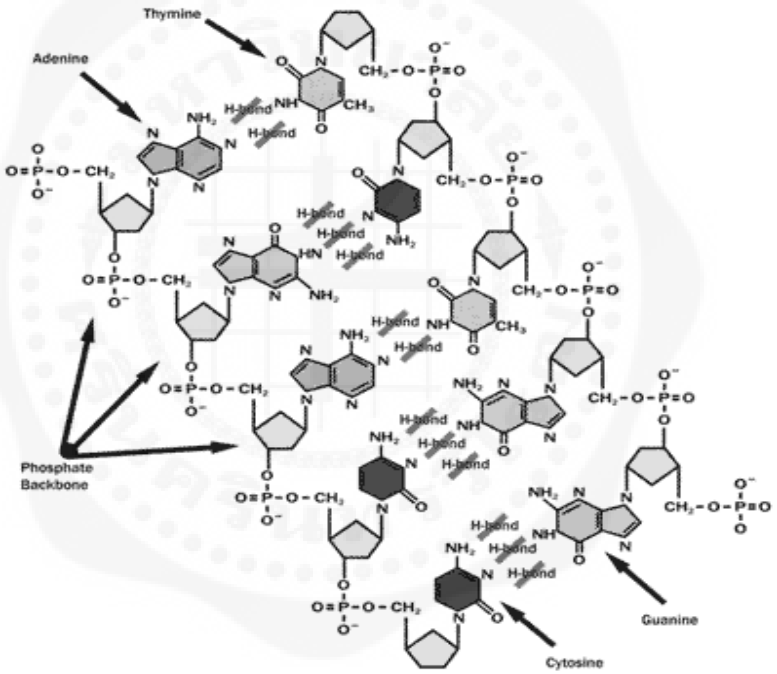

Figure 7 Configurations of DNA and the hybridization principle [74].

Generally, the detection of particular DNA sequence is carried out by gel electrophoresis of DNA fragments amplified by polymerase chain reaction (PCR) using primers which are specific complementary sequence with the chosen region of DNA. Although, gel electrophoresis is simple and effective for detection of PCR products, ethidium bromide which is a common stain is a carcinogen [77]. As an alternative way to gel electrophoresis, DNA probe

has been widely used for detection of specific DNA sequences by hybridization. In this method, the probe is usually labeled with a radioisotope, enzyme, and fluorescent tag, these labeling and detection process require long and tedious steps [22].

The large demand for low-cost genetic assays has lead to the development of portable and easy-to-use biosensors. These systems should be able to perform the analysis in a very short time and with a very limited amount of specimen. Micro-fabricated structures, based on micro and nano-technology can satisfy these requirements and also allow a high degree of parallelism and sensitivity.

The biosensor technologies have been intensively investigated because of their promise for rapid consuming, high specificity, and low cost. Therefore, DNAbased biosensor is a promising alternative detection method by base pairing property in DNA. The specificity of DNA base pairing can be used as a biorecognition [23]. This biosensor has been based on electrochemical [71], optical [78], and piezoelectric transducer [22,72,79,80]. This I s a great potential market for simple, cheap, rapid, and quantitative detection of specific genes. Areas of application include clinical, veterinary, medico-legal, environment, and food industry. DNA-based biosensors require any non-labeling such as radio isotope, enzyme, and fluorescence tag. Therefore, the piezoelectric transducer appears to be a suitable and simple device for direct detection and label free monitoring of complementary olignucleotide hybridization [22].

Piezoelectric DNA based biosensor

A piezoelectric (PZ) quartz crystal or quartz crystal microbalance (QCM) biosensor [73, 81] is an extremely sensitive mass sensor, capable of measuring subnanogram levels of mass changes, and it consists of a thin quartz disc sandwiched between a pair of electrodes. Due to the piezoelectric properties of quartz, it is possible to excite the crystal to oscillation by applying an AC voltage across its electrodes [82].

The term “piezoelectric” is derived from the Greek word “*piezen*” meaning “to press”. Therefore, the piezoelectric effect means “pressure electricity” The theoretical foundation for using piezoelectricity was first pioneered by Raleigh in 1885, but the first investigation was performed by Jacques and Pierre Curie in 1880 [83], who observed a mechanical stress to a quartz crystal which induces an electrical potential across the crystal surface. The piezoelectric

effects can be found in natural crystals but are very rare. The crystal has to go through a polarization process to obtain the piezoelectric property [84].

The piezoelectric device as a mass sensor arises from the linear relationship between the change in mass at the crystal surface and the change in oscillating frequency [84]. The vibration of piezoelectric crystals produces an oscillating electric field that the resonant frequency of the crystals depends on parameters associated with the phases adjacent to the crystal and the physical properties such as size, cut density, and shear modules [85]. The change in mass is identified by a corresponding change in the frequency of vibration of the crystal.

A resonant oscillation is achieved by including the crystal into an oscillation circuit where the electric and the mechanical oscillations are near to the fundamental frequency of the crystal. The fundamental frequency depends upon the thickness of the wafer, its chemical structure, its shape and its mass. Some factors can influence the oscillation frequency, like the thickness, the density and the shear modulus of the quartz that are constant, and the physical properties of the adjacent media (density or viscosity of air or liquid). As shown by Sauerbrey (1959), changes in the resonant frequency are simply related to the mass accumulated on the crystal. The fundamental frequency increases as the piezoelectric thickness decreases [86].

Thus for detection of analytes in air (the 'dip-and dry') method the frequency change is simply related to the change in mass:

$$\Delta F = \frac{-2 f_0^2 \Delta m}{A\sqrt{\mu_q \rho_q}} \qquad (1)$$

Where ΔF = measured frequency shift (Hz)

f_0^2 = the fundamental resonant frequency of the crystal (Hz)

Δm = mass change (g)

A = area of electrode surface (cm^2)

μ_q = shear modules of quartz crystal = 2.947×10^{11} $g/cm^2 \times s^2$

ρ_q = density of quartz crystal = 2.648 g/cm^3

Gas phase mass sensitivity is determined by the piezoelectric quartz crystal of fundamental frequency as described in equation 1. Mass sensitivity increases as the fundamental frequency of the quartz crystal increases which the fundamental frequency increases as the quartz crystal thickness decreases. Thus, one approach to increase sensitivity is to fabricate thinner crystal which in turn increases the operating frequency and sensitivity. Clearly, miniaturization can only be performed within physical limits. The size cannot be reduced below a certain value without affecting the durability of the device. However, recent fabrication designs have been tested that provide fundamental frequencies of 30 MHz [87]. The most commonly used crystals are 5–15 MHz quartz disks with a 10–16 mm diameter. For a fundamental frequency of 10 MHz and an electrode surface area of 0.22 cm^2, the gas phase mass sensitivity is approximately 1 Hz per nanogram [88].

There are two types of piezoelectric devices; surface acoustic wave (SAW) and the piezoelectric crystal

1. SAW crystal can oscillate at several hundreds of MHz that are replaced by 9-14 MHz of the piezoelectric crystal. In this device, an acoustic wave is generated by application of an alternating voltage across a pattern of interlaced metal electrode such as gold. These devices are mass sensitive more than piezoelectric quartz crystal because mass sensitivity is directly related to the operating frequency. However, SAW devices present various problems when applied to a biological sensing system because biological materials can severely reduce surface acoustic wave [85].

2. Piezoelectric quartz crystal, the piezoelectric resonator is made from piezoelectric materials which has specific dimension and orientation with respect to the crystallographic axes of material. The resonator consists of one or more pairs of conducting electrodes which are deposited by vacuum vaporization [89]. The electric field is applied between the electrodes cause mechanical vibration or oscillation at the particular frequency in the resonator. These vibrations or oscillations will produce a reverse electrical potential which caused by the interaction coupling between the mechanical properties of the piezoelectric resonator and the electrical potential is termed the piezoelectric effect. The quartz crystal resonators are covered with metals such as gold, silver, or platinum by evaporation on the quartz surface, which are used as electrodes. There are various types of materials that exhibit the piezoelectric effect

such as quartz, tourmaline, zinc oxide, or aluminium nitrite, but quartz usually used in analytical applications [89].

A piezoelectric quartz crystal resonator is cut slab from natural or synthetic crystal of the quartz. The quartz crystal plate must be cut in the specific orientation with respect to the crystal axes [89]. The properties of a quartz crystal depend on the plane in which it is cut. The AT-cut is normally employed which has an orientation of approximately 35° to the z-axis or optical axis in figure 8. Since the AT-cut crystal has a temperature coefficient near zero, then the resonant frequency is stable over a wide range of temperature. Therefore, the AT-cut crystal has been used in majority of the piezoelectric work [83].

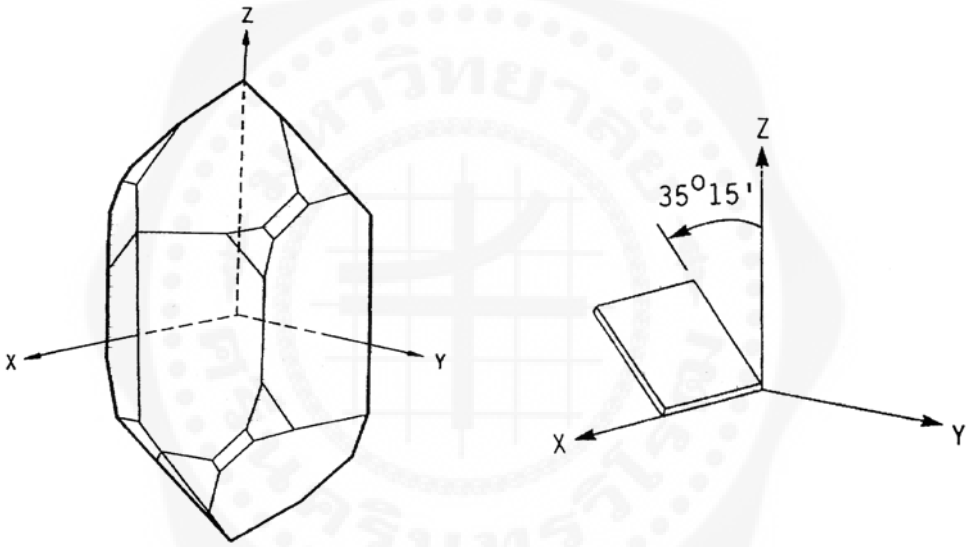

Figure 8 The orientation angle of AT- cut quartz crystal [85].

There are other terms to describe piezoelectric quartz crystal such as quartz crystal microbalance (QCM) and thickness shear mode (TSM). The AT-cut quartz crystal is a piezoelectric material which functions in microbalance mode as quartz crystal microbalance. TSM can describe the motion of crystal's vibration [89]. Quartz crystal has different vibration modes, which are grouped into flexure, extensional, face shear, and thickness shear mode. The thickness shear mode is also divided into fundamental mode and third overtone thickness shear. The thickness shear mode of vibrations is the type of vibrations that using AT-cut resonator [90]. When an appropriate alternating electrical potential is applied to gold electrode

on opposite side of the piezoelectric crystal, the crystal will oscillate at specific frequency. If increasing in mass at the interface, the oscillation frequency will decrease when the analyte binds with the coated surface. The frequency change is directly proportional to the increase in mass and correlated with analyte binding [91].

Dip and dry piezoelectric sensing (gas phase or stepwise) applications are advantageous in that the frequency signal can in some cases be interpreted through the use of the Sauerbrey relation; although, the method is sensitive to errors due to hydration, humidity, and solvent retention. The time consuming and tedious nature of the analysis scheme suggest the dip and dry method is not likely to ever become a routinely used analytical procedure. Furthermore, the application of solution phase piezoelectric sensing is far superior in that real-time data analysis can be conducted and the system can be configured for automated analysis [17].

Real time DNA piezoelectric based biosensor

Quartz crystal sensing system to liquid phase measurement failed because the crystal ceased to oscillate when submerged in solution. To sense solution phase analytes either the sample was converted into a gas or a tedious dipping procedure was used [92,93]. These problems have been addressed by developing oscillator circuits that allow for crystal immersion in solution [94] or through the use of specially designed crystal flow through and/or batch reaction cells where solution contacts only one crystal surface [17,94-97].

The theoretical foundation for using piezoelectricity was first pioneered by Kanazawa and Gordon in 1985 [19], but the first attempt to use an acoustic device as a liquid phase sensor by Konash and Bastiaans in 1980 [18], who used as a liquid chromatography detector where one crystal face was exposed to a flowing organic solution.

The system had poor sensitivity and reproducibility, but they demonstrated the quartz crystal could produce stable oscillations in liquid.

When a crystal is dipped into a solution or real time, the oscillating frequency depends on the solvent used. The question as to which factors determine the frequency is important for understanding the mechanism of oscillation of a crystal in solution and for its potential development as a sensor in solution [20,98]. When an over layer is thick, the relationship between the *f* and D*m* is no longer linear and corrections are necessary. The coupling of the

crystal surface to a liquid drastically changes the frequency when a quartz crystal oscillates in contact with a liquid that a shear motion on the surface generates motion in the liquid near the interface.

Thus for detection of analytes in liquid phase method which derived a relationship that expresses the change in oscillation frequency of a quartz crystal in contact with a fluid,

$$\Delta F = f_0^{3/2}\left(\frac{\rho_L \eta_L}{\pi \mu_q \rho_q}\right)^{1/2} \qquad (2)$$

Where ΔF = measured frequency shift (Hz)

$f_0^{3/2}$ = resonant frequency of the unloaded quartz crystal (Hz)

ρ_L = density of liquid in contact with the quartz crystal

η_L = viscosity of liquid in contact with the quartz crystal

μ_q = shear modulus of quartz crystal = 2.947×10^{11} g/cm^2×s^2

ρ_q = density of quartz crystal = 2.648 g/cm^3

The penetration depth of this sheer wave depends on $(\left(\pi f_0 \mu_q \rho_q\right)^{-1/2}$. Kanasawa and Gordon (equation 2) [20] demonstrated stress that ΔF in solution is linear function of $(\rho_L \eta_L)^{1/2}$ except for salts and high polymer solutions. They, in fact, tested the linearity of depence of the frequency decrease on $(\rho_L \eta_L)^{1/2}$ using many solvents selected on the basis of their different viscosity, density and electrical conductivity. In 1994, Bruckenstein and shay observed that quartz crystal with on face exposed to dilute aqueous solutions near temperature induced frequency change by several kilohertz [98].

Kanazawa and Gordon described the frequency response in fluid phases in terms of the physical parameters of the quartz crystal and analyte solution by considering the coupling of quartz crystal shear wave to a dampened shear wave propagating into the fluid [20,99]. The depth of the shear wave penetration varied with the square root of the bulk liquid viscosity. The decay length corresponded to the effective thickness of the liquid in motion with the quartz crystal. This liquid layer was treated as a sheet of mass attached to the quartz crystal surface. The model treated the fluid layer as continuous which no slip boundary between the quartz crystal surface and the fluid was allowed. The equation was verified by contacting a single

quartz crystal surface with solutions of glucose and ethanol. The oscillation frequency in pure water was taken as a reference. The decrease in frequency varied as the solution viscosity and density product increased.

Liquid phase systems are designed using a myriad of conditions. The most common method employs the use of a contact cell where one crystal surface is adjacent to the solution. The contact cell is configured in a flow or batch mode and the solution is typically introduced using a peristaltic or syringe pump. In flow cells, the volume of solution flowing over the crystal surface is commonly less than 100 mL [100,101] but some flow cells have been designed for solution contact volumes of up to 7 mL [102]. No generalities can be made concerning the volume of solution in a batch contact cell which volumes range from a few microliters to nominally one liter. Alternatively, the whole crystal can be in contact with the solution phase. Here, either the quartz crystal surface is masked to avoid solution contact [103,104] or the oscillator circuit is designed to allow the crystal to oscillate while immersed in solution [105,106]. Many conventional quartz crystal designs do not allow for dual electrode contact with a solution to avoid short-circuiting due to exposure to a common conductive solution. Further, with full solution contact more than just the piezoelectrically active surface interacts with the solution. This may cause calibration inconsistencies [107]. On the other hand, immersion in solution allows for detection of changes in solution conductivity. This could be advantageous, or a serious draw back, depending on the type of analysis performed.

This technique has been investigated for monitoring nucleic acid hybridization by immobilized the crystal with nucleic acid probe and detecting the mass change after hybridization with specific target sequence in solution, Fawcett et al [108] were the first group to describe a piezoelectric biosensor for DNA immobilizing ssDNA onto the quartz crystal and detecting the mass change after hybridization. The advantages of this technique are not only the high sensitivity but also the label less operation. Additionally, frequency change can be followed in real time [22].

The drawback of quartz crystal microbalance is non-specific adsorption of molecules present in real matrices. Piezoelectric biosensor is a mass sensor which has surface for binding with any molecules which can potentially interfere the reaction. However, previous experiments with piezoelectric, DNA probes and hybridization of oligonucleotides clearly demonstrated that using appropriate chemistry immobilization, non-specific binding can be

effectively minimized [22,91]. Method to improve the sensitivity of the piezoelectric biosensor can be improved by using higher frequency of quartz, but this device is often difficult to operate in liquid because of fragility and frequency stability problems. Alternatively, the selectivity can be improved by improving the quality of the surface of the crystal and the immobilization method [79].

For most biosensor techniques, a biological component is immobilized on the quartz crystal surface. The signal is generated in response to adsorbate recognition. The sensitivity of direct analyte detection through an immobilized ligand is limited by the number of binding sites available to interact. This is beneficial for characterization of conditions associated with a reaction but may be a limitation in terms of detection sensitivity. One technique used to increase the sensitivity of piezoelectric biosensor is to relate the first-derivative of the change in frequency versus time to the analyte concentration [109,110]. Additionally, a number of analysis schemes have been proposed that do not rely on direct mass attachment to the crystal surface [111-113].

Liquid phase piezoelectric techniques for monitoring cellular process have been described [114,115]. Piezoelectric biosensor integrated in a flow injection analysis (FIA) system has the advantage to work continuously and to monitor on-line the binding of the analyte A cell growth sensor was developed by Ebersole et al. to detect metabolites without immobilization of a biological entity [115]. This was the first sensor capable of detecting metabolic responses and division rates of viable cells. The authors indicated production of metabolic acids is a useful marker of cell metabolism and growth and utilized this relation in their sensor design. Detection of metabolic processes was based on adhesion of a polymer to the quartz crystal. The polymer precipitated from solution in response to titration of its carboxylate groups by the metabolic acids which converted the polymer to its isoelectric form. Ebersole et al. also reported solution phase detection of DNA hybridization [116]. Matsuda et al. monitored real time platelet adhesion in plasma [117]. Moa et al. reported DNA piezoelectric sensor, based on the nanoparticle amplification method, was developed for detection of *Escherichia coli* O157:H7 by using a thiolated single-stranded DNA (ssDNA) probe specific to *E. coli* O157:H7 *eaeA* gene was immobilized onto the piezoelectric sensor surface through self-assembly [118]. Eun et al. have developed a piezoelectric DNA-sensor based on DNA-RNA hybridization for the detection of two orchid viruses, *Cymbidium mosaic virus* (CymMV) and *Odontoglossum ringspot virus*

(ORSV). Specific oligonucleotide probes modified with a mercaptohexyl group at the 5′-phosphate end were directly immobilized onto 10-MHz [119]. Wong et al. have demonstrated DNA piezoelectric biosensing method for real-time detection of E. coli O157:H7 in a circulating-flow system was developed in this study. The thioled surface of the Au electrode could be immobilized by many inner Au nanoparticles, then more thiolated single-stranded DNA (ssDNA) probes which were specific to E. coli O157:H7 eaeA gene could be fixed through Au-SH bonding [120]. Wu et al were developed DNA piezoelectric biosensing method for real-time detection of Escherichia coli O157:H7 in a circulating-flow system was developed in this study. Specific probes for the detection of E. coli O157:H7 gene eaeA, synthetic oligonucleotide targets (30 and 104 mer) and PCR-amplified DNA fragments from the E. coli O157:H7 eaeA gene (104 bp), were used to evaluate the efficiency of the probe immobilization and hybridization with target DNA in the circulating-flow quartz crystal microbalance (QCM) device [121].

Self-assembled monolayer (SAM) probe immobilization

The immobilization technique is used to help the biological element attached with the sensor surface. This step not only helps for attachment between biological element and transducer, but also helps in stability for reusing if the immobilization is strong enough. The immobilization of the nucleic acid probe onto the transducer surface plays an important role in performance of DNA sensor. The immobilization step leads to well defined probe orientation, readily accessible to the target. This process depends on the nature of physical transducer and method that used for attachment of DNA probe to the surface [80,85].

There are various common immobilization methods for biosensor such as the using of direct physical adsorption on a solid surface, entrapment in a matrix, covalent coupling to functional groups on the electrode [122]. The covalent binding method can improve uniformity, density, distribution of bound molecules, and reproducibility of surface and instability, diffusion, aggregation, and inactivation of biomolecules. Glutaraldehyde, carbodiimide, and succinimide esters are widely used for covalent binding method [123].

The self-assembled monolayer is one of immobilization method by covalent binding. This method is rapidly grown since the discovery of these structures and ability to modify the physical and chemical property of surface. Self-assembled monolayer is molecular assembly

obtained by immersion of an appropriate substrate into a solution containing molecules that specific with the surface. The term “self assembly” involves arrangement of atoms and molecules into an ordered or even aggregate of functional entities without the intervention of mankind towards an energetically stable form [124]. SAM is distinguished from ordinary surfactant monolayer by the fact that one end of the molecule is designed to have a favorable and specific interaction with the solid surface of the substrate [125]. The self assembled monolayer have been composed from different types of simple organic molecules, such as alkanethiols and silane compounds on different substrate such as on metal oxide and gold surface substrate. The SAM system is extremely versatile and can provide a method for *in vitro* development of bio-surface.

The simple method involved in immobilizing self-assembly monolayer makes attractive strategy for achieving better control in the orientation and molecular organization of biomolecules at interfaces. SAM is easy formation of ordered, pinhole free and stable monolayer. More significantly, the easy method for SAM formation and compatibility with metal substrates such as gold or silver provided benefits for biosensor application such as only needed minimum amount of molecules. The stability and organization of the SAM depend on the forces of attraction between the immobilized molecules and the binding force between the surfaces and the binding group [126]. Thiols on gold form very well-assembled monolayer which is highly resistant to washing due to the strong chemisorption of the sulfur atoms. There is a rapid reaction between –SH group and gold atom with formation of S-Au bond. After the initial fast adsorption of thiols, the akyl side chains assemble together to maximize the van der Waal’s interaction [127].

The SAM is successfully used in previous study by Caruso et al [79] immobilized oligonucleotides directly on the gold quartz crystals, by forming a self-assembled monolayer, and also used biotin-oligonucleotides to immobilize them on avidin-modified gold quartz crystals. Zhou et al [91] compared different immobilization methods (direct chemical bonding and avidin-biotin interaction) and different immobilization architectures (oriented oligonucleotide monolayer and multilayer created by self-assembling of alternating DNA and polymers). The researcher observed the biotinylated DNA films that provided fast sensor responses and high hybridization efficiencies, due to the spacer group that conferred better accessibility, and that multilayered films increased the sensor sensitivity, indicating that the complementary DNA can

penetrate into the multilayer sensing film, but also increased the sensor response time because of the more difficult transport of the complementary sequence [91].

Generally, detection of single copy gene by piezoelectric quartz crystal DNA-based biosensor requires PCR for amplifying target DNA [22,128]. However, PCR is still time consuming and requires expensive reagents and machines. Development of piezoelectric DNA-based biosensor for direct detection of highly repeated sequences using nonamplified genomic DNA has been reported recently. Minnunni et al [128-130] detected satellite 13 DNA from genomic DNA of *Bos taurus*. They also applied this method for direct detection of single copy gene in non-amplified genomic DNA from *Nicotiana glauca* tobacco plant. They detected the promoter region (35S) that present in various GMOs and can be used as a marker for GMO screening [131]. They also applied this method for direct detection of sequences in nonamplified genomic DNA is described. The system relies on real-time and label-free detection of the hybridization reaction between an immobilized probe and the complementary sequence in solution. From above described, DNA piezoelectric biosensor can possibly be used for direct detection in non-amplified bacterial genomic DNA. Kaewphinit et al were developed the DNA-piezoelectric biosensor for direct detection in non-amplified bacterial genomic DNA of *M. tuberculosis*. The method involved in immobilization of specific synthetic biotinylated probe that was designed from IS*6110* gene-specific for *M. tuberculosis* [132].

CHAPTER 3

MATERIALS AND METHODS

Oligonucleotide design

All oligonucleotide DNA probe and complementary DNA target for the detection of *M. tuberculosis* were designed based on the nucleotide sequence of IS*6110* gene retrieving from NCBI (Accession number AJ242908.1) [133]. The gene had 2,645 bp in length and was aligned against IS*6110* of *M. microti* and *M. bovis*. Nucleotide sequences at position 1,474 -1,493 (19 bp) were selected for synthesis of DNA probe and complementary DNA target due to its specificity to *M. tuberculosis*. For DNA probe synthesis, the linker of TTTTTT was added to the 5' end with the thiol and biotin modified oligonucleotide probe (table 1).

The accuracy of probe was confirmed by using BLAST nucleotide free program provided by NCBI [134]. The probe is specific to *M. tuberculosis* putative secretion system-associated gene cluster. This probe was thiol-modified oligonucleotide at 5' end to form SH group and gold atom with formation of S-Au bond interaction and biotin-modified oligonucleotide probe at 5' end to biotin labeling for used as piezoelectric DNA based biosensor. The synthetic complementary DNA target was chosen for hybridization with probe. The blocking 1 and blocking 2 were used for annealing with the ssDNA of bacterial target sequence after denatuaration method. This blockings were biotinylated at 3' end to form avidin-biotin interaction and thiol-modified oligonucleotide at 3' end to form DNA conjugated gold particle for used mass enhancement as piezoelectric biosensor. For PCR-amplified DNA from real samples, the primer pair RMTB, FMTB specific for the IS*6110* was used for the amplification of target DNA fragments as 209 bp.

Table 1 Oligonucleotide sequences of DNA probe and complementary DNA target designed from IS*6110* sequence.

Name	Nucleotide sequence 5' to 3'
Thiol-modified oligonucleotide probe	SH-$(CH_2)_6$-TTTTTTGTGGCCATCGTGGAAGCGA
Biotin-modified oligonucleotide probe	Biotin-TTTTTTGTGGCCATCGTGGAAGCGA
Blocking 1	ATCGTGGTCCTGCGGGCTTTTTTTTT-$(CH_2)_3$-SH
Blocking 2	ATCGTGGTCCTGCGGGCTTTTTTTTT-Biotin
Complementary DNA target	TCGCTTCCACGATGGCCAC
Primer FMTB	AAAGCCCGCAGGACCACGAT
Primer RMTB	GTGGCCATCGTGGAAGCGA

Isolation of genomic DNA

Standard strain from cultivation including *Mycobacterium tuberculosis* (H37RVKK11-20) was provided from Department of Communicable Disease, Ministry of Public Health Thailand. *Mycobacterium avium* complex, *Pseudomonas aeruginosa*, *Escherichia coli*, *Staphylococcus aureus*, and *Enterococcus faecalis* were collected from Department of Pathology, Faculty of Medicine, Srinakharinwirot University. The clinical sputum 200 samples; 150 samples as positive infection of *M. tuberculosis* and 50 samples as negative of non-*M. tuberculosis* and other microorganism were corrected from Department of Pathology, Faculty of Medicine, Srinakharinwirot University and Bureau of Tuberculosis, Ministry of Public Health Thailand.

M. tuberculosis (H37RVKK11-20 strains) grown on Lowenstein-Jensen (LJ) slant medium was plated in 10 mL sterile normal saline tube and vertexed. After was adjusted to a 0.5 McFarland standards scale set (BioMerieux, German) approximately 1.5×10^8 CFU/mL (1 McFarland standards scale set 3×10^8 CFU/mL) [135]. M. tuberculosis was diluted under 9 different conditions as 10^8, 10^7, 10^6, 10^5, 10^4, 10^3, 10^2,10^1, and 10^0 CFU/mL from 0.5 McFarland standards (1.5×10^8 CFU/mL).

Two loops of standard strains which were cultured on LJ-medium or 0.5 µL of sputum. Extraction was prepared by one ml DNAzol® (Invitrogen, USA) reagent was used for extraction. The mixture was inverted for several times and centrifuged at 4,000xg for 10 minutes. The

supernatant of both methods was individually transferred to other vial and precipitated by adding 0.5 ml of cold absolute ethanol which showed visible DNA as a cloudy precipitate and then mixed again by inversion and left at room temperature for 1-3 minutes prior to centrifugation at 4,000xg for 10 minutes. The supernatant was discarded and the DNA pellet was washed twice with 0.8 -1.0 mL of 70% ethanol by inverting the tubes 3-6 times. The mixture was then centrifuged at 13,000xg for 10 minutes to allow DNA to settle and ethanol was removed by decanting. The genomic DNA was air-dried for 2 hours, and distilled water was added and kept at 4°C. Total DNA concentration and DNA purity were measured by spectrophotometer analysis. The absorbance at 260 nm was used for calculating the concentration of nucleic acid. One absorbance at 260 nm is equivalent to approximately 50 µg/ml of DNA. DNA purity was calculated by using the ratio of A260/A280. The ratio of A260/A280 should be 1.8-2.0.

Fragmentation of genomic DNA by restriction enzyme

The genomic DNA was digested by restriction enzyme to obtain DNA fragments containing the target sequence. The restriction enzyme used in this study was selected by using NEBcutter 2.0 freeware [136]. From restriction mapping of putative IS*6110* system-associated gene cluster of *M. tuberculosis*, many enzymes can digest the genomic DNA of *M. tuberculosis* and result in various sizes of DNA fragments. Therefore, *Bst*DSI (*Btg* I) (SIB enzyme, USA) was chosen for digesting the genomic DNA to obtain DNA fragment containing the IS*6110* secretion system sequence. After digestion, the fragment containing the target sequence was calculated to be 218 bp long.

Genomic DNA of partial IS*6110* gene of purified *M. tuberculosis* DNA was performed by using *Bst*DSI restriction enzyme. All reactions were manipulated in 50 µL containing genomic DNA in 5 µL of 10X buffer (33 mM Tris-acetate (pH 7.9), 10 mM Magnesium acetate, 66 mM Potassium acetate, and 0.1 mg/mL BSA), and 10 units of *Bst*DSI restriction enzyme. Sterile distilled water was added to adjust volume to 50 µL. The *Bst*DSI digestion was allowed to proceed at 37 °C for 14 – 16 hours. The reaction was inactivated by heating at 65 °C for 20 minutes. The success reaction had been confirmed by electrophoresis analysis, which has been performed by using an agorose gel (1.5% in TBE electrophoresis buffer).

Synthesis of DNA-gold particle conjugates

The protocol for the synthesis of DNA-gold particle conjugates was similar to previously reported [137]. Twenty nm gold colloid (Sigma, USA) was contained approximately 0.01% $HAuCl_4$ suspended in 0.01% tannic acid with 0.04% trisodium citrate, 0.26 mM potassium carbonate, and 0.02% sodium azide as a preservative. All unconjugated gold nanoparticles were added with thiol-modified oligonucleotide. After 20 minutes, a solution of 1 M PBS (100 mM PB, 1 M NaCl, pH 7.0) was gradually added to the solution until the salt concentration reached 0.1 M. This solution was aged for 16 hrs at room temperature. After that, the solution was centrifuged, and the precipitate was washed by 100 µL of 0.1 M PBS. This washing process was repeated for three times, and the final product was diluted in 100 µL of 0.1 M PBS.

Synthesis of avidin-gold particle conjugates

Twenty nm gold nanoparticles were added to optimize avidin concentration. In order to synthesize the avidin-coated gold particles, avidin and NaCl were added to the 20 nm diameter gold particle suspension. The solution was centrifuged at 12000 rpm, 4°C for 70 min to remove excess avidin and increase the concentration of gold particles [120].

Real time piezoelectric system design

An experimental flow cell was developed by mounting the crystal between two O-ring seals inserted in an acrylic cell. One face of the quartz crystal was exposed to a 50 µL flow-through chamber, which was connected to an inlet and outlet-flow tube drove by the peristaltic pump (ISM 834, USA). The whole flow cell was placed in a shielding box to avoid some environmental interference. The apparatus included a peristaltic pump to assure a 10 µL/min constant flow of the solutions. The experiments were performed at the room temperature. The experimental piezoelectric biosensor setup consisted of the 12 MHz AT-cut piezoelectric quartz wafer with gold electrode was used for preparing DNA-piezoelectric based biosensor. The gold electrode that fabricated on the quartz wafer has diameter of 4 mm and thickness of 1000 Å. Oscillation counting device was used for measuring the frequency change of the quartz crystal after the addition of immobilization material. The major component of this device composes of

microcontroller, oscillation circuit and read out display. The experimental setup was monitored by a microcomputer with a diver interface programmed by National Instruments LabVIEW.

Preparation of quartz crystal surface for real time

The method used to prepare piezoelectric DNA sensor in this study was modified by Wu and co-works (121). The quartz crystals, which consist of a 12 MHZ AT cut quartz crystal slab with a layer of a gold electrode on each side were (0.125 cm^2 in area on each side) obtained from Kyocera-Kinseki Co.,Ltd., Thailand.

The gold electrode surface of quartz crystals were cleaned by using Piranha solution (30% H_2O_2: H_2SO_4 = 1:3) for 30 seconds. The crystals were then thoroughly washed with distilled water and used immediately afterward. Initially, immobilization of thiol-modified oligonucleotide probe on gold electrode surface by using 4-(2-hydroxyethyl)-1-piperazine-ethanesulfonic acid (HEPES) (Sigma, USA) buffer (0.05 M HEPES, 0.2 M NaCl, pH 7.5) was passed through the flow system. The inlet/outlet pumps were controlled to deliver 50 μL of solution to the detection cell. After the baseline was stabilized, 20 μL of thiol-modified oligonucleotide probe in buffer (1M KH_2PO_4, pH 3.8) was added into the cell through the reagent reservoir and the pump was stopped for 20 minutes and added 1 mM of 6-mercapto-hexanol (MCH) was completed for 30 minutes which MCH helps reduce nonspecific binding of the thiol-modified oligonucleotide to the gold surface, After the immobilization the pump was restarted again. The detection cell was washed using the buffer for 5 minutes prior to injection of DNA target (figure 9a).

Another, immobilization biotin-modified oligonucleotide probe on gold electrode surface by using HEPES buffer was passed through the flow system. The inlet/outlet pumps were controlled to deliver 50 μL of solution to the detection cell. After the baseline was stabilized, 1mM 3-mercaptopropionic acid (MPA) (Sigma, USA) aqueous solution for 1 hour, washed with buffer. To activate the monolayer, 100 mg/mL 1-ethyl-3(3-dimethylaminopropil) carbodiimide ethanolic solution (EDC) (Sigma, U.S.A) was placed on the surface. Then 100 mg/mL *N*-hydroxysuccinimide aqueous solution (NHS) (Fluka, Switzerland) was immediately add and left to react on the surface of gold electrode to form MPA monolayer for 30 minutes. The surface was then rinsed with buffer. An aliquot of 0.1 mg/mL avidin HEPES buffer was placed on the electrode surface for at least 1 hour.

Then, the quartz crystal was exposed to a 1 mM ethanolamine (Fluka, Switzerland) for 30 minutes, rinsed with distilled water and HEPES buffer. The DNA biotinylated probes were placed over the gold electrode surface for 20 minutes. Then, the probes were rinsed with immobilization buffer. All experiment, this stage the quartz crystal was ready for the hybridization (figure 9b).

Hybridization assay

The hybridization with the oligonucleotides target was performed. Twenty microliters of the oligonucleotides target were placed on the surface of gold electrode which was previously immobilized with DNA probe (thiol, thiol/MCH, biotin probe). After another interval of 30 minutes (pump stopping), the cell was washed by buffer for 5 minutes. At the same time, 20 µL DNA target were driven by pump to after pass through the denatured (95 ˚C) for 5 minites and then rapidly passing through the cold down (50 ˚C) for 1 minute prior to a rapid transfer to the detection cell. The flow rate was maintained with a slow flow at 30 µL/min of denaturing fragmentation of genomic DNA by restriction enzyme and transferring solution between reactors and delivering samples to the detection cell. After the denatured fragmentation of genomic DNA was injected into the piezoelectric biosensor for 15 - 20 minutes, the cell was washed by the buffer again prior to the recording of frequency shift after a stable frequency was reached. For the regeneration of the probe modified electrode, 1 mM HCl was added to the electrode surface for 30 seconds, following by a thorough washing using the buffer solution (figure 9a, 9b).

Optimization of quartz crystal for detections

Optimization of flow rate injection

The HEPES buffer was passed through the flow system at various flow rates from 5, 10, 20, 30, 40, 50, 60, 70, 80, 90, 100, and 150 µL/min to the flow cell. The inlet/outlet pumps were controlled to deliver 500 µL of solution to the detection flow cell. The flow rate of peristaltic pump which gave the most stability frequency was chosen for using in all experiments of this study.

Optimization of oligonucleotide probe

Thiol-modified oligonucleotide probe; the probe at various concentrations from 0.25, 0.50, 0.75, 1.00, 1.5, and 2.0 μM were immobilized on the quartz crystal for 30 minutes at room temperature. The resonant frequency was measured as the amount of synthetic DNA target.

Thiol-modified oligonucleotide probe/MCH; the probe at various concentrations from 0.25, 0.50, 0.75, 1.00, 1.5, and 2.0 μM were immobilized on the quartz crystal for 30 minutes at room temperature and added 1 mM of 6-mercaptohexanol (MCH) was completed for 30 minutes which MCH helps reduce nonspecific binding of the thiol-modified oligonucleotide to the gold surface. The resonant frequency was measured as the amount of synthetic DNA target.

Biotin-modified oligonucleotide probe; the probe at various concentrations from 0.50, 0.75, 1.00, 1.5, and 2.0 μM were selected. Each concentration was immobilized on quartz crystals that pretreated with 0.1 mg/mL avidin binding to 15 mM MPA/ 200 mM EDC/ 50 mM NHS monolayer.

The each concentration of DNA probe which gave the highest frequency shift was chosen for using in all experiments of this study.

Study of the responses of the synthetic complementary DNA target

The optimum concentration of DNA probe was chosen for preparing DNA piezoelectric biosensor. The synthetic DNA target at various concentrations 0, 0.25, 0.50, 0.75, 1.00, 1.50, and 2.00 μM were hybridized with thiol-modified oligonucleotide probe/MCH and biotin-modified oligonucleotide probe at room temperature for 20 minutes. The frequency shift was measured in hertz (Hz).

Shelf life study of DNA probe on quartz crystal

The optimum concentration of thiolated probe and biotinylated probe on quartz crystal was stored at 4 °C for 0, 1, 3, 5, 10, 30, 60, 90, 120, and 150 days by closing the cap of quartz crystal. After storage, the quartz crystal of various time points, the quartz crystal was

hybridized with 1.00 μM of synthetic DNA target at room temperature for 20 minutes. The frequency shift was measured in Hz.

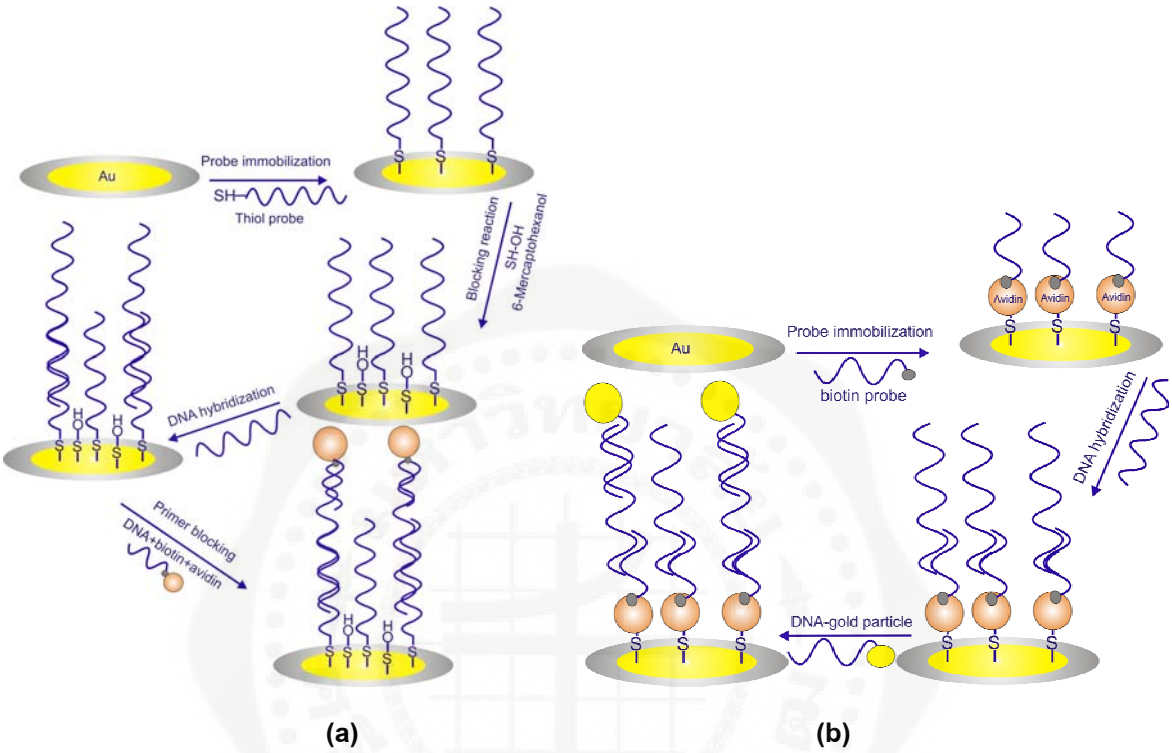

Figure 9 Schematic diagram of immobilization and hybridization method. (a) Thiol-modified oligonucleotide probe and Thiol-modified oligonucleotide probe/MCH immobilization and (b) Biotin-modified oligonucleotide probe immobilization.

Development sensitivity of hybridization of DNA target with DNA probe

Generally, simple thermal treatment of bacterial target DNA is sufficient to give a significant analytical signal when amplified bacterial DNA fragment is used in DNA biosensor technique. But this treatment was not enough for non-amplified genomic DNA because of reannealing of bacterial target DNA. Minnuni et al [129, 130] used the blocking oligonucleotides for blocked the bacterial target DNA after simple thermal treatment. This method increases the efficiency of hybridization between DNA probe and non-amplified genomic DNA. For this reason, different denaturation methods have been studied as shown in figure 10.

- Thermal denaturation plus blocking oligonucleotides: The bacterial DNA was heated at 95 °C for 5 minutes and then cooled at 50 °C for 1 minute for adding the blocking 1 oligonucleotides attached 20 nm gold nanoparticle (Sigma, USA). After that, the bacterial DNA was hybridized with the optimum DNA probe at room temperature for 20 minutes and the frequency shift was measured (figure left).

- Thermal denaturation plus blocking oligonucleotides: The bacterial DNA was heated at 95 °C for 5 minutes and then cooled at 50 °C for 1 minute for adding the blocking 2 oligonucleotides attached avidin. After that, the bacterial DNA was hybridized with the optimum DNA probe at room temperature for 20 minutes and the frequency shift was measured (figure center).

- Thermal denaturation plus blocking oligonucleotides: The bacterial DNA was heated at 95 °C for 5 minutes and then cooled at 50 °C for 1 minute for adding the blocking2 oligonucleotides attached avidin conjugated gold nanoparticle. After that, the bacterial DNA was hybridized with the optimum DNA probe at room temperature for 20 minutes and the frequency shift was measured (figure right).

The optimal DNA digestion was diluted with hybridization buffer and loaded onto the quartz crystals. The concentration of DNA target sequence was 0, 0.5, 1, 5, 10, 20, and 30 μg/mL. The concentration of DNA target sequence hybridized which gave the highest frequency shift was chosen for using in experiments of this study.

Optimization of blocking oligonucleotide/gold nanoparticle conjugation

Initially, the HEPES buffer was passed through the flow system. The inlet/outlet pumps were controlled to deliver 50 μL of solution to the detection cell. After the baseline was stabilized, 20 μL of thiol-modified oligonucleotide probe concentrations were diluted buffer (1M KH_2PO_4, pH 3.8) The detection cell was then washed using the HEPES buffer to remove unbound probes prior to injection an aqueous solution of 1 mM MCH was added into each well and left for 30 mins at room temperature to block any non-specific interaction site and washed using the HEPES buffer to remove unbound. After that thermal denaturation capture with blocking 1 oligonucleotides and then cooled at 50 °C for 1 minute for adding the block1 oligonucleotides (1 μM) capture with gold nanoparticle-modified varies concentration at 10%, 20%, 25%, 50%, 75%, and 100% Hz. After that, the bacterial DNA was hybridized with the

probe for 20 minutes and the frequency change was measured. The concentration of gold nanoparticle-modified oligonucleotide which gave the highest frequency change was chosen for using in experiments of this study.

The optimization of gold particle-modified oligonucleotide was sectioned with the glass knives under ultramicrotome (model RMC ultramicrotome MT-7000). Ultra-thin sections (approximately 80 to 90 nanometers) were mounted on grids, and then DNA-gold particles were viewed in JEOL-1200EXII (Japan) transmission electron microscope (TEM) operating at 80 KV.

Optimization of blocking avidin-modified oligonucleotide

The HEPES buffer was passed through the flow system. The inlet/outlet pumps were controlled to deliver 50 µL of solution to the detection cell. After the baseline was stabilized, 20 µL of thiol-modified oligonucleotide probe concentrations were diluted buffer The detection cell was then washed by using the HEPES buffer to remove unbound probes prior to injection an aqueous solution of 1 mM MCH was added into each well and left for 30 minutes to block any non-specific interaction site and washed using buffer to remove unbound. After that thermal denaturation capture with blocking 2 oligonucleotides which the bacterial DNA was heated at 95 °C for 5 minutes and then cooled at 50 °C for 1 minute for adding the blocking 2 oligonucleotides (1 µM) capture with avidin-modified at varies concentration from 0.025, 0.05, 0.075, 0.1, and 0.2 mg/mL. After that, the bacterial DNA was hybridized with the probe for 20 minutes and the frequency shift was recorded.

The concentration of blocking oligonucleotide/avidin conjugated which gave the highest frequency shift was chosen for using in experiments of this study.

The optimization of DNA capture with avidin was sectioned with the glass knives under ultramicrotome (model RMC ultramicrotome MT-7000). Ultra-thin sections (approximately 80 to 90 nanometers) were mounted on grids, and then DNA-gold particles were viewed in JEOL-1200EXII (Japan) transmission electron microscope (TEM) operating at 80 KV.

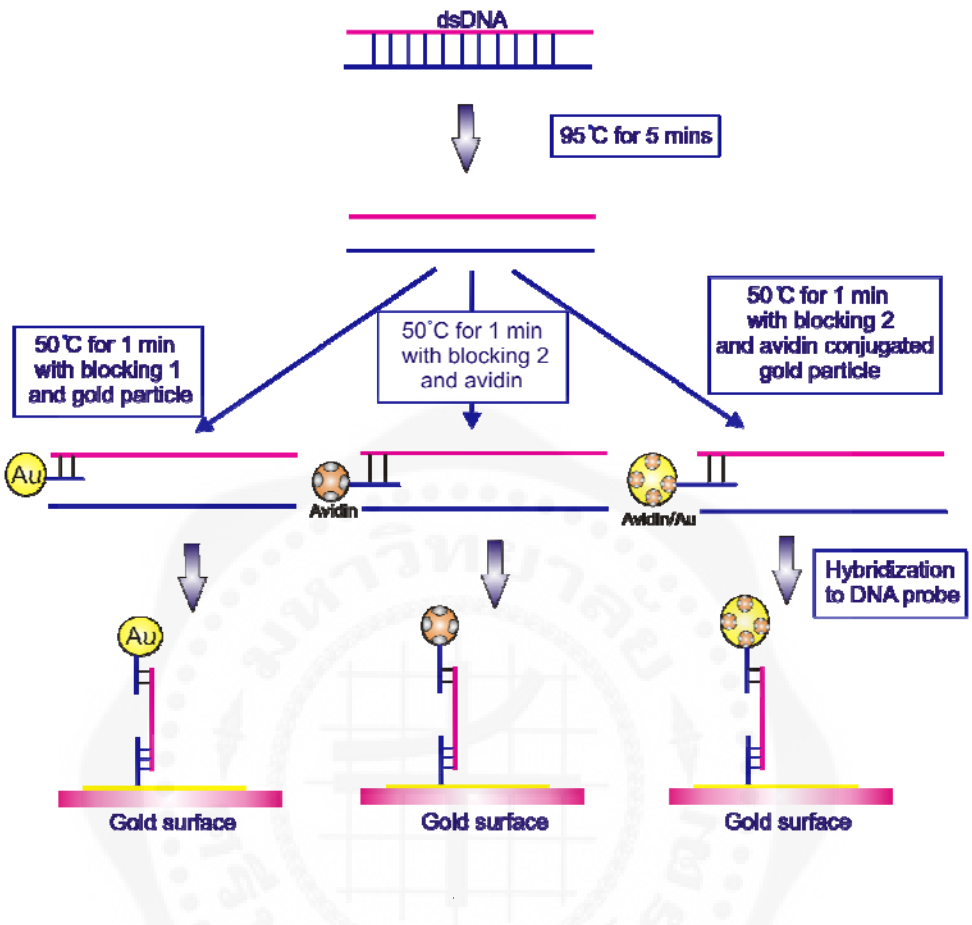

Figure 10 Schematic diagram of denaturation method.

Optimization of blocking avidin/gold particle-modified oligonucleotide

The buffer was passed through the flow system. The inlet/outlet pumps were controlled to deliver 50 µL of solution to the detection cell. After the baseline was stabilized, 20 µL of thiol-modified oligonucleotide probe concentrations were diluted buffer The detection cell was then washed by using the HEPES buffer to remove unbound probes prior to injection an aqueous solution of 1 mM MCH was added into each well and left for 30 minutes to block any non-specific interaction site and washed using the HEPES buffer to remove unbound. The bacterial DNA was heated at 95˚C for 5 minutes and then cooled at 50˚C for 1 minute for adding the block 2 oligonucleotides (1 µM) capture with avidin/gold particle-modified varies concentration at 10%, 20%, 25%, 50%, 75% and 100% v/v. After that, the bacterial DNA was hybridized with the probe at room temperature for 20 minutes and the frequency change was

measured. The concentration of avidin/gold particle-modified oligonucleotide which gave the highest frequency shift was chosen for using in experiments of this study.

The optimization of DNA/avidin/gold particle was sectioned with the glass knives under ultramicrotome (model RMC ultramicrotome MT-7000). Ultra-thin sections (approximately 80 to 90 nanometers) were mounted on grids, and then DNA-gold particles were viewed in JEOL-1200EXII (Japan) TEM operating at 80 KV.

Study of the evaluation of DNA piezoelectric based biosensor system specificity

The hybridizations with the target oligonucleotides were performed. Three quartz crystals were assayed with the target solution in total 50 µL. *M. Tuberculosis* (H37RVKK11-20), *M. avium* complex, *P. aeruginosa*, *E. coli*, *S. aureus*, and *E. faecalis*, and hybridization buffer were separately added to each quartz crystal.

All genomic DNA of specimens were performed using *Bst*DSI restriction enzyme. The digested DNA fragments were denature at 95 °C for 5 minutes to generate single stranded DNA, then the reaction was subsequently incubated at 50 °C 1 minute in present of blocking oligonucleotides. This temperature was the appropriated for the annealing of the blocking oligonucleotides to the complementary DNA sequences. This denaturation procedure combined the thermal dissociating effect with the steric hindrance cased by the binding of two oliglonucleotides to the separated DNA strands. This method relied on the use of Block 1 or Block 2 oliglonucleotides added to the sample. One oliglonucleotide was complementary to the strand containing the target, but bound laterally not to overlap with them. By the interaction between the thermally separated DNA strands and these oliglonucleotides, re-association between dsDNA strand could be prevented. Afterwards, the DNA digestion was diluted with hybridization buffer and loaded onto the quartz crystals. The concentration range of DNA target was 10 µg/mL after that DNA target capped with 25%v/v oligonucleotide capture with avidin/gold nanoparticle modified. The hybridization reactions were allowed to proceed for 20 mins. The crystals were washed well with hybridization buffer to remove the unbound oligonucleotides, subsequently the resonance frequency was measured.

Study of precision and accuracy of device

Fifteen microliters of 1.5 μM DNA thiol-modified oligonucleotide probes were hybridized with 1.5 μM synthetic DNA target into the piezoelectric biosensor for 15 - 20 minutes, the cell was washed by the buffer again prior to the recording of frequency shift after a stable frequency was reached. Each experiment was performed triplicate with different piezoelectric biosensor devices. All data were presented as the mean ± standard deviation (S.D.) that compared for standard device as oscilloscope (Intek GDS 800)

The accuracy of a measurement system is the degree of closeness of measurements of a quantity to its actual (true) value. The precision of a measurement system, also called reproducibility or repeatability, is the degree to which repeated measurements under unchanged conditions show the same results.

Study of the quartz crystal reusing

The reused quartz crystals were achieved by treating with 50 μL of 1 mM HCl for 1 minute. HCl hydrolyzed the hydrogen bonding between optimal DNA probe concentration and complementary DNA target IS*6110*. The separation of double strand complementary DNA target were rinsed to remove unbound the surfactant with hybridization buffer and immediately hybridized with complementary DNA target.

The detection of the piezoelectric biosensor compared PCR method

The piezoelectric biosensor detected genomic DNA of partial IS*6110* sequence of *M. tuberculosis* DNA was performed using *Bst*DSI restriction enzyme that non amplified DNA compared a procedure for PCR amplification was performed in 25 μL volume. The reaction contains genomic DNA in 10x PCR buffer, 50 mM MgCl2, 20 mM dNTP, 20 μM each of primers (RMTB, FMTB), 1 unit of *Taq* DNA polymerase and distilled water. The PCR amplification was performed using DNA thermal cycle apparatus. Each cycle consist of pre-denaturation at 94°C for 5 minutes, denaturation at 94°C for 1 minute, annealing at 53°C for 1 minute , extension at 72°C for 1 minute and Post-extension at 72°C for 7 minutes. The PCR products were analyzed using electrophoresis in 2% agarose gel at 100 volt for approximately 30 minutes prior to ethidium bromide staining and record the DNA band under ultraviolet light.

All methods were detected 200 samples; 150 positive samples and 50 as negative samples (*M. avium* complex and other microorganism).

CHAPTER 4

RESULTS

Electronic circuits design for real time

The oscillation frequency counter unit for piezoelectric biosensor device was designed by measurement of frequency up to 20 MHz as shown in figure 11.

To establish the circuit, the switches SW1 was turn-on and turn-off switches for distribution of the electric potential by using the power supply at 12 V/DC.

The diode D11 allowed electricity to flow in only one direction. C100 capacitors was used in circuit to block the flow of direct current, while allowing alternating current to pass, to filter out interference, to smooth the output of power supplies. U4 and C102 were the regulator circuit for maintaining the level of the voltage to 5V in the microcontroller U1.

C80 and C91 were frequency high signal filter from IC output. IC of U5 converted series circuit communications from a microcontroller USB to communicate with a PC via port USB.

ISO1 and ISO2 as opto-isolator were devices that used a short optical transmission path to transfer an electronic signal between elements of a circuit, typically, a transmitter and a receiver, while keeping them electrically isolated, which used to isolate ground between circuits and PC.

Frequency circuit was comprised with U2 as the frequency generation with quartz crystal.

L1 and C101 were a tank circuit suitable for generating frequency transmission energy to quartz crystal which can oscillate in the liquid.

U60 decorated frequency generating output which could give square wave. The frequency input might be higher than the speed of the microcontroller overload therefore, the circuit needed designed frequency divider circuit by using IC U61. IC was dividing by 4 counters by using timing generator 4 seconds. The device allowed measurement up to 30 MHz by 1 Hz resolution required 10 seconds of sampling time.

Calculations and processing part with supply voltage were input of microcontroller, which runs output from written program. The major of function received input button and

interface with PC via U5. Frequency counter was input during the period of time. The frequency input was calculated from the equation.

$$F = n / t.$$

F = frequency

n = number of waveforms in time period.

t = time period

After measurement and calculation of frequency, the result was read out by LCD display or recorded by a computer with the aid of LabVIEW interface software.

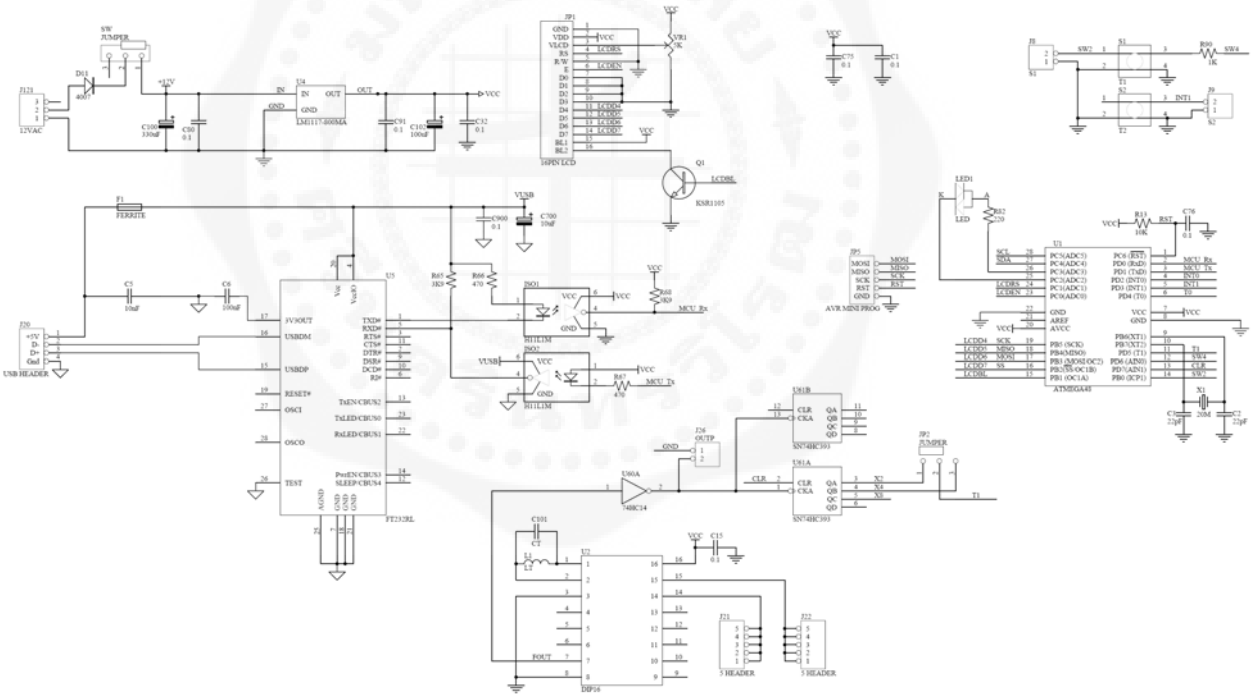

Figure 11 Electronic circuit of oscillation frequency counters for real time piezoelectric biosensor equipment.

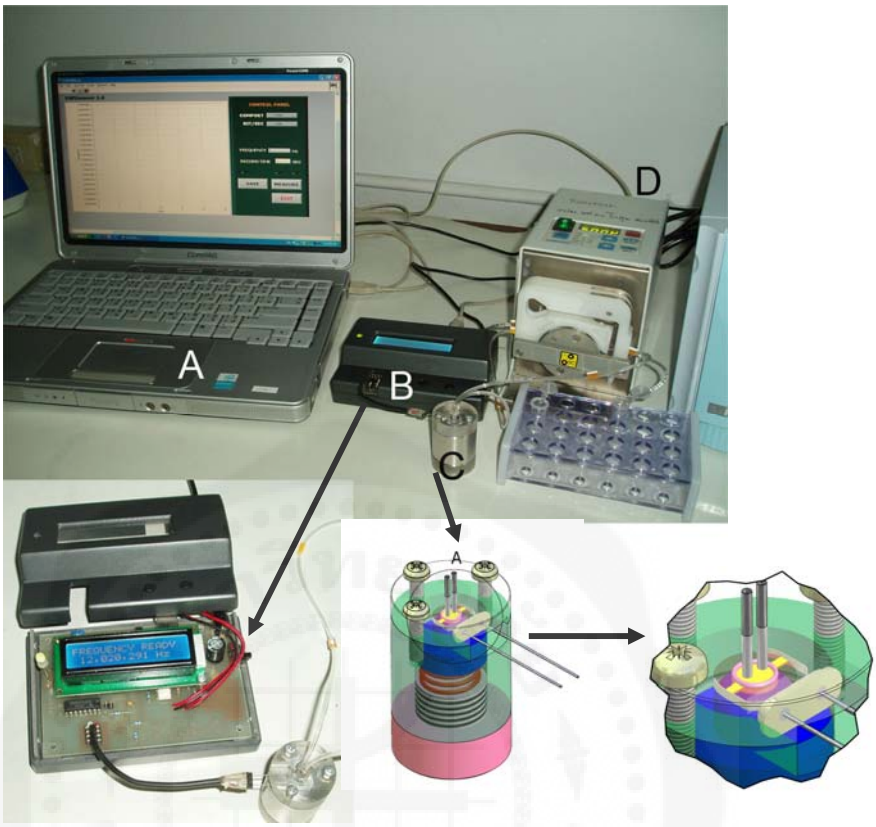

Figure 12 DNA piezoelectric based biosensor system in real time. (A) Data recorded by a computer with the aid of LabVIEW interface software. (B) Picture of oscillation counting device was used for measuring the frequency shift of the quartz crystal after the addition of immobilization material. (C) Picture of flow cell detection. (D) Picture of peristaltic pump.

Optimization of quartz crystal for detections

Optimization of flow rate injection

The HEPES buffer was passed through the flow system at various flow rates from 5, 10, 20, 30, 40, 50, 60, 70, 80, 90, 100, and 150 µL/min to the flow cell. The inlet/outlet pumps were controlled to deliver 500 µL of solution circulation to the detection flow cell. After HEPES buffer was passed through the flow system, the frequency change was increase when change the flow rate changed but frequency was stable after 2 – 3 minutes. Figure 13 showed the relationship between flow rate and frequency shift, which the flow rate was stable from 5 to 100 µL/min.

The flow rate of peristaltic pump at 30 µL/min was chosen for using in all experiments of this study because it was slow enough to allow DNA target in suspension to bind to the surface before being swept away, yet fast enough to prevent accumulation of particulates. Moreover, the liquid inlet through the flow cell was prevented bubbles formation during piezoelectric biosensor experiments.

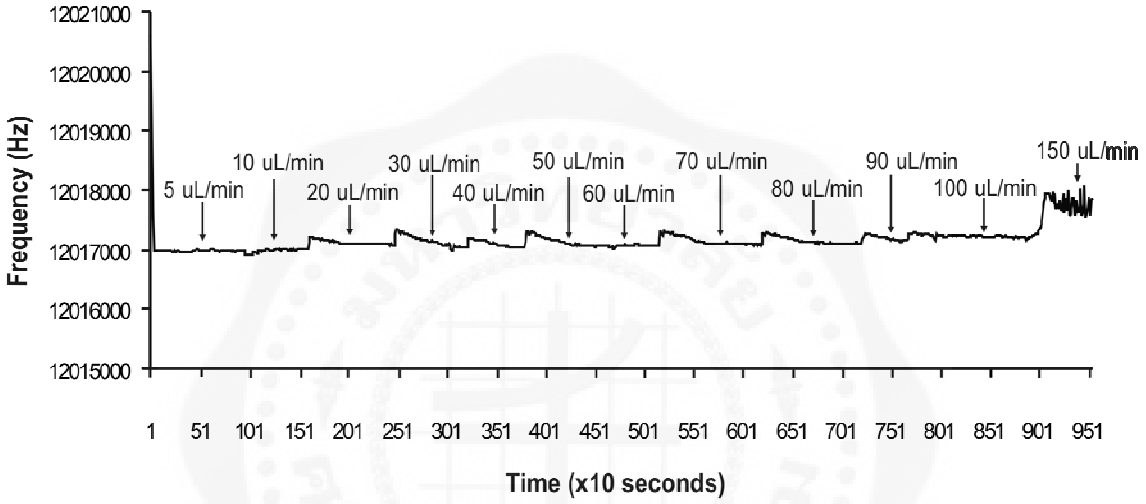

Figure 13 Frequency shift of quartz crystal by flow rate injection.

Optimization of oligonucleotide probe

Biotin-modified oligonucleotide probe; the concentrations of DNA biotin-modified oligonucleotide probe ranging from 0.50, 0.75, 1.00, 1.50, and 2.00 µM were selected. Each concentration was immobilized on quartz crystals that pretreated with 0.1 mg/mL avidin binding to 15 mM MPA/ 200 mM EDC/ 50 mM NHS monolayer.

Each concentration of biotin-modified oligonucleotide probe immobilization was used for 8 pieces of quartz crystal. The frequency shift was averaged from -195±7.27, -239±13.12, -265±11.45, -263±10.75, and -260±7.15 Hz as shown in table 2, respectively.

The frequency shift of each concentration (n=8) of biotin-modified oligonucleotide probe immobilization was presented as mean ±S.D. as shown in figure 14. The frequency shift

increased in relation with the concentration of biotin-modified oligonucleotide probe which was stabled from concentration 1.00, 1.50, and 2.00 μM.

Thiol-modified oligonucleotide probe/MCH; the probe at various concentrations from 0.25, 0.50, 0.75, 1.00, 1.5, and 2.0 μM were immobilized on the quartz crystal for 30 minutes at room temperature and 1 mM of 6-mercaptohexanol (MCH) was added and completed for 30 minutes which MCH helped reducing nonspecific binding of the DNA thiolated to the gold surface. After that, 1.0 μM of the synthetic DNA target was hybridized with the thiolated probe/ MCH at room temperature for 20 minutes. The resonant frequency was measured as the amount of synthetic DNA target. Each concentration of probe immobilization was used for 8 pieces of quartz crystal. The frequency shift was averaged from -64±6.04, -121±4.98, -183±8.49, -203±6.86, and -209±7.42 Hz as shown in table 3, respectively.

The frequency shift of each concentration (n=8) of thiol-modified oligonucleotide probe/MCH immobilization was presented as mean ±S.D. as shown in figure 14. The frequency shift increased in relation with the concentration of thiol-modified oligonucleotide probe/MCH which was stabled from concentration 1.5 and 2.0 μM.

Thiol-modified oligonucleotide probe; the probe at various concentrations from 0.25, 0.50, 0.75, 1.00, 1.5, and 2.0 μM were immobilized on the quartz crystal for 30 minutes at room temperature. The frequency change was measured. After that, 1.0 μM of the synthetic DNA target was hybridized with the thiol-modified oligonucleotide probe at room temperature for 20 minutes. The resonant frequency was measured as the amount of synthetic DNA target. Each concentration of probe immobilization was used for 8 pieces of quartz crystal. The frequency shift was averaged from -36±4.36, -78±4.9, -101±4.8, -107±9.69, and -105±7.49 Hz as shown in table 4, respectively.

The frequency shift of each concentration (n=8) of thiol-modified oligonucleotide probe immobilization was presented as mean ±S.D. as shown in figure 14. The frequency shift increased in relation with the concentration of thiol-modified oligonucleotide probe which was stabled from concentration 1.00, 1.5, and 2.0 μM.

The frequency shifts related to the increasing of all the probe concentration which thiol and biotin-modified oligonucleotide probe stabled at concentration 1.00, 1.50, and 2.00 μM but thiol-modified oligonucleotide probe/ MCH stabled at concentration 1.50, and 2.00 μM. The

biotin-modified oligonucleotide probe at concentration 1.00 μM gave the highest frequency shift which higher thiol-modified oligonucleotide probe, respectively. The thiol-modified oligonucleotide probe/MCH at concentration 1.50 μM gave the highest frequency shift. Therefore, the optimum concentration of biotin-modified oligonucleotide probe and thiol-modified oligonucleotide probe was 1.00 μM but thiol-modified oligonucleotide probe/MCH was 1.50 μM which was used in all experiments in this study.

Table 2 The frequencies were shifted at various concentration of biotin-modified oligonucleotide probe.

Quartz (pieces)	**Biotin-modified oligonucleotide probe at various concentration (μM)**				
	0.50	0.75	1.00	1.50	2.00
1	-187 Hz	-236 Hz	-263 Hz	-268 Hz	-252 Hz
2	-190 Hz	-213 Hz	-254 Hz	-260 Hz	-250 Hz
3	-194 Hz	-251 Hz	-273 Hz	-244 Hz	-259 Hz
4	-189 Hz	-232 Hz	-272 Hz	-261 Hz	-255 Hz
5	-203 Hz	-249 Hz	-287 Hz	-259 Hz	-264 Hz
6	-193 Hz	-233 Hz	-248 Hz	-284 Hz	-271 Hz
7	-210 Hz	-238 Hz	-266 Hz	-269 Hz	-260 Hz
8	-197 Hz	-258 Hz	-259 Hz	-257 Hz	-269 Hz
$\overline{X} \pm SD$	-195±7.27 Hz	-239±13.12 Hz	-265±11.45 Hz	-263±10.75 Hz	-260±7.15 Hz

Table 3 The frequencies were shifted at various concentration of thiol-modified oligonucleotide probe/MCH.

Quartz	Thiol-modified oligonucleotide probe/MCH at various concentration (μM)				
(pieces)	0.50	0.75	1.00	1.50	2.00
1	-55 Hz	-118 Hz	-180 Hz	-192 Hz	-195 Hz
2	-57 Hz	-113 Hz	-185 Hz	-200 Hz	-201 Hz
3	-64 Hz	-127 Hz	-189 Hz	-209 Hz	-219 Hz
4	-65 Hz	-122 Hz	-167 Hz	-210 Hz	-216 Hz
5	-61 Hz	-119 Hz	-176 Hz	-213 Hz	-211 Hz
6	-74 Hz	-121 Hz	-182 Hz	-198 Hz	-213 Hz
7	-68 Hz	-117 Hz	-198 Hz	-203 Hz	-212 Hz
8	-70 Hz	-128 Hz	-183 Hz	-197 Hz	-207 Hz
$\overline{X} \pm SD$	-64±6.04 Hz	-121±4.98 Hz	-183±8.49 Hz	-203±6.86 Hz	-209±7.42 Hz

Table 4 The frequencies were shifted at various concentration of thiol-modified oligonucleotide probe.

Quartz	Thiol-modified oligonucleotide probe at various concentration (μM)				
(pieces)	0.50	0.75	1.00	1.50	2.00
1	-30 Hz	-87 Hz	-100 Hz	-92 Hz	-106 Hz
2	-35 Hz	-74 Hz	-103 Hz	-97 Hz	-100 Hz
3	-39 Hz	-71 Hz	-97 Hz	-111 Hz	-99 Hz
4	-38 Hz	-78 Hz	-92 Hz	-107 Hz	-95 Hz
5	-27 Hz	-73 Hz	-99 Hz	-103 Hz	-108 Hz
6	-37 Hz	-81 Hz	-109 Hz	-120 Hz	-120 Hz
7	-38 Hz	-77 Hz	-105 Hz	-112 Hz	-112 Hz
8	-40 Hz	-82 Hz	-102 Hz	-117 Hz	-103 Hz
$\overline{X} \pm SD$	-36±4.36 Hz	-78±4.9 Hz	-101±4.8 Hz	-107±9.69 Hz	-105±7.49 Hz

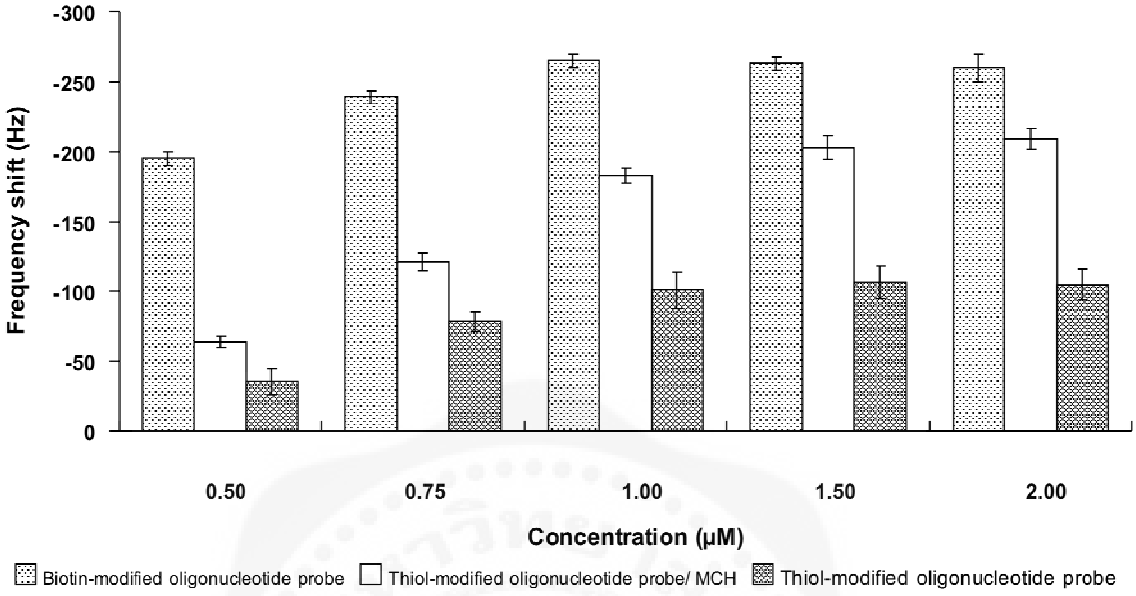

Figure 14 The immobilization relationship between concentration of each probe and frequency shift.

Study of the responses of the synthetic complementary DNA target

The optimum concentration of each DNA probe was chosen for preparing DNA piezoelectric biosensor. The synthetic DNA target at various concentrations 0, 0.25, 0.50, 0.75, 1.00, 1.50, and 2.00 μM were hybridized with thiol-modified oligonucleotide probe/MCH and biotin-modified oligonucleotide probe at room temperature for 20 minutes. The frequency shift was measured in hertz (Hz).

Each concentration of hybridization of complementary DNA target was used for 3 pieces of quartz crystals. The frequency shift of 1.50 μM thiol-modified oligonucleotide probe/MCH was averaged from -3±3.82, -30±2.64, -82±5.00, -116±12.50, -155±11.97, -185±5.74, and -183±13.27 Hz, as shown in table 5, respectively. The frequency shift of 1.0 μM biotin-modified oligonucleotide probe was averaged from -2±1.29, -44±3.56, -61±6.53, -107±14.53, -144±11.21, -209±6.68, and -184±5.29 Hz, as shown in table 6, respectively. In figure 15 showed the relationship between concentration of synthetic DNA target and frequency shift after hybridized with thiol-modified oligonucleotide probe/MCH and biotin-modified oligonucleotide probe. When frequency shift was decreased, concentration of complementary

DNA target was increased. At 0.25 μM was the least of concentration which the tool showed the minimum of frequency shift of thiol-modified oligonucleotide probe/MCH and biotin-modified oligonucleotide probe at -30±2.64 and -44±3.56 Hz, respectively.

The frequency shift related to the increasing of synthetic DNA target concentration which stabled since concentration 1.50 and 2.00 μM. The optimum concentration of all DNA probe can hybridize with the synthetic DNA target at lowest concentration 0.25 μM.

Table 5 Thiol-modified oligonucleotide probe was hybridized with synthetic DNA target at various concentration and frequency shifts.

Quartz (pieces)	**Thiol-modified oligonucleotide probe (1.50 μM) hybridized with synthetic DNA target at various concentration (μM)**						
	0	0.25	0.5	0.75	1.0	1.5	2.0
1	-5 Hz	-28 Hz	-77 Hz	-125 Hz	-141 Hz	-178 Hz	-177 Hz
2	-1 Hz	-34 Hz	-89 Hz	-98 Hz	-140 Hz	-192 Hz	-170 Hz
3	+3 Hz	-29 Hz	-81 Hz	-125 Hz	-152 Hz	-184 Hz	-201 Hz
$\overline{X}$	-3 Hz	-30 Hz	-82 Hz	-116 Hz	-155 Hz	-185 Hz	-183 Hz
SD	3.82	2.64	5.00	12.50	11.97	5.74	13.27

Table 6 Biotin-modified oligonucleotide probe was hybridized with synthetic DNA target at various concentration and frequency shifts.

Quartz (pieces)	**Biotin-modified oligonucleotide probe (1.00 μM) hybridized with synthetic DNA target at various concentration (μM)**						
	0	0.25	0.5	0.75	1.0	1.5	2.0
1	-2 Hz	-47 Hz	-69 Hz	-100 Hz	-171 Hz	-202 Hz	-189 Hz
2	-4 Hz	-39 Hz	-61 Hz	-132 Hz	-160 Hz	-207 Hz	-170 Hz
3	-1 Hz	-46 Hz	-53 Hz	-124 Hz	-172 Hz	-218 Hz	-183 Hz
$\overline{X}$	-2 Hz	-44 Hz	-61 Hz	-107 Hz	-144 Hz	-209 Hz	-184 Hz
SD	1.29	3.56	6.53	14.53	11.21	6.68	5.29

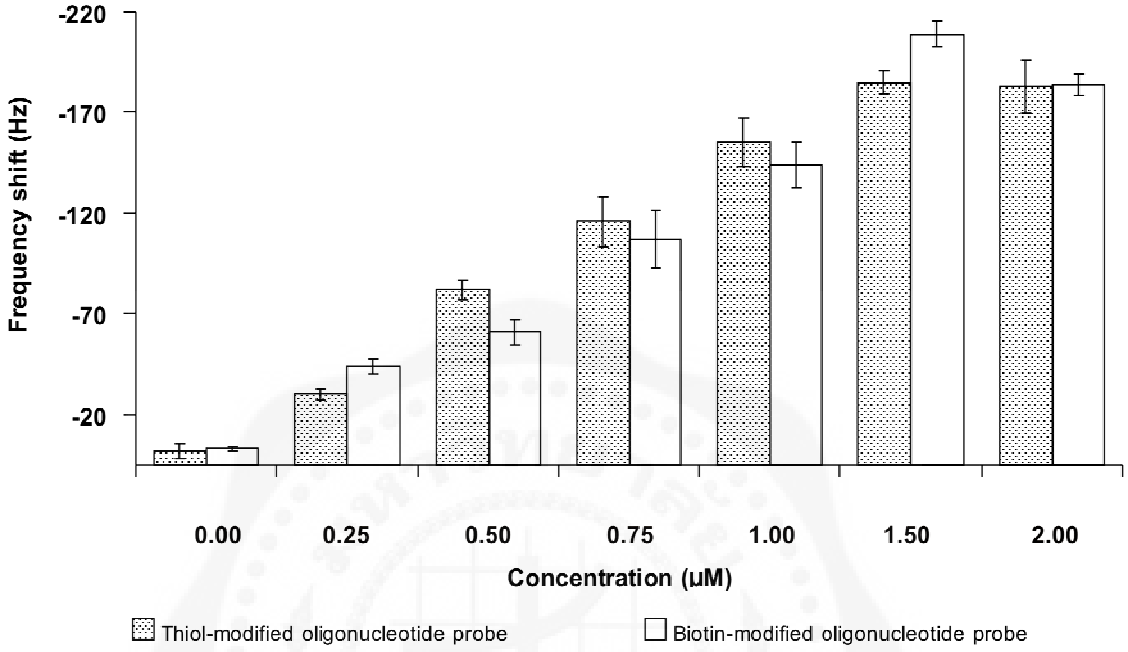

Figure 15 The hybridization relationship between concentration of synthetic complementary DNA target and frequency shift.

Shelf life study of DNA probe on quartz crystal

The biotin-modified oligonucleotide probe at concentration 1.00 µM and thiol-modified oligonucleotide probe/MCH at concentration 1.50 µM were stored for 0, 1, 3, 5, 10, 30, 60, 90, 120, and 150 days at 4 °C by closing the cap. After storage at various times, each probe was hybridized with 1.50 µM synthetic DNA target. The inlet/outlet pumps were controlled to deliver 50 µL of solution circulation of flow rate at 30 µL/min to the detection flow cell for 20 minutes at room temperature. Each quartz crystal of thiol-modified oligonucleotide probe/MCH immobilization was measured the frequency shift as shown in table 7. The frequency shift of each storage time (n=3) was presented as mean ± S.D. as shown in figure 16. The storage time at 0, 1, 3, 5, 10, 30, 60, 90, and 120 days gave similar frequency shifts. The storage time at 150 days gave frequency shift was lower than the frequency shift of other storage time.

The frequency shift of each quartz crystal of biotin-modified oligonucleotide probe immobilization was measured the frequency shift as shown in table 8. The frequency shift of

each storage time (n=3) was presented as mean ± S.D. as shown in figure 16. The storage time at 0, 1, 3, 5, and 10 days gave similar frequency shifts. The storage time at 30, 60, 90, 120, and 150 days gave frequency shift was lower than the frequency shift of other storage time, respectively.

The thiol-modified oligonucleotide probe/MCH probe at concentration 1.50 μM gave the most stable frequency shift after hybridization with 1.50 μM of synthetic DNA target. Consequently, this thiol-modified oligonucleotide probe/MCH at concentration 1.50 μM can store at 4°C for 120 days. The optimum concentration of thiol-modified oligonucleotide probe was 1.50 μM which was used in all experiments in this study.

Table 7 The frequencies were shifted after storage thiol-modified oligonucleotide probe at various times.

Quartz (pieces)	**Frequency shift (Hz) after storage probe at various times (Days)**									
	0	1	3	5	10	30	60	90	120	150
1	-155	-157	-145	-175	-153	-141	-169	-141	-163	-132
2	-150	-150	-159	-169	-140	-163	-150	-162	-157	-144
3	-154	-159	-150	-149	-161	-150	-157	-158	-139	-131
$\overline{X}$	-153	-155	-151	-164	-151	-151	-159	-154	-153	-136
SD	2.16	3.87	5.80	11.12	8.66	9.04	7.85	9.11	10.19	5.91

Table 8 The frequencies were shifted after storage biotin-modified oligonucleotide probe at various times.

Quartz (pieces)	Frequency shift (Hz) after storage probe at various times (Days)									
	0	1	3	5	10	30	60	90	120	150
1	-150	-156	-145	-151	-137	-131	-117	-93	-80	-74
2	-148	-149	-153	-143	-144	-119	-105	-95	-86	-56
3	-167	-158	-149	-159	-141	-135	-97	-87	-77	-73
$\bar{X}$	-155	-154	-149	-151	-141	-128	-106	-92	-81	-68
SD	8.52	3.87	3.26	6.53	2.88	6.80	8.22	3.42	3.74	8.26

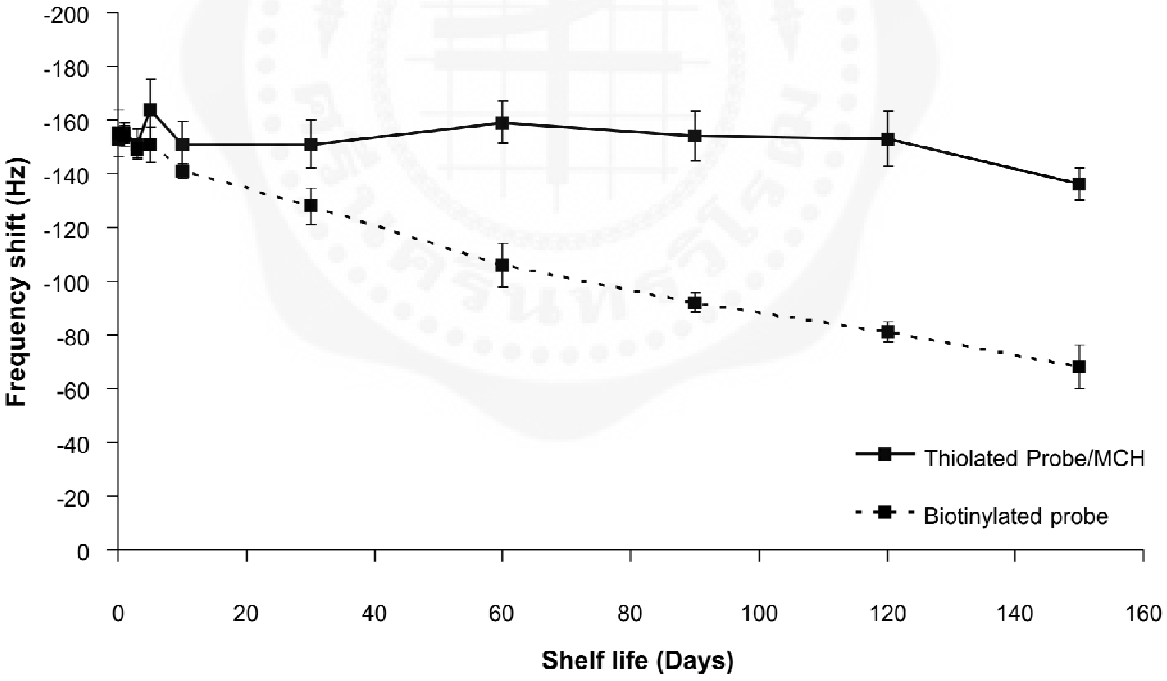

Figure 16 The hybridization relationship between synthetic DNA target hybridization with each probe after storage and frequency shift.

Development sensitivity of hybridization of DNA target with DNA probe

Preliminary experiment was conducted with non-amplified genomic DNA previously treated with the restriction enzyme (*Bst*DSI). The genomics of DNA digestion were mixed with blockings oligonucleotide. By the interaction between the thermally separated DNA strands and these oliglonucleotides, re-association on surface of quartz crystal between dsDNA could be prevented. All samples were hybridized with 1.50 μM of thiol-modified oligonucleotide probe for 20 minutes. After washed unbound, the frequency shifts were recorded as shown in table 9. Figure 17 showed the relationship among the concentrations of DNA digestion ranged from 0, 0.5, 1, 5, 10, 20, and 30 μg/mL, frequency shift averaged from -6± 3.74, -31±2.08, -59±6.53, -109±5.74, -137±7.42, -148±6.85, and -140±8.04 Hz, respectively.

The frequency shift of each denaturation method (n=3) was presented as mean ± S.D. as shown in figure 17. The frequency shifts related to the increasing of DNA target concentration which stabled since concentration dilution at 10, 20, and 30 μg/mL. The DNA target sequence at concentration 10 μg/mL gave the highest frequency change. Therefore, the optimum concentration of DNA target sequence dilution was 10 μg/mL capture signal enhancement (avidin, gold nanoparticle, avvidin/gold nanoparticle) which was used in all experiments in this study.

Table 9 The frequencies were shifted at various concentration of thiol-modified oligonucleotide probe.

Quartz (pieces)	**Thermal denaturation plus blocking oligonucleotides at various concentration (μg/mL)**						
	0	1	5	10	20	40	50
1	-6 Hz	-31 Hz	-67 Hz	-110 Hz	-145 Hz	-143 Hz	-132 Hz
2	-2 Hz	-34 Hz	-59 Hz	-102 Hz	-127 Hz	-158 Hz	-137 Hz
3	-11 Hz	-29 Hz	-51 Hz	-116 Hz	-138 Hz	-144 Hz	-151 Hz
$\overline{X}$	-6 Hz	-31 Hz	-59 Hz	-109 Hz	-137 Hz	-148 Hz	-140 Hz
SD	3.74	2.08	6.53	5.74	7.42	6.85	8.04

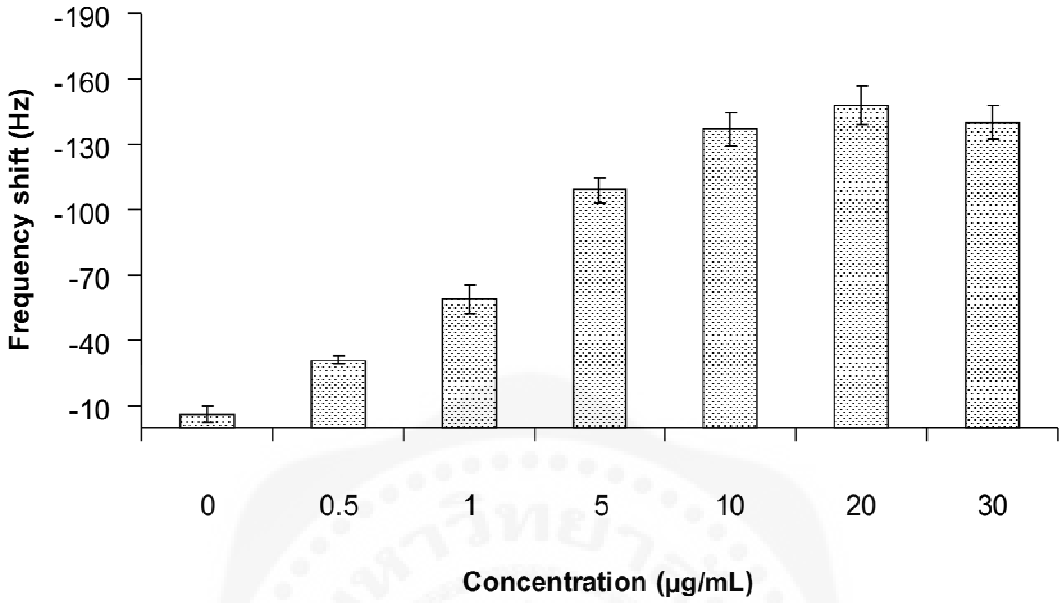

Figure 17 The hybridization relationship between concentrations of DNA digestion and frequency shift.

After that thermal denaturation plus blocking oligonucleotides which the bacterial DNA was heated at 95°C for 5 minutes and then cooled at 50°C for 1 minute for adding the blocking 2 oligonucleotides (1 µM) capture with mass enhancement for increasing sensitivity. In the figure 18 showed schematic illustrations of the steps involved in thiol-modified oligonucleotide probe/MCH immobilization, probes hybridized with DNA target, and signal amplification. The frequency shift of the detection process was shown. (A) DNA target was hybridized with thiol-modified oligonucleotide probe by blocking 2 oligonucleotides capture with avidin. (B) DNA target was hybridized with thiol-modified oligonucleotide probe by blocking 1 oligonucleotides capture with gold nanoparticle. (C) DNA target was hybridized thiol-modified oligonucleotide probe by blocking 2 oligonucleotides capture with avidin/gold nanoparticle conjugation.

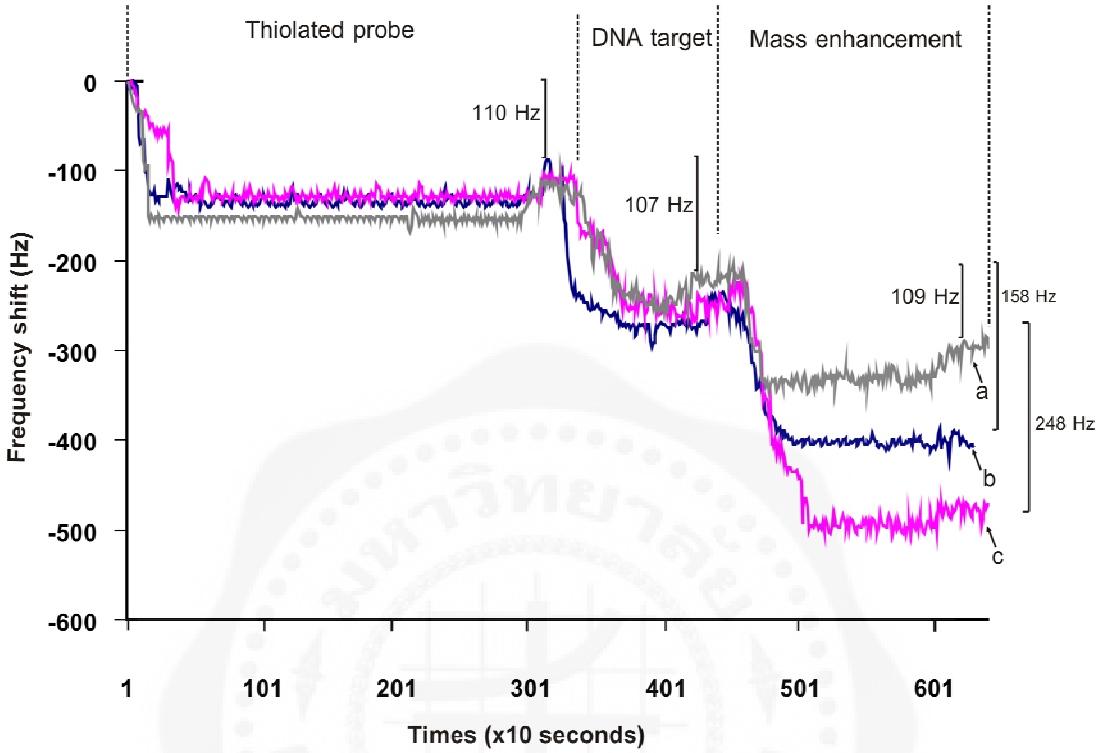

Figure 18 Schematic illustrations of the steps involved in thiol-modified oligonucleotide probe/MCH immobilization, probes hybridized with DNA target, and signal amplification. The frequency shift of the detection process was shown. (A) DNA target was hybridized with thiol-modified oligonucleotide probe by blocking 2 oligonucleotides capture with avidin. (B) DNA target was hybridized with thiol-modified oligonucleotide probe by blocking 1 oligonucleotides capture with gold nanoparticle. (C) DNA target was hybridized with thiol-modified oligonucleotide probe by blocking 2 oligonucleotides capture with avidin/gold nanoparticle conjugation.

Optimization of avidin -modified blocking 2 oligonucleotide

The bacterial DNA digestion was heated at 95°C for 5 minutes and then cooled at 50°C for 1 minute for adding the blocking 2 oligonucleotides (1 μM) capture avidin as mass enhancement varies concentration of avidin at 0.025, 0.05, 0.075, 0.10, and 0.20 mg/mL. The frequency shift was averaged from -36±10.23, -70±3.56, -92±4.51, -89±2.94, and -95±8.37 Hz,

as shown in table 10, respectively. In figure 19 showed the relationship between concentration of avidin as signal enhancement and frequency shift. The frequency shifts related to the increasing of avidin as signal enhancement concentration which stabled since concentration 0.075, 0.10, and 0.20 mg/mL.

Table 10 The frequencies were shifted at various concentration of blocking 2 oligonucleotides capture with avidin as signal amplification.

Concentrations	**blocking 2 oligonucleotides capture with avidin**			
(mg/mL)	Quartz	Probe (1.50 μM)	Target (10 μg/mL)	mass enhancement (avidin)
0.025	1	-70 Hz	-156 Hz	-37 Hz
	2	-84 Hz	-155 Hz	-23 Hz
	3	-90 Hz	-150 Hz	-48 Hz
	$\overline{X}$	-81 Hz	-154 Hz	-36 Hz
	SD			±10.23
0.05	1	-84 Hz	-152 Hz	-65 Hz
	2	-90 Hz	-155 Hz	-73 Hz
	3	-83 Hz	-151 Hz	-72 Hz
	$\overline{X}$	-86 Hz	-153 Hz	-70 Hz
	SD			±3.56
0.075	1	-87 Hz	-152 Hz	-92 Hz
	2	-90 Hz	-178 Hz	-87 Hz
	3	-81 Hz	-167 Hz	-98 Hz
	$\overline{X}$	-86 Hz	-166 Hz	-92 Hz
	SD			±4.51

Table 10 (Continued).

Concentrations	**blocking 2 oligonucleotides capture with avidin**		
(mg/mL)	Quartz	Probe (1.50 µM)	Target (10 µg/mL) mass enhancement (avidin)
0.1	1	-78 Hz	-180 Hz	-92 Hz
	2	-78 Hz	-156 Hz	-90 Hz
	3	-84 Hz	-164 Hz	-85 Hz
	$\overline{X}$	-80 Hz	-167 Hz	-89 Hz
	SD			±2.94
0.2	1	-84 Hz	-171 Hz	-87 Hz
	2	-80 Hz	-169 Hz	-100 Hz
	3	-73 Hz	-168 Hz	-99 Hz
	$\overline{X}$	-79 Hz	-169 Hz	-95 Hz
	SD			±8.37

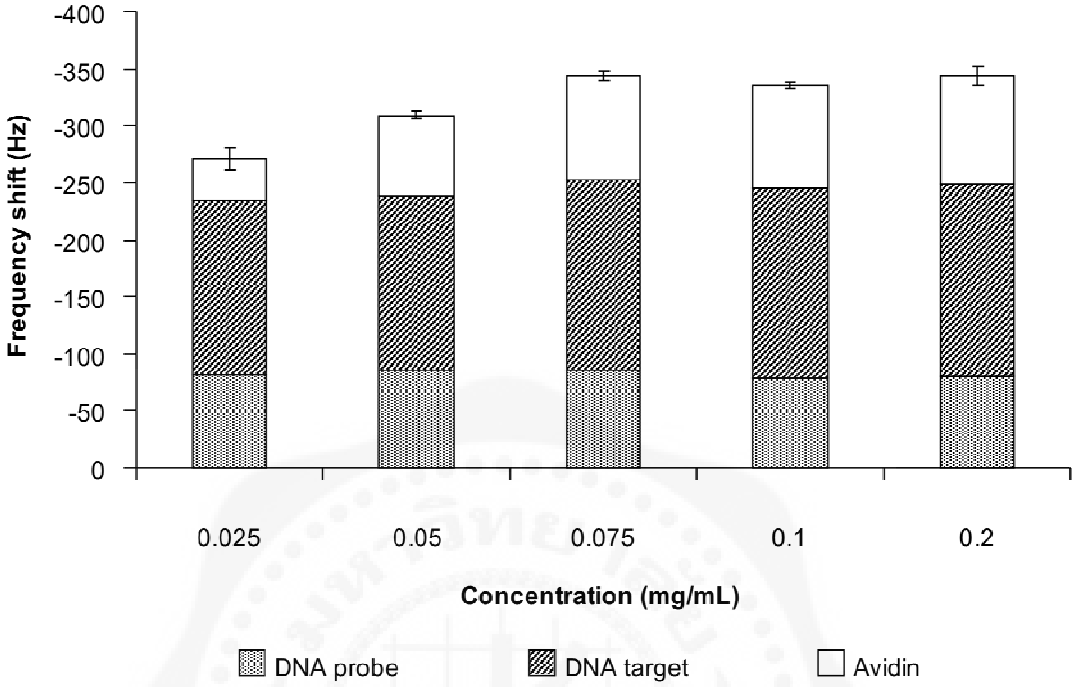

Figure 19 The hybridization relationship between concentrations of blocking 2 oligonucleotide capture avidin as signal enhancement and frequency shift.

Optimization of gold nanoparticle -modified blocking 1

The bacterial DNA digestion was heated at 95°C for 5 minutes and then cooled at 50°C for 1 minute for adding blocking 1 (1.00 μM) capture gold nanoparticle as mass enhancement varies concentration of gold nanoparticle at 10, 20, 25, 50, 75, and 100 %v/v. The frequency shift was averaged from -47±1.73, -91±3.87, -138±2.65, -158±4.65, -166±6.03, and -163±12.97 Hz, as shown in table 11, respectively. In figure 20 showed the relationship between concentration of gold nanoparticle signal amplification and frequency shift. The frequency shifts related to the increasing of gold nanoparticle signal amplification concentration which stabled since concentration 25, 50, 75, and 100 %v/v.

Table 11 The frequencies were shifted at various concentration of blocking 1 oligonucleotides capture with gold nanoparticle as signal amplification.

Concentrations	**blocking 1 oligonucleotides capture with gold nanoparticle**			
(%v/v)	Quartz	Probe (1.50 μM)	Target (10 μg/mL)	gold nanoparticle
10	1	-88 Hz	-151 Hz	-48 Hz
	2	-91 Hz	-151 Hz	-49 Hz
	3	-88 Hz	-155 Hz	-45 Hz
	$\overline{X}$	-89 Hz	-152 Hz	-47 Hz
	SD			±1.73
20	1	-86 Hz	-158 Hz	-95 Hz
	2	-89 Hz	-151 Hz	-93 Hz
	3	-87 Hz	-152 Hz	-86 Hz
	$\overline{X}$	-87 Hz	-154 Hz	-91 Hz
	SD			±3.87
25	1	-81 Hz	-170 Hz	-134 Hz
	2	-83 Hz	-178 Hz	-140 Hz
	3	-81 Hz	-173 Hz	-139 Hz
	$\overline{X}$	-82 Hz	-172 Hz	-138 Hz
	SD			±2.65
50	1	-74 Hz	-173 Hz	-164 Hz
	2	-82 Hz	-164 Hz	-156 Hz
	3	-81 Hz	-154 Hz	-153 Hz
	$\overline{X}$	-79 Hz	-164 Hz	-158 Hz
	SD			±4.65

Table 11 (Continued).

Concentrations	**blocking 1 oligonucleotides capture with gold nanoparticle**			
(%v/v)	Quartz	Probe (1.50 μM)	Target (10 μg/mL)	gold nanoparticle
75	1	-78 Hz	-155 Hz	-158 Hz
	2	-76 Hz	-151 Hz	-171 Hz
	3	-82 Hz	-150 Hz	-169 Hz
	$\overline{X}$	-79 Hz	-152 Hz	-166 Hz
	SD			±6.03
100	1	-82 Hz	-152 Hz	-153 Hz
	2	-87 Hz	-152 Hz	-181 Hz
	3	-88 Hz	-154 Hz	-154 Hz
	$\overline{X}$	-86 Hz	-153 Hz	-163 Hz
	SD			±12.97

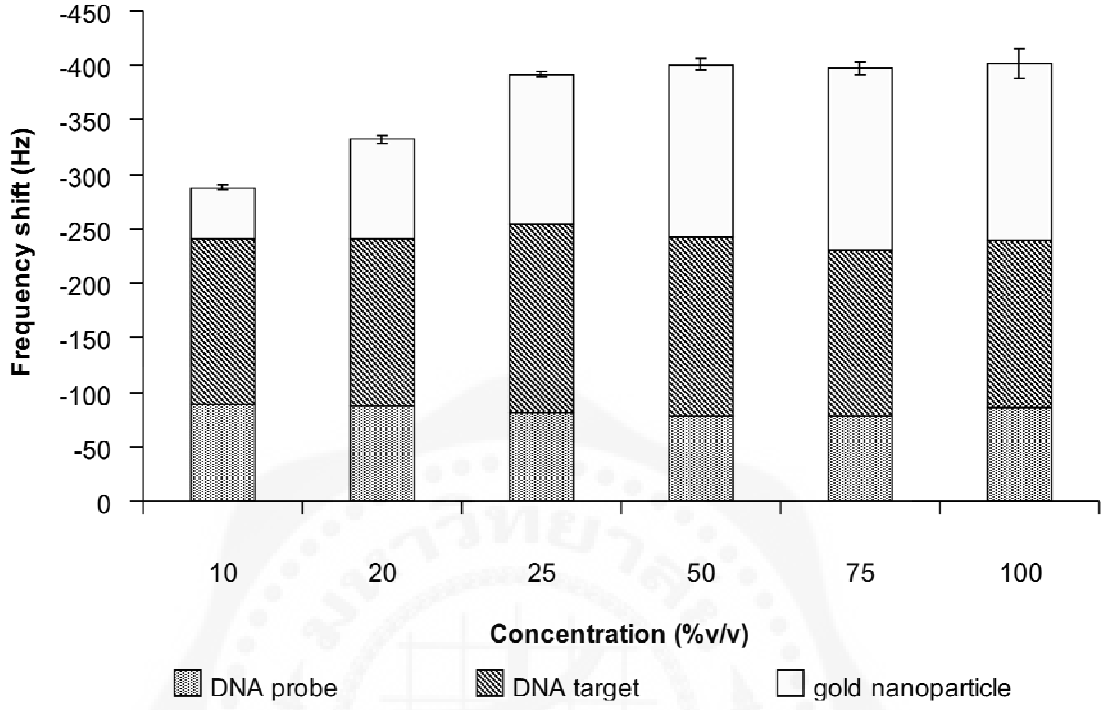

Figure 20 The hybridization relationship between concentrations of blocking 1 oligonucleotide capture gold nanoparticle as signal enhancement and frequency shift.

Optimization of avidin/gold nanoparticle-modified blocking

The bacterial DNA digestion was heated at 95°C for 5 minutes and then cooled at 50°C for 1 min for adding the blocking 2 oligonucleotides (1.00 μM) capture avidin/gold nanoparticle as signal amplification varies concentration of avidin/gold nanoparticle at 10, 20, 25, 50, 75, and 100 %v/v. The frequency shift was averaged from -91±5.31, -146±1.73, -195±5.32, -203±3.42, -198±2.51, and -191±2.56 Hz, as shown in table 12, respectively. In figure 21 showed the relationship between concentration of avidin/gold nanoparticle signal amplification and frequency shift. The frequency shifts related to the increasing of avidin/gold nanoparticle concentration which stabled since concentration 25, 50, 75, and 100 %v/v.

The frequency shift of blocking 2 oligonucleotides capture avidin/gold nanoparticle was higher than the frequency shift of blocking 1 oligonucleotides capture with gold nanoparticle and blocking 2 oligonucleotides capture with avidin, respectively.

The optimization of DNA target sequence (10 µg/mL), oligonucleotides capture avidin (0.075 mg/mL), gold nanoparticle (25 %v/v), and avidin/gold nanoparticle (25 %v/v) were sectioned with the glass knives under ultramicrotome (model RMC ultramicrotome MT-7000). Ultra-thin sections (approximately 80 to 90 nanometers) were mounted on grids, and then were viewed in JEOL-1200EXII transmission electron microscope (TEM) operating at 80 KV, as shown in figure 22.

Table 12 The frequencies were shifted at various concentration of blocking 2 oligonucleotides capture with avidin/gold nanoparticle as signal amplification.

Concentrations	**blocking 2 oligonucleotides capture with avidin/goldnanoparticle**			
(%v/v)	Quartz	Probe (1.5 µM)	Target (10 µg/mL)	avidin/gold nanoparticle
10	1	-84 Hz	-134 Hz	-84 Hz
	2	-80 Hz	-130 Hz	-91 Hz
	3	-73 Hz	-144 Hz	-97 Hz
	$\bar{X}$	-79 Hz	-136 Hz	-91 Hz
	SD			±5.32
20	1	-78 Hz	-135 Hz	-148 Hz
	2	-78 Hz	-146 Hz	-142 Hz
	3	-84 Hz	-132 Hz	-147 Hz
	$\bar{X}$	-80 Hz	-138 Hz	-146 Hz
	SD			±1.73

Table 12 (continued).

Concentrations (%v/v)	blocking 2 oligonucleotides capture with avidin/goldnanoparticle			
	Quartz	Probe (1.50 µM)	Target (10 µg/mL)	avidin/gold nanoparticle
25	1	-80 Hz	-134 Hz	-201 Hz
	2	-78 Hz	-139 Hz	-195 Hz
	3	-84 Hz	-147 Hz	-188 Hz
	$\overline{X}$	-81 Hz	-140 Hz	-195 Hz
	SD			±5.32
50	1	-80 Hz	-149 Hz	-200 Hz
	2	-73 Hz	-143 Hz	-208 Hz
	3	-77 Hz	-146 Hz	-202 Hz
	$\overline{X}$	-77 Hz	-146 Hz	-203 Hz
	SD			±3.42
75	1	-80 Hz	-145 Hz	-199 Hz
	2	-74 Hz	-143 Hz	-201 Hz
	3	-78 Hz	-148 Hz	-195 Hz
	$\overline{X}$	-77 Hz	-145 Hz	-198 Hz
	SD			±2.51
100	1	-79 Hz	-138 Hz	-187 Hz
	2	-73 Hz	-149 Hz	-193 Hz
	3	-81 Hz	-138 Hz	-192 Hz
	$\overline{X}$	-78 Hz	-142 Hz	-191 Hz
	SD			±2.56

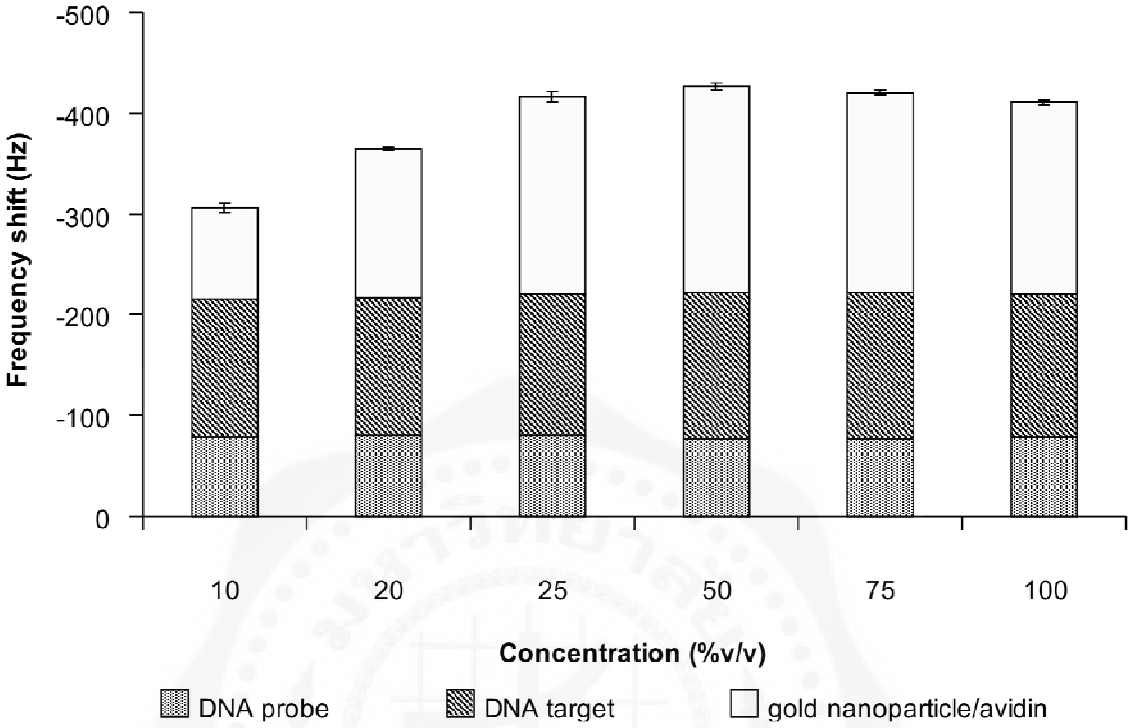

Figure 21 The hybridization relationship between concentrations of blocking 2 oligonucleotide capture avidin/gold nanoparticle as signal enhancement and frequency shift.

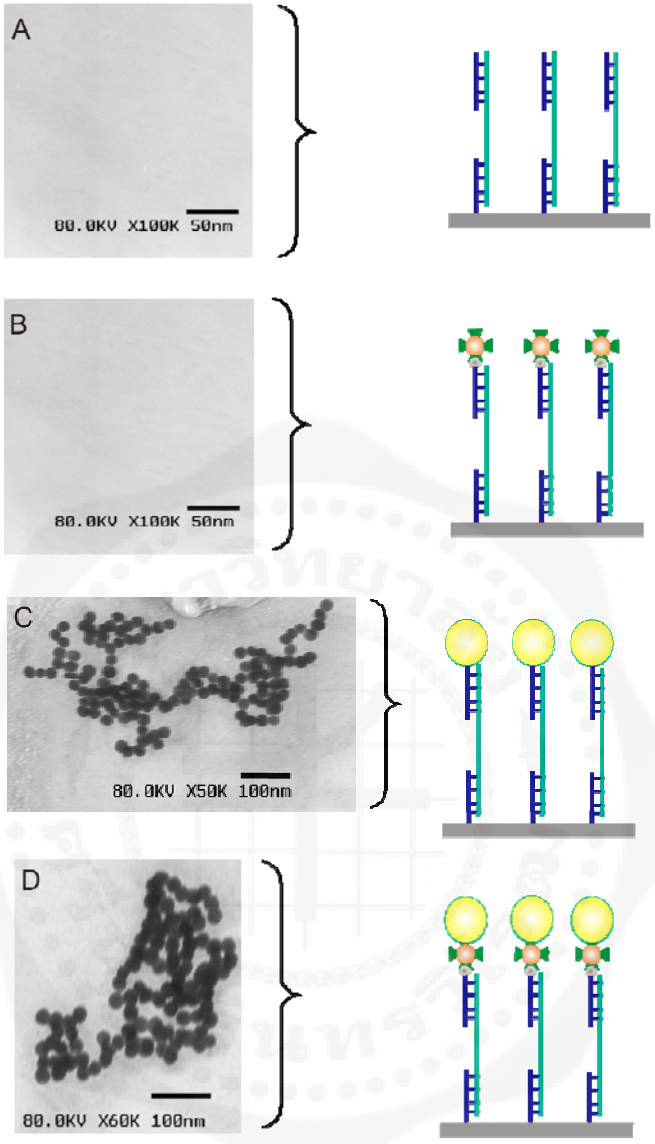

Figure 22 TEM images of the surface of a piezoelectric biosensor. (A) The surface of quartz was immobilized with thiol-modified oligonucleotide probe/MCH and hybridized with target sequences without mass enhancement. (B) The surface of quartz was hybridized with target sequences via blocking 2 oligonuclotides capture avidin as mass enhancement. (C) The surface of quartz was hybridized with target sequences via blocking 1 oligonuclotides capture gold nanoparticle as mass enhancement. (D) The surface of quartz was hybridized with target sequences via blocking 2 oligonuclotides capture avidin/gold nanoparticle as mass enhancement.

Study of the evaluation of DNA piezoelectric based biosensor system specificity

The specificity was detected by using *M. tuberculosis* (H37RVKK11-20), *M. avium* complex, *P. aeruginosa*, *E. coli*, *S. aureus*, and *E. faecalis*. The hybridization buffer was the negative control. All genomic DNA digested samples were denatured by thermal denaturation plus primer blocking capture with avidin/gold nanoparicle (25%v/v) and hybridized with 1.5 μM of thiol-modified oligonucleotide probe for 20 minutes at room temperature. The frequency shift of each sample (n=3) of denaturation methods was presented as mean ± S.D. as shown in table 13. *M. tuberculosis* gave frequency shift with higher frequency shift than of *M. avium* complex, *P. aeruginosa*, *E. coli*, *S. aureus*, and *E. faecalis* of denaturation plus primer blocking capture with avidin/gold nanoparticle methods, as shown in figure 23. Therefore, the thermal denaturation plus blocking capture avidin/gold particle for preparation of target DNA could differentiate *M. tuberculosis* from *M. avium* complex and other microorganism.

Table 13 The frequency shift of quartz crystal for evaluation of DNA-piezoelectric based biosensor system specificity.

Quartz (pieces)	**Frequency change (Hz) after bacteria target DNA hybridization**						
	Buffer	*M. avium*	*P. aeruginosa*	*E. coli*	*S. aureus*	*E. faecalis*	*M. tuberculosis*
1	-7 Hz	-4 Hz	-2 Hz	-6 Hz	-16 Hz	-14 Hz	-357 Hz
2	+3 Hz	-6 Hz	-4 Hz	-8 Hz	-14 Hz	-6 Hz	-360 Hz
3	-1 Hz	-3 Hz	-12 Hz	-15 Hz	-9 Hz	-8 Hz	-377 Hz
$\overline{X}$	-2 Hz	-4 Hz	-7 Hz	-10 Hz	-13 Hz	-9 Hz	-364 Hz
SD	4.12	1.29	4.43	3.87	3.32	3.06	8.83

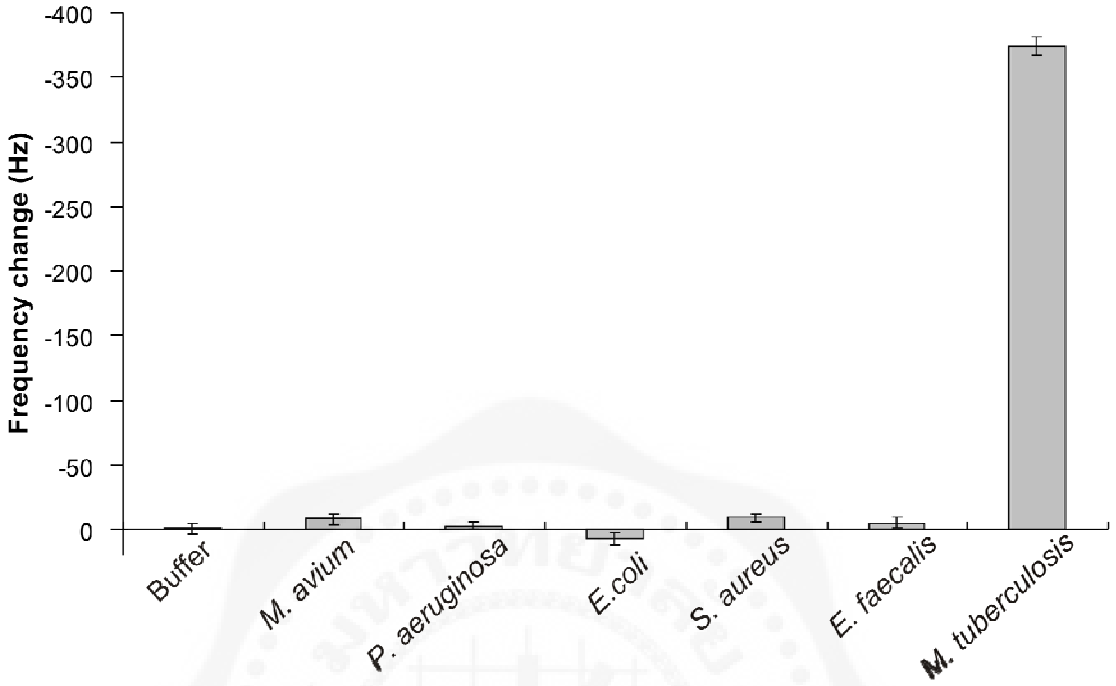

Figure 23 Specificity test of DNA-piezoelectric biosensor on *Bst*DSI-digested DNA of *M. tuberculosis* H37RVKK11-20 (positive control), *M. avium* complex, *P. aeruginosa*, *E. coli*, *S. aureus*, and *E. faecalis* (negative control) against hybridization buffer (blank).

Study of quantitative detection of non-amplification DNA

The genomics DNA digestion were mixed with blockings 2 oligonucleotide. By the interaction between the thermally separated DNA strands and these oliglonucleotides, re-association on surface between dsDNA could be prevented. The sensitivity of real time DNA-piezoelectric biosensor depends on the mass change on the gold surface. Therefore, in the detection with avidin/gold nanoparticle modified oligonucleotide (25 %v/v) for signal amplification. Table 14 and 15 showed the relationship among the concentrations of *M. tuberculosis* from $1.5x10^{0}$ - $1.5x10^{8}$ CFU/mL combined with avidin/gold nanoparticle modified oligonucleotide as mass enhancement, frequency shift averaged -15±5.32, -19±5.32, -21±6.14, -40±6.66, -83±9.63, -151±9.09, -252±10.28, -337±7.77, and 383±6.95 Hz, respectively and the frequency shift without mass enhancement conjugation was averaged -17±5.32, -13±3.32, -17±6.56, -19±4.55, -17±3.70, -53±2.89, -82±12.57, -84±6.38, and 101±5.35 Hz, respectively.

The blank showed the background of frequency shift as -17±3.56 Hz in the samples with mass enhancement and frequency shift as -7±2.16 Hz in the samples without mass amplification as shown in figure 24. The results indicate that the binding of biotin-modified blocking 2 oligonucleotide capture with avidin/gold nanoparticles was higher sensitivity than without conjugation.

Table 14 The frequencies were shifted at various concentration of *M. tuberculosis* (CFU/mL) with mass enhancement.

Quartz (pieces)	**Concentration of *Mycobacterium tuberculosis* 1.5×10^n (CFU/mL) after frequency shift (Hz)**									
	Blank	0	1	2	3	4	5	6	7	8
1	-12	-9	-16	-13	-46	-80	-141	-265	-335	-393
2	-20	-15	-23	-21	-31	-73	-163	-240	-346	-380
3	-19	-22	-19	-28	-44	-96	-149	-250	-330	-377
$\overline{X}$	-17	-15	-19	-21	-40	-83	-151	-252	-337	-383
SD	3.56	5.32	2.89	6.14	6.66	9.63	9.09	10.28	7.77	6.95

Table 15 The frequencies were shifted at various concentration of *M. tuberculosis* (CFU/mL) without mass enhancement.

Quartz (pieces)	**Concentration of *Mycobacterium tuberculosis* 1.5×10^n (CFU/mL) after frequency shift (Hz)**									
	Blank	0	1	2	3	4	5	6	7	8
1	-8	-13	-6	-25	-24	-13	-49	-65	-79	-95
2	-9	-21	-13	-9	-20	-17	-53	-95	-80	-100
3	-4	-18	-19	-18	-13	-22	-56	-86	-93	-108
$\overline{X}$	-7	-17	-13	-17	-19	-17	-53	-82	-84	-101
SD	2.16	3.32	5.32	6.56	4.55	3.70	2.89	12.57	6.38	5.35

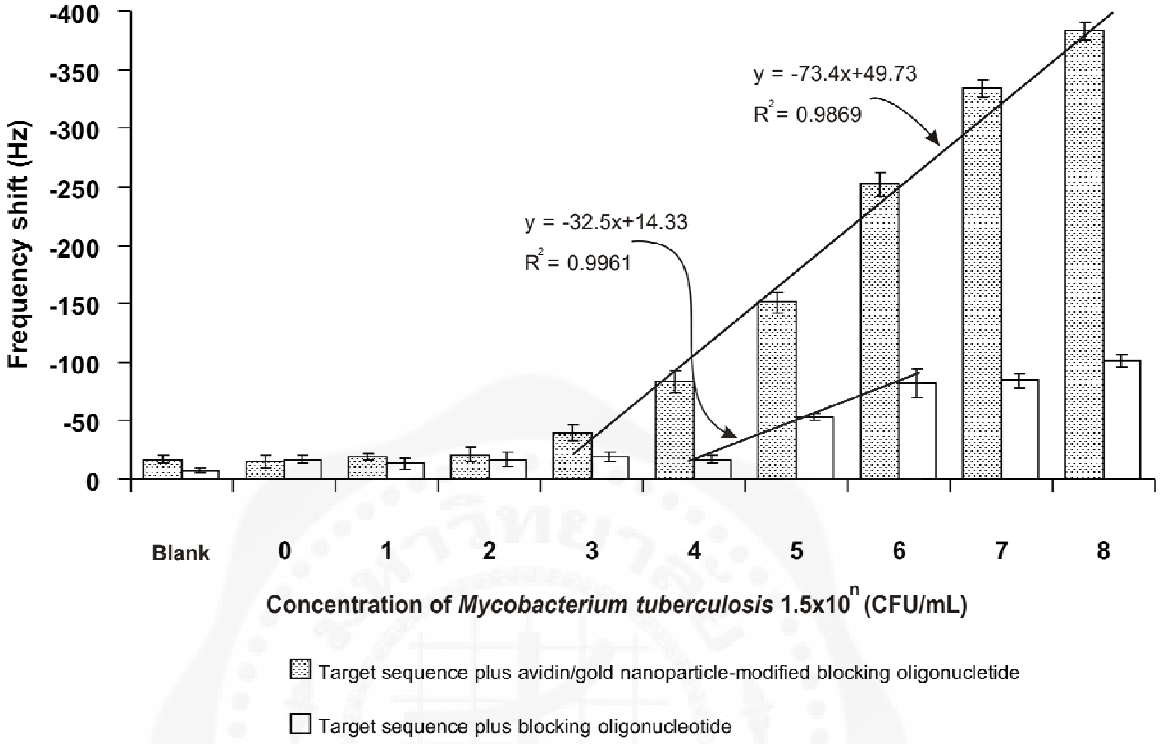

Figure 24 Sensitivity of the real time DNA piezoelectric biosensor was detected target sequence of *M. tuberculosis* by using combined with avidin/gold nanoparticle and without mass enhancement for signal amplification. Different of target sequence was $1.5x10^{0}$ – $1.5x10^{8}$ CFU/mL by detection with real time piezoelectric biosensor system.

Study of precision and accuracy of device

The accuracy of a measurement system was the degree of closeness of measurements of a quantity to its actual (true) value. Table 14 showed the accuracy of piezoelectric biosensor device compared to oscilloscope as reference of which frequencies shift average were -146±4.08 and 185.9±1.16 Hz, respectively. The accuracy of the frequency shift of piezoelectric biosensor device was lower than the frequency shift of oscilloscope as shown in figure 25.

The precision of a measurement system, also called reproducibility or repeatability, was the degree to which repeated measurements under unchanged conditions showed the same results. Table 14 showed the accuracy of piezoelectric biosensor device compared to

oscilloscope as reference of which frequencies shift error bar were 4.08 and 1.16 Hz, respectively. The precision of the frequency shift error bar of piezoelectric biosensor device was more similar to oscilloscope of which piezoelectric biosensor in this study was high precision as shown in figure 25.

Table 16 The accuracy and precision of DNA piezoelectric biosensor device comparison oscilloscope as reference and frequency shift.

Measurement (times)	**Frequency shift after synthetic DNA target hybridization**	
	Piezoelectric biosensor	Oscilloscope
1	-145 Hz	-185 Hz
2	-142 Hz	-185 Hz
3	-146 Hz	-185 Hz
4	-143 Hz	-185 Hz
5	-146 Hz	-187 Hz
6	-148 Hz	-187 Hz
7	-143 Hz	-186 Hz
8	-143 Hz	-187 Hz
9	-149 Hz	-186 Hz
10	-146 Hz	-186 Hz
11	-144 Hz	-186 Hz
12	-147 Hz	-185 Hz
13	-158 Hz	-186 Hz
14	-156 Hz	-186 Hz
15	-148 Hz	-186 Hz
16	-144 Hz	-186 Hz
17	-146 Hz	-186 Hz
18	-143 Hz	-187 Hz
19	-143 Hz	-186 Hz
20	-147 Hz	-186 Hz
$\overline{X}$	-146 Hz	-185.9 Hz
SD	4.08	1.16

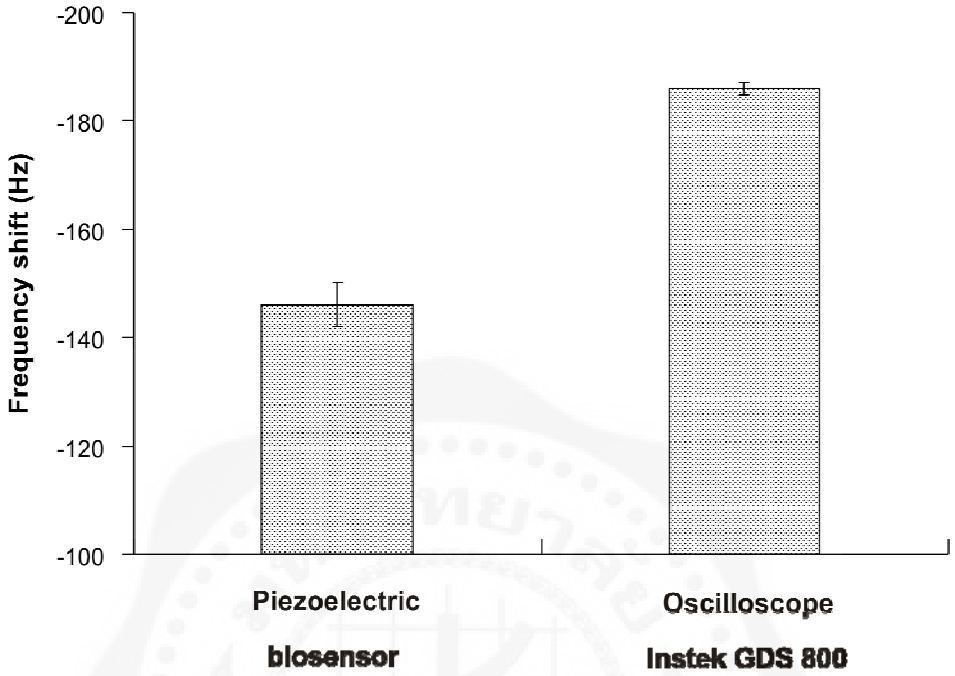

Figure 25 The precision and accuracy of device was compared with oscilloscope and frequency shift.

Study of the quartz crystal reusing

The reusing surface of each quartz crystal was performed with 50 µL of 1 mM HCl. HCl hydrolyzed the hydrogen bonding between DNA thiol-modified oligonucleotide probe and complementary DNA target. The separations of double stranded into single stranded oligonucletide by using concentration of the DNA digestion at the highest frequency shift. The frequency shift averages were -150±3.11, -148±15.55, -145±6.35, -139±7.33,-131±7.33, -125±3.87, -127±16.74, -111±6.35, -81±3.74, -101±5.00, and -97±3.56 Hz, respectively .The cycles of reusing could be performed 10 times, without affecting the sensor performance as shown in table 17 and figure 26.

Table 17 The cycles of reusing between thiol-modified oligonucleotide probe/MCH hybridized with synthetic DNA target.

Quartz (pieces)	Frequency shift (Hz) after quartz crystal reusing (Times)										
	0	1	2	3	4	5	6	7	8	9	10
1	-146	-166	-154	-149	-141	-121	-127	-117	-91	-102	-94
2	-153	-149	-143	-133	-126	-130	-148	-118	-125	-94	-102
3	-152	-128	-139	-134	-125	-123	-107	-97	-112	-106	-95
$\bar{X}$	-150	-148	-145	-139	-131	-125	-127	-111	-81	-101	-97
SD	3.11	15.55	6.35	7.33	7.33	3.87	16.74	6.35	3.74	5.00	3.56

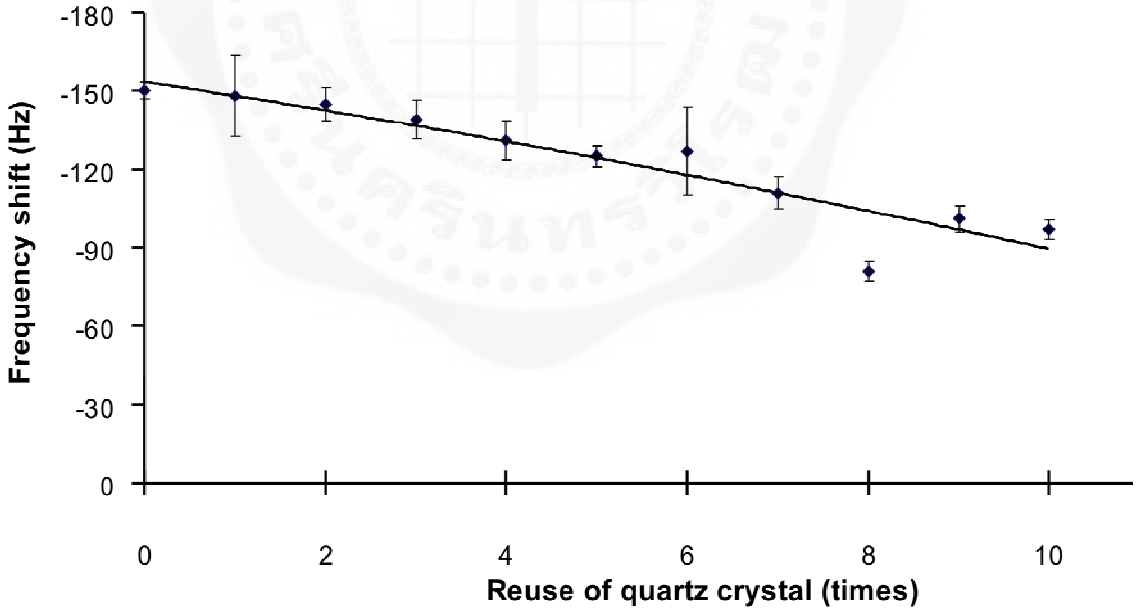

Figure 26 The relationship of reused quartz crystals between cycles of reusing and frequency shift.

The detection of the piezoelectric biosensor compared PCR method

Preliminary experiment was conducted with non-amplified genomic DNA previously treated with the restriction enzyme (*Bst*DSI). The genomics DNA digestion were mixed with blockings oligonucleotide capped avidin/gold nanoparticle conjugation for signal amplification. By the interaction between the thermally separated DNA strands and these oliglonucleotides, re-association on surface of quartz crystal between dsDNA could be prevented.

The PCR was accomplished with FMTB/RMTB primer pair and annealing temperature at 53 °C. Each PCR amplicon was detected with the IS*6110* sequence on 2% agarose gel electrophoresis. The results were shown in figure 27. It was found that all of PCR amplicon from 150 specimens of *M. tuberculosis* presented the specific band around 209 bp which the sequence of IS*6110*. Whereas, all of 50 non-*M. tuberculosis* samples were not presented DNA band in gel electrophoresis as shown in figure 28 .

*Bst*DSI-digested genomic DNA from 150 specimens of *M. tuberculosis* and 50 specimen of *M. avium* complex and other microorganism were tested by using piezoelectric biosensor in comparison to the result of PCR technique as shown in table 18.

One hundred fifty specimens of *M. tuberculosis* were decreased in frequency shift (Hz) after the hybridization reaction with thiol-modified oligonucleotide probe. The interaction with 50 non-*M. tuberculosis* samples did not result in a significant measurable frequency and also did not observe the band of PCR amplicon. Both of those results were well correlated. It can be concluded that specific IS*6110* sensor with IS*6110* probe had high specificity for detection.

The PCR targeting 209 bp of IS*6110* was analyzed by using gel electrophoresis to confirm the successful amplification of PCR products. The data revealed that the results obtained from piezoelectric biosensor were corresponded to those of PCR techniques.

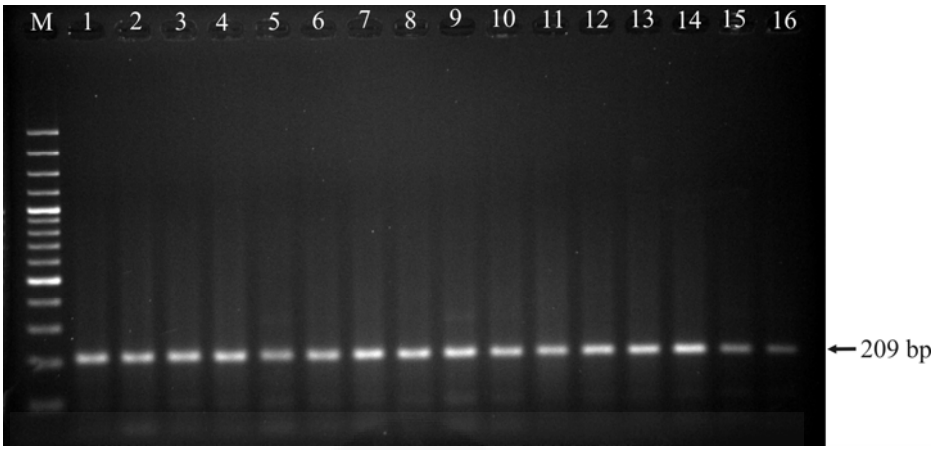

Figure 27 Example analysis of PCR positive samples amplicon by 2% agarose gel electrophoresis. DNA sample was run in agarose gel electrophoresis with 100 volts for 30 minutes. Lane M =100 base pair DNA ladder, lane 1 to lane 16 were M. tuberculosis samples presented the specific band around 209 bp from 150 samples which the sequence of IS*6110*.

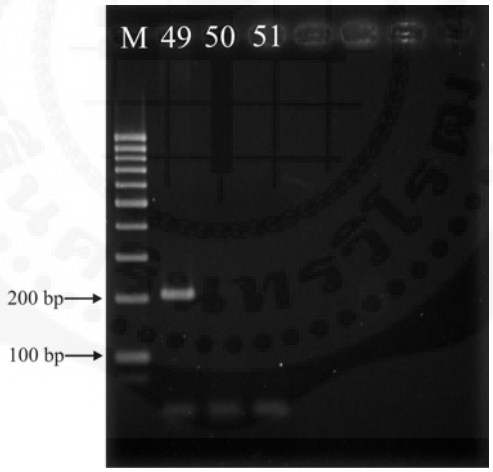

Figure 28 Example analysis of PCR negative samples amplicon by 2% agarose gel electrophoresis.DNA sample was run in agarose gel electrophoresis with 100 volts for 30 minutes. Lane M =100 base pair DNA ladder, lane 1 was M. tuberculosis (H37RVKK11-20) samples presented the specific band around 209 bp which the sequence of IS*6110*. Lane 2 and land 3 was showed the negative samples (*M. avium* complex *and P. aeruginosa*, respectively).

Table 18 Samples identified with DNA-piezoelectric based biosensor, tested with specific sensors carrying the IS*6110* probes compared with the PCR method.

Methods	Number of clinical specimens		
	Positive	**Negative**	**Total**
PCR technique	150	50	200
Piezoelectric biosensor technique	150	50	200

CHAPTER 5
DISCUSSION

Real time (liquid phase) setup measurement for affinity studies consisted of the piezoelectric biosensor, driving electronics and a flow-through system. The quartz crystal was sandwiched between two soft rubber o-rings because reasonable force should be applied to prevent damage of thin and fragile quartz crystals.

The piezoelectric quartz crystals with gold electrodes and the basic resonant frequency of 12 MHz are the most common used as electrode because it is easy to handle during immobilization. Higher frequency quartz is more fragile than lower frequency quartz because it is too thin to handle which higher frequencies are not routinely used.

The modified quartz crystals were fixed in a flow-through cell between two soft rubber o-rings which only one side of the crystal was in contact with the flowing solution. The electrodes of the crystal were connected to a gate oscillating circuit based on the integrated TTL oscillator driver 74LS320. Consequently, oscillating circuit driving the quartz crystal should provide enough energy to the crystal for smooth oscillation in the presence of liquid [138]. The integrated form of this oscillator will provide much higher energy to the quartz crystal resulting in improved performance under variable conditions. Better stability was obtained by using carefully designed lever oscillators consisting of individual transistors. Oscillator circuit was chosen from several conditions in laboratory by focusing on high frequency stability and IC supplier in Thailand.

The output frequency was measured by AVR microcontroller to computer. A home made software Labview (for Windows) interface was used for data storage. The delay interval between two data points was 10 seconds, whereas achieved resolution of the frequency from the counter was 1 Hz.

Piezoelectric quartz crystal in real time biosensor has the advantage of being an inexpensive sensor with digital output that can be operated online and in real time, as well cheap, easy to use, and rapid for detection. This biosensor can be avoiding sensitivity to errors due to hydration, humidity, time consuming, solvent retention, and expect to routinely analytical procedure.

Therefore, this study was focused on development of the DNA-piezoelectric biosensor for direct detection of artificial DNA target of IS*6110 M. tuberculosis* in real time thus quartz crystals have been used to construct the piezoelectric biosensor in-house.

The efficiency of flow rate as 30 µL/min was chosen for using in all experiments of this study because it was slow enough to allow DNA target in suspension to bind to the surface before being swept away, yet fast enough to prevent accumulation of particulates. Moreover, the liquid inlet through the flow cell was prevented bubbles formation during piezoelectric biosensor experiments. In real time system may be effect oscillation signal error from accumulation of samples hybridization which can be prevent by washing non-specific with HEPES buffer.

The thiol-modified oligonucleotide probe, thiol-modified oligonucleotide probe/MCH, and biotin-modified oligonucleotide probe were immobilized on the quartz crystal for 20 minutes. After that, the frequency shifts were recorded as shown in figure 14. The frequency shifts related to the increasing of all the probe concentration of which thiol and biotin-modified oligonucleotide probe stabled at concentration 1.00, 1.50, and 2.00 µM but thiol-modified oligonucleotide probe/ MCH stabled at concentration 1.50, and 2.00 µM. The biotin-modified oligonucleotide probe at concentration 1.00 µM gave the highest frequency shift which higher thiol-modified oligonucleotide probe, respectively. The thiol-modified oligonucleotide probe/MCH at concentration 1.50 µM gave the highest frequency shift. Therefore, the optimum concentration of biotin-modified oligonucleotide probe and thiol-modified oligonucleotide probe was 1.00 µM but thiol-modified oligonucleotide probe/MCH was 1.50 µM which was used in all experiments in this study.

Therefore, the concentration of thiol-modified oligonucleotide probe at 1.50 µM was chosen for using in all experiments of this study. The probe at this concentration gave the highest frequency change of 1.50 µM synthetic DNA target hybridization. This result was different with to previous studies [121] which used the thiol-modified oligonucleotide probe at concentration of 1.00 µM in piezoelectric biosensor. This concentration showed the minimal amount of probe to use in this system. This can lead to a lower cost of piezoelectric biosensor preparation.

The relationship study between DNA probe (1.00 µM biotin-modified and 1.50 µM thiol-modified) and synthetic DNA target hybridization at various concentrations was shown in figure 15. The resonant frequency shifts proportionally related to the increasing of synthetic DNA target concentration. The decreasing of resonant frequency was almost linear with the increase of synthetic DNA target concentration up to concentration of 0.25

μM. The optimum concentration of DNA probe could hybridize with the synthetic DNA target at lowest concentration 0.25 μM. The frequency changes proportionally related to the increasing of synthetic DNA target concentration. The decreasing of resonant frequency was almost linear with the increase of synthetic DNA target concentration up to concentration of 1.50 μM. At concentrations more than 1.50 μM, the frequency changes were stable. This indicated that the saturation concentration of synthetic DNA target hybridization was 1.50 μM. This result was different from that reported by Wu and colleagues [121] which the saturation of synthetic target DNA hybridization of others studies were 1.00 μM. Therefore, this system could detect the minimal synthetic target at 0.25 μM. This could lead to a decrease amount of target used by this biosensor.

The result of shelf-life study of thiol-modified oligonucleotide probe/MCH after storage at 4°C by closing the cap of quartz crystal was shown in figure 16. The frequency shift of 1.50 μM synthetic DNA target hybridization after storage at various times ranging from 0-120 days was similar. The frequency shift of 1.50 μM synthetic DNA target hybridization after storage at 120 and 150 days was significant but The frequency shift of 1.00 μM biotin-modified oligonucleotide probe was hybridized with 1.50 μM synthetic DNA target after storage at various times ranging from 0-10 days is similar. Therefore, The thiol-modified oligonucleotide probe/MCH probe at concentration 1.50 μM gave the most stable frequency shift after hybridization with 1.50 μM of synthetic DNA target. Consequently, this thiol-modified oligonucleotide probe/MCH at concentration 1.50 μM could be stored at 4°C for 120 days. The optimum concentration of thiol-modified oligonucleotide probe was 1.50 μM which was used in all experiments in this study because thiol-modified oligonucleotide probe/MCH was higher stability. The shelf-life of probe on DNA piezoelectric biosensor of Caruso and coworks [79] and Tombelli and colleagues [80] reported the storage time at 4°C for several weeks without losing the activity.

Normally, the thermal denaturation was used for denaturation of PCR amplified target DNA. However in non-amplified genomic DNA, the blocking oligonucleotides were added in this denaturation step. This blocking could prevent the reannealing of ssDNA to increase the efficiency of DNA target hybridization. Moreover, the blocking oligonucleotides were used for development of DNA target sequence hybridization. The result of this improvement study was shown in figure 17. The frequency shifts related to the increasing of DNA target concentration which stabled since concentration dilution at 10, 20, and 30 μg/mL. The DNA target sequence at concentration 10 μg/mL gave the highest frequency change. Therefore, the optimum concentration of DNA target sequence dilution was 10

μg/mL capture signal enhancement (avidin, gold nanoparticle, avidin/gold nanoparticle) in this study.

However in non-amplified genomic DNA, the blocking oligonucleotides were added in this denaturation step. This blocking can prevent the reannealing of single-stranded DNA to increase the efficiency of DNA target hybridization. Therefore, the blocking oligonucleotides were used for improvement of DNA target hybridization. The thermal plus blocking oligonucleotides gave the frequency change (indecreasing the resonant frequency) higher than only thermal denaturation. This result showed the similarity with previous studies [129,130] which the thermal plus blocking oligonucleotides gave the frequency changes higher than the frequency change of thermal denaturation only.

These thermal plus blocking oligonucleotides method could be improved the sensitivity by using mass enhancement (avidin, avidin/gold nanoparticle, and gold nanoparticle) was capped with blocking oligonucleotides. The frequency shift of blocking 2 oligonucleotides capture 25% (v/v) avidin/gold nanoparticle was higher than the frequency shift of blocking 1 oligonucleotides capture with 25% (v/v) gold nanoparticle and blocking 2 oligonucleotides capture with 0.075 mg/mL avidin, respectively. This study used 20 nm diameter of gold nanoparticle as optimal for the surface immobilization of piezoelectric biosensor and the consequent sensitivity improvement because the hybridization was highest maximum value when the average diameter of nanoparticles was 20 nm and then decreased with the increasing of particle size [139]. Therefore, the frequency shift of the sensor was decreased accompanied by an increase of nanoparticle size applied in the static solution [140,139]. The particle with an average diameter of 20 nm afforded the best hybridization rate, probably as previous report [139]. In addition, gold nanoparticle modified blocking oligonuclotide deposited onto the piezoelectric sensor were depended on the DNA hybridization efficiency between the specific probe and target sequences [141,142]. The gold nanoparticles could be attributed to the steric hindrance effect which the larger nanoparticles could not move as independently as the smaller nanoparticles and the larger nanoparticles connected to the DNA target hinder the approach of further nanoparticles [140]. In this study, the real time piezoelectric biosensor could be detected *M. tuberculosis* by using thermal denaturation only to detect limit of 1.5×10^5 CFU/mL and thermal denaturation capture avidin/gold nanoparticle to detect limit of 1.5×10^3 CFU/mL. Moreover, piezoelectric biosensor could be developed a sensitivity of detection DNA based on gold nanoparticles amplification which detected *E. coli* O157:H7 cells to limit of 2.0×10^3 CFU/mL [143], 1.3×10^3 CFU/mL [24], and 2.67×10^2 CFU/mL [118]. Chen and colleagues [144] detected Dengue virus to

limit of 2 PFU/mL by gold nanoparticle signal amplified. Gill and co-works [145] detected *M. tuberculosis* by using gold nanoparticle probes for colorimetric detection to limit of 10 CFU/ml. Uludag and colleagues [146] studied the hybridisation with neutrAvidin capture for signal enhancement for the detection of HSV viral nucleic acids at 5.2 x 10^{-11} M concentration. In addition, they have some biosensor for the detection of *M. tuberculosis* such as electrochemical biosensor was detected short sequence synthetic target [58], optical biosensing was development for detection of multidrug resistant tuberculosis. To complete the biosensor system, the individual elements of the biosensor was optimized to its maximum sensitivity for the electrochemiluminescent optical signal, which is produced during the DNA hybridization event [147].

The interaction between 3' end of thiol-modified oligonucleoyide (Blocking oligonucleotide) capture avidin, gold nanoparticle, or avidin/gold nanoparticle on surface was strongly affected by the particle size. The highly accuracy was counted particle size with TEM image in this study. Moreover, the particle size could be counted by scan electron microscope image (SEM) [144,148-150], TEM image [140], UV spectroscopy [149], Atomic force microscope (AFM) [137] or gel electrophoresis [151].

The detection of genomic DNA target by using a quartz crystal piezoelectric normally has less probability to hybridize with DNA probe due to the steric hindrance effect of DNA secondary structure and lower amount of specific DNA sequence than the detection limit of general analytical technique. The alternative solution to solve this problem was restricted enzymatic digestion of the DNA samples without any previous amplification step to separate small DNA fragments [21,129]. However, sensitivity of genomic detection may be break cell of reagent. In this study was used DNazol® reagent which can be break cell up to 70 – 100%.

The steric effect on oligonucleotide immobilization onto a solid surface and DNA target hybridization in a real time DNA piezoelectric biosensor was improved in this study. It could be increased in the hybridization efficiency by added of 6 dT to the 5' end of the probes. This confirmed the studies that reported the poly dT at 5' end of probes might reduce steric hindrance in three-dimensional space also the addition of the spacer during DNA hybridization caused the increase of molecule collision [152,153]. It is also proposed that during DNA target sequence hybridization, spacers have been shown to reduce steric interference, making the probe end closet to the surface of the device more accessible [153].

The specificity was tested by using *Mycobacterium tuberculosis* (H37RVKK11-20), *Mycobacterium avium* complex, *Escherichia coli*, *Pseudomonas aeruginosa*, *Staphylococcus*

aureus and *Enterococcus faecalis*. The hybridization buffer was the negative control (NC) as shown in figure 23. The amount of non-amplification (DNA target) could effect the determination of specific IS*6110* sensor. The dilutions of digested genomic DNA could be performed to reach the appropriate concentration within the limit of this sensor. The binding of target DNA sequences was inhibited when an excess amount of target DNA sequence complementary to the DNA probe. This is due to the formation of double-stranded in the solution by the two single strands of the DNA target at high concentration. Hence, blocking oligonucleotides capture with avidin/gold nanoparticle were used for protection of the DNA fragments form self-assembly. Also, avidin/gold nanoparticle as mass enhancement was signal amplification. Therefore, the thermal denaturation plus blocking oligonucleotides for preparation of target DNA could differentiate *M. tuberculosis* from *M. avium* complex and other microorganism. This result showed that the frequency change of *M. tuberculosis* was lower than the frequency change of *M. avium* complex and other microorganism. This result was similar to the report of previous study [7,8,11] which used IS*6110* target for detection of *M. tuberculosis* by PCR technique. The specific IS*6110* target was used to differentiate *M. tuberculosis* from non-*M. tuberculosis*. However, this objective was only to present the capability of sensor in term of analytical specificity for *Mycobacterium tuberculosis* (H37RVKK11-20) against with *M. avium* complex, *E. coli*, *P. aeruginosa*, *S. aureus* and *E. faecalis* which some bacteria not required respiratory infection. This specificity of real time DNA-based biosensor was reported testing by using other organism which is not closely related to *M. tuberculosis* only but may not report about specificity to bacteria in respiratory infection.

The accuracy of a measurement system was the degree of closeness of measurements of a quantity to its actual (true) value. The precision of a measurement system, also called reproducibility or repeatability, was the degree to which repeated measurements under unchanged conditions showed the same results. This result showed that the precision of frequency shift error bar of piezoelectric biosensor device gave similar to oscilloscope of which piezoelectric biosensor in this study was high precision as shown in figure 25.

The reusability of the crystal use was a crucial part to develop the sensor. This biosensor system was evaluated its reusability by washing the used biosensor with 1 mM HCl solution for 1 minute to remove the attached target DNA. The regenerated surface was then applied new DNA sample solution to test the hybridization ability of probe on the sensor surface. It was found that the washed sensor maintained its ability to hybridize with

new DNA sample for at least 10 times without significant functional surface deterioration as shown in figure 26.

The direct detection of 150 *M. tuberculosis* samples was decreased in frequency value (Hz) after the hybridization reaction with DNA probe. The interaction with 50 non-*M. tuberculosis* samples did not result in a significant measurable frequency and also did not observe the band of PCR amplicon which the clinical sputum 150 samples as positive infection of *M. tuberculosis* and 50 samples as negative of non-*M. tuberculosis* and other microorganism were corrected from Department of Pathology, Faculty of Medicine, Srinakharinwirot University and Bureau of Tuberculosis, Ministry of Public Health Thailand.

The data revealed that the results obtained from piezoelectric biosensor were corresponded to those of PCR techniques. It could be concluded that specific IS*6110* gene sensor with DNA probe had high specificity for detection. For the detection in clinical samples, the proposed method presented 100% result agreement with PCR regarding both to positive and negative samples. However, it had been reported that IS*6110* and its homologue could be detected by nested-PCR in some mycobacteriae other than *M. tuberculosis* [154]. It meant that the specificity of these detection methods based on IS*6110* was not only on account of IS*6110* itself but also the possession of IS*6110* among bacteria strains. Therefore, this developed method had possibility to get false-positive results in clinical specimens containing non-*M. tuberculosis*.

Only some strains of *M. tuberculosis* possessed low copy numbers of IS*6110* as previous report [155]. However, most of *M. tuberculosis* contained 2-5 copies. This method should be appropriate for detection of those possible low copy numbers of IS*6110* strains.

Practically, the digested DNA from sputum sample was diluted for 1:100 before apply to the sensor. The 1:20 dilution of sample should be appropriate for detection of those possible low copy numbers of IS*6110* strains. Also the samples 1:100 dilutions can be reduced viscosity of real time system because of the usually higher viscosity of the sample which will be signal record error from DNA target adhesion to quartz crystal surface.

The normal clinical sample for diagnosis of tuberculosis was lymphnode aspirates, cerebrospinal fluid, ascitic fluid, pleural fluid, sputum, and others. The sputum specimen has the highest possibility to get heavy contamination with other organisms. The result showed that satisfied performance of this biosensor system still remained in case of sputum samples.

This real time piezoelectric DNA-based biosensor required 4 hours for preparation the DNA probe immobilized and DNA target hybridized on the quartz crystal. In other report,

Wu and colleagues [121] studied the circulating-flow system of piezoelectric biosensor for real-time detection of *E. coli* O157:H7 by using 1 day for preparation. The advantage of this biosensor for detection of *M. tuberculosis* was non-labeling, easy to use, and direct detection of non-amplified genomic DNA which reduces the PCR step. PCR technique required the well-trained personnel to handle the process and this amplification process required such an additional processing time, reagents and device which effected to the cost of assay.

Finally, this study was new finding direct detection without PCR which could be beneficial for further routinely clinical development as portable device for sensitivity, specificity, cheap, easy to use, and rapid for detection of *M. tuberculosis*.

REFERENCES

REFERENCES

1. Lee RB, Li W, Chatterjee D, Lee RE. Rapid structural characterization of the arabinogalactan and lipoarabinomannan in live mycobacterial cells using 2D and 3D HR-MAS NMR: structural changes in the arabinan due to ethambutol treatment and gene mutation are observed. Glycobiology 2005;15(2):139 -51.
2. WHO. Global tuberculosis control: epidemiology, strategy, financing, WHO report 2009. Retrieved September 3, 2009, from URL: http://www.who.int/tb/ publications/global_report/2009/en/html.
3. Bureau of tuberculosis, Strategic for Management of Tuberculosis and development of management organizations. Document conference proceeding, Aug 3-4,2009; Prince palace hotel, Bangkok, Thailand, Retrieved September 3, 2009, from URL: http://www.tbthailand.org.
4. De C Ramos M, Soini H, Roscanni GC, Jaques M, Villares MC, Musser JM. Extensive Cross-Contamination of Specimens with *Mycobacterium tuberculosis* in a reference laboratory, J Clin Microbiol 1999;37:916-9.
5. Haldar S, Chakravorty S, Bhalla M, De Majumdar S, Tyagi JS. Simplified detection of Mycobacterium tuberculosis in sputum using smear microscopy and PCR with molecular beacons. J Med Microbiol 2007;56:1356-62.
6. Ozkutuk A, Terek G, Coban H, Esen N. Is it valuable to examine more than one sputum smear per patient for the diagnosis of pulmonary tuberculosis?. Jpn J Infect Dis 2007;60:73-5.
7. Shah DH, Rishendra V, Bakshi CS, Singh RK. A multiplex-PCR for the differentiation of *Mycobacterium bovis* and *Mycobacterium tuberculosis*. FEMS Microbiol Lett 2002;214:39-43.
8. Singh KK, Muralidhar M, Kumar A, Chattopadhyaya TK, Kapila K, Singh MK, et al. Comparison of in house polymerase chain reaction with conventional techniques for the detection of Mycobacterial tuberculosis DNA in granulomatous lymphadenopathy. J Clin Pathol 2000;53:355-61.
9. Delacourt C, Poveda JD, Churean C, et al. Use of polymerase chain reaction for improved diagnosis of tuberculosis in children. J Pediatr 1995;126:703-9.
10. Fité E, Fernández-Figueras MT, Prats R, Vaquero M, Morera J. High prevalence of *Mycobacterium tuberculosis* DNA in biopsies from sarcoidosis patients from catalonia, Spain. Respiration 2006;73:20-6.

11. Sekar B, Selvaraj L, Alexis A, Ravi S, Arunagiri K, Rathinavel L. The utility of IS*6110* sequence based polymerase chain reaction in comparison to conventional methods in the diagnosis of extra-pulmonary tuberculosis. Indian J Med Microbiol 2008;26:352-5.

12. Kai E, Sawanta S, Ikebukuro K, Honda T, Karube I. Detection of PCR products in solution using surface plasmon resonance. Anal Chem 1999;71:796-800.

13. Mahaisavariya P, Chaiprasert A, Khemngern S, Manonukul J, Tingtoy N. Detection and identification of *Mycobacterium* species by polymerase chain reaction (PCR) from paraffin-embedded tissue compare to AFB staining in pathological sections. J Med Assoc Thai 2005;8:108-13.

14. Pfaller MA. Application of new technology to the detection, identification, and antimicrobial susceptibility testing of mycobacteria. Am J Clin Pathol 1994; 101:329-37.

15. Paramasivan CN, Kamala T, Herbert D. Appraisal of techniques for identification and characterization of non-tuberculosis mycobacteria. Ind J Tub 1996; 43:67-74.

16. Spangler BD, Tyler BJ. Capture agents for a quartz crystal microbalance-continuous flow biosensor: functionalized self-assembled monolayers on gold. Anal Chim Acta 1999;399:51-62 .

17. Lee YG, Chang KS. Application of a flow type quartz crystal microbalance immunosensor for real time determination of cattle bovine ephemeral fever virus in liquid. Talanta 2005;65:1335-42.

18. Konash PL, Bastiaans GJ. Piezoelectric crystals as detectors in liquid chromatography. Anal Chem 1980;52:1929-31

19. Kanazawa KK, Gordon JG. Frequency of a quartz microbalance in contact with liquid, Anal Chem 1985;57:1770-1

20. Kanasawa KK, Gordon JG. A liquid phase piezoelectric detector. Anal Chem 1985; 57:1771-5.

21. Chunyan Y, Tangyou Z, Jin T, Rong W, Qinghai C, Ming C, et al. Hybridization assay of hepatitis B virus by QCM peptide nucleic acid biosensor. Biosens Bioelectron 2008;23:879-85.

22. Tombelli S, Mascini M, Sacco C, Turner A. A DNA piezoelectric biosensor assay coupled with a polymerase chain reaction for bacterial toxicity determination in environmental samples. Anal Chim Acta 2000;418:1-9.

23. Junhui Z, Hong C, Ruifu Y. DNA based biosensors. Biotechnol Adv 1997;15:43-58.

24. Xia H, Wang F, Huang Q, Huang J, Chen M, Wang J. Detection of *Staphylococcus epidermidis* by a quartz crystal microbalance nucleic acid biosensor array using Au nanoparticle signal amplification. Sensors 2008;8:6453-70.
25. Mo XT, Zhou YP, Lei H, Deng L. Microbalance-DNA probe method for the detection of specific bacteria in water. Enz Microbial Techno 2002;30:583-9.
26. He F, Liu S. Detection of *P. aeruginosa* using nano-structured electrode separated piezoelectric DNA biosensor. Talanta 2004;62:271-7.
27. Grange JM. Mycobacteria and human disease. Maryland, USA. Edward Arnold Publisher 1998:119-37.
28. WHO. Global Tuberculosis Control: surveillance, planning, financing. WHO report 2005. Geneva: World Health Organization 2005.
29. Raviglione MC, Narain JP, Kochi A. HIV-associated tuberculosis in developing countries: clinical features, diagnosis, and treatment. Bulletin of World Health Organisation 1992;70:515-26.
30. Msamanga GI, Fawzi WW. The double burden of HIV infection and tuberculosis in sub-Saharan Africa. New Eng J Med 1997;337:849-51.
31. Wandwalo E. The role of direct observation of tuberculosis treatment and collaborative TB and HIV/AIDS interventions. Centre for International Health. University of Bergen. Bergen-Norway 2005:1-64.
32. Dye, C., S. Scheele, P. Dolin, V. Pathania, and M. C. Raviglione. Consensus statement. Global burden of tuberculosis: estimated incidence, prevalence, and mortality by country. WHO Global Surveillance and Monitoring Project. JAMA 1999;282:677-86.
33. Murray CJ, Lopez AD. Mortality by cause for eight regions of the world: Global Burden of Disease Study. Lancet 1997;349:1269-76.
34. Murray CJ, Salomon J A. Modeling the impact of global tuberculosis control strategies. Proc Natl Acad Sci USA 1998;95:13881-6.
35. Camus JC, Pryor MJ, Medigue C, Cole ST. Re-annotation of the genome sequence of *Mycobacterium tuberculosis* H37Rv. Microbiol 2002;148:2967-73.
36. Basso LA, da Silva LH, Fett-Neto AG, de Azevedo WF Jr, Moreira Ide S, Palma MS, et al. The use of biodiversity as source of new chemical entities against defined molecular targets for treatment of malaria, tuberculosis, and T-cell mediated diseases--a review. Mem Inst Oswaldo Cruz 2005;100:475-506.

37. Brennan PJ. Structure, function, and biogenesis of the cell wall of *Mycobacterium tuberculosis.* Tuberculosis 2003.83:91-7.
38. Larsen MH, Biermann K, Jacobs WR. Laboratory Maintenance of Mycobacterium tuberculosis. Curr Protoc Microbiol 2007 Chapter 10:Unit 10A.1.
39. Image tuberculosis. Retrieved September 3, 2009, from URL:http://feww.files.wordpress-.com/2008/10/tb.jpg.
40. John C. Microbiology: an introduction to infectious disease. New York; Elsevier 1984:401-16.
41. Wells WF. On air-borne infection: study II, droplets and droplet nuclei. Am J Hygiene 1934;20:611-8.
42. Louden RG, Roberts RM. Droplet expulsion from the respiratory tract. Am Rev Dis 1966;95:435-42.
43. Riley RL, Mills CC, Nyka W, et al. Aerial dissemination of pulmonary tuberculosis: a two-year study of contagion in a tuberculosis ward. Am J Hygiene 1959; 70:185-96.
44. Comstock GW, Livesay VT, Woolpert SF. The prognosis of a positive tuberculin reaction in childhood and adolescence. Am J Epidemiol 1974;99:131-8.
45. Sutherland I. Recent studies in the epidemiology of tuberculosis, base on the risk of being infected with tubercle bacilli. Adv Tuberc Res 1976;19:1- 63.
46. Schluger NW, Rom WN. The host immune response to tuberculosis. Am J Respir Crit Care Med 1998;157:679-91
47. Palwatwichai A. Tuberculosis in Thailand. Respirology 2001;1:65-70.
48. Dowdy DW, Lourenço MC, Cavalcante SC, Saraceni V, King B, Golub JE. Impact and cost-effectiveness of culture for diagnosis of tuberculosis in HIV-infected Brazilian adults. PLoS One 2008;3:e4057.
49. Silver H, Sonnenwirth AC, Alex N. Modifications in the fluorescence microscopy technique as applied to identification of acid-fast bacilli in tissue and bacteriological material. J Clin Pathol 1966;19:583-8.
50. Mascellino MT, Rossi F, Iegri F, Iona E. Rapid detection of mycobacteria by combining a radiometric detection system with DNA probes. New Microbiol 1994;17:249-53.
51. Telenti M, de Quirós JF, Alvarez M, Santos Rionda MJ, Mendoza MC. The diagnostic usefulness of a DNA probe for Mycobacterium tuberculosis complex (Gen-

Probe) in Bactec cultures versus other diagnostic methods. Infection 1994;22:18-23.

52. Salfinger M, Morris AJ. The role of the microbiology laboratory in diagnosing mycobacterial diseases. Am J Clin Pathol 1994;101(4 Suppl 1):S6-13.
53. Shi RR, Zhang JY, Yuan XQ, Sun ZG, Li CY. Detection of streptomycin resistance in Mycobacterium tuberculosis clinical isolates by denaturing high-performance liquid chromatography and DNA sequencing. Zhonghua Yi Xue Za Zhi 2008; 88:1376-9.
54. Van Embden JD, Cave MD, Crawford JT, Dale JW, Eisenach KD, Gicquel B, et al. Strain identification of Mycobacterium tuberculosis by DNA fingerprinting: recommendations for a standardized methodology. J Clin Microbiol 1993; 31:406-9.
55. Sjobring U, Mecklenberg M, Andersen AB, Miorner H. Polymerase chain reaction for detection of Mycobacterium tuberculosis. J Clin Microbiol 1990;28:2200-4.
56. Cave MD, Eisenach KD, Templeton G, Salfinger M, Mazurek G, Bates JH, et al. Stability of DNA fingerprint pattern produced with IS6110 in strains of Mycobacterium tuberculosis. J Clin Microbiol 1994;32:262-6.
57. Neuman MR, Perlaky SC, Michalski JP. Detection of TB in liquid and vapor phases by an antibody-based piezoelectric biosensor. IEEE-EMBC and CMBEC. Theme 7: Instrumentation 1995:1563-4.
58. Wang J, Rivas G, Cai X, Dontha N, Shiraishi H, Luo D, et al. Sequence-specific electrochemical biosensing of *M. tuberculosis* DNA. Anal Chim Acta 1997; 337:41-8.
59. Ross BC, Raios K, Jackson K, Dwyer B. Molecular cloning of a highly repeated DNA element from *Mycobacterium tuberculosis* and its use as an epidemiological tool. J Clin Microbiol 1992;30:942-6.
60. Charlesworth B, Sniegowski P, Stephan W. The evolutionary dynamics of repetitive DNA in eukaryotes. Nature 1994;371:215-20.
61. Blot M. Transposable elements and adaptation of host bacteria. Genetica 1994;93:5-12.
62. Thierry D, Cave MD, Eisenach KD, Crawford JT, Bates JH, Gicquel B, Guesdon J L. IS6110, an IS-like element of Mycobacterium tuberculosis complex. Nucleic Acids Res 1990;18:188.
63. Kurepina NE, Sreevatsan S, Plikaytis BB, Bifani PJ, Connell ND, Donnelly R J, et al. Characterization of the phylogenetic distribution and chromosomal insertion

sites of five IS6110 elements in Mycobacterium tuberculosis: non-random integration in the dnaA-dnaN region. Tuberc Lung Dis 1998;79:31-42.

64. McHugh TD, Gillespie SH. Nonrandom association of IS*6110* and *Mycobacterium tuberculosis*: implications for molecular epidemiological studies. J Clin Microbiol 1998;36:1410-3.
65. Kurabachew M, Enger O, Sandaa RA, Skuce R, Bjorvantn B. A multiplex polymerase chain reaction assay for genus-, group- and species-specific detection of mycobacteria. Diagnos Microbiol Infect Dis 2004;49:99-104.
66. Oggioni MR, Fattorini L, Li B, De Milito A, Zazzi M, Pozzi G, et al. Identification of *Mycobacterium tuberculosis* complex, *Mycobacterium avium* and *Mycobacterium intracellulare* by selective nested polymerase chain reaction. Molecular Cellular Prob 1995;9:321-6.
67. Mchugh TD, Newport LE, Gillespie SH. IS*6110* Homologs are present in multiple copies in mycobacteria other than tuberculosis-causing mycobacteria. J Clinic Microbiol 1997;35:1769-71.
68. Collingsy AF, Carusozx F. Biosensors: recent advances. Rep Prog Phys 1997;60:1397-445.
69. Newman JD, Tigwell LJ, Warner PJ, Turner APF. Biosensors: boldly going into the new millennium. Sensor Review 2001;21:268-71.
70. Byfield MP, Abuknesha RA. Biochemical aspects of biosensors. Biosens Bioelectron 1994;373-400.
71. Masaaki K, Takashi K, Masato S, Sakiko K, Miyuki O, Shinichiro I, et al. Electrochemical DNA quantification based on aggregation induced by Hoechst 33258. Electrochem Commun 2004;6:337-43.
72. Tombelli S, Minunni M, Santucci A, Spiriti MM, Mascini M. A DNA-based piezo- electric biosensor: strategies for coupling nucleic acid to piezoelectric devices. Talanta 2006;68:806-12
73. Carter RM, Mekalanos JJ, Jacobs MB, Lubrano GJ, Guilbault GG. Quartz crystal microbalance detection of *Vibrio cholerae O*139 serotype. J Immunol Methods 1995;187;121-5.
74. Structure of DNA. Retrieved September 3, 2009, from URL: http://www.mindfiesta.com-/images/article/DNA_clip_image001.gif
75. Watson JD, Crick FHC. Genetical implications of the structure of deoxyribonucleic acid. Nature 1953;171:964-7.

76. Rodahl M, Hook C, Frederiksson C, Keller CA, Krozer A, Brzezinski P, et al . Simultaneous frequency and dissipation factor QCM measurements of biomolecular adsorption and cell adhesion. Faraday Discuss 1997;107:229-47.
77. Glynou K, Ioannou PC, Christopoulos TK, Syriopoulou V. Oligonucleotide functionalized gold nanoparticles as probes in a dry-reagent strip biosensor for DNA analysis by hybridization. Anal Chem 2003;75:4155-60.
78. Jun L, Weihong T, Kemin W, Dan X, Xiaohai Y, Xiaoxiao H, et al. Ultrasensitive optical DNA biosensor based on surface immobilization of Molecular Beacon by a bridge structure. Analyt Scienc 2001;17:1149-53.
79. Caruso F, Rodda E, Furlong DN. Quartz crystal microbalance study of DNA immobilization and hybridization for nucleic acid sensor development. Anal Chem 1997,69:2043-9.
80. Tombelli S, Mascini M, Turner APF. Improved procedures for immobilization of oligonucleotides on gold coated piezoelectric quartz crystals. Biosens Bioelectron 2002;17:929-36.
81. In'acio P, Marat-Mendes JN, Dias CJ. Development of a biosensor based on a piezoelectric film. Taylor & Francis 2003;293:351-6.
82. Joshua K. QCM based DNA biosensor. Chem 2006;243:1-7.
83. Curie J, Curie P. An oscillating quartz crystal mass detector. Rendu 1880;91:294-7.
84. Sharma A, Rogers KR. Biosensors. Meas Sci Technol 1994;5:461-72.
85. O'Sullivan CK, Guilbault GG. Commercial quartz crystal microbalances-theory and applications. Biosens Bioelectron 1999;14:663-70.
86. Sauerbrey G. The use of quartz oscillators for weighing thin layers and for microweighing. J Phys 1959;155:206-22.
87. Lin Z, Yip CM, Joseph IS, Ward MD. Operation of an ultrasensitive 30-MHz quartz crystal microbalance in liquids. Anal Chem 1993;65:1546-51.
88. Smith AL, Shirazi HM. Principles of quartz crystal microbalance/heat conduction calorimetry: Measurement of the sorption enthalpy of hydrogen in palladium. Thermochimica Acta 2005;432:202-11.
89. Bunde RL, Jarvi EJ, Rosentreter J. Piezoelectric quartz crystal biosensors. Talanta 1998;46:1223-36.
90. Janshoff A, Galla HJ, Steinem C. Piezoelectric mass-sensing devices as biosensors-An alternative to optical biosensors?. Angrew Chem Int Ed 2000;39:4004-32.

91. Zhou XC, Huang LQ, Li SFY. Microgravimetric DNA sensor based on quartz crystal microbalance: comparison of oligonucleotide immobilization methods and the application in genetic diagnosis. Biosens Bioelectron 2001;16:85-95.

92. Alder JF, McCallum JJ. Piezoelectric crystals for mass and chemical measure- ments, A review. Analyst 1983;108:1169-89.

93. McCallum JJ. Piezoelectric devices for mass and chemical measurements: an update, A review. Analyst 1989;114:1173-89.

94. Christopher Barnes, Development of quartz crystal oscillators for under-liquid sensing. Sens Actuat A: Physic 1991;29:59-69.

95. Talib ZA, Baba Z, Kurosawa S, Sidek HAA, Kassim A,Yunus WMM. Frequency behavior of a quartz crystal microbalance in contact with selected solutions. Am J App Sci 2006;3:853-8.

96. Suri CR. Quartz crystal based microgravimetric immunobiosensors. Sens Trans 2006;66:543-52.

97. Chou SF, Hsu WL, Hwang JM, Chen CY. Determination of alpha-fetoprotein in human serum by a quartz crystal microbalance-based immunosensor. Clin Chem 2002;48(6 Pt 1):913-8.

98. Bruckenstein S, Shay M. Dual quartz microbalance oscillator circuit. Anal Chem 1994;66:1847-55.

99. Kanazawa KK, Gordon JG. The oscillation frequency of a quartz resonator in contact with a liquid. Anal Chim Acta 1985;175:99-105.

100. Carter RM, Jacobs MB, Lubrano GJ, Guilbault GG. Piezoelectric detection of ricin and affinity-purified goat anti-ricin antibody. Anal Lett 1995;28:1379-86.

101. Minunni M, Skladal P, Mascini MA. Piezoelectric quartz-crystal biosensor as a direct affinity sensor. Anal Lett 1994;27:1475-87.

102. Muratsugu M, Ohta F, Miya Y, Hosokawa T, Kurosawa S, Kamo N, et al. Quartz crystal microbalance for the detection of microgram quantities of human serum albumin: relationship between the frequency change and the mass of protein adsorbed. Anal Chem 1993;65:2933-7.

103. Kurosawa S, Tawara E, Kamo N, Kobatake Y. Oscillating frequency of piezoelectric quartz crystal in solutions. Anal Chim Acta 1990;230:41-49.

104. Muratsugu M, Kurosawa S, Kamo N. Detection of antistreptolysin O antibody: application of an initial rate method of latex piezoelectric immunoassay. Anal Chem 1992;64:2483-2487.

105. Muramatsu H, Dicks JM, Tamiya E, Karube I. Piezoelectric crystal biosensor modified with protein A for determination of immunoglobulins. Anal Chem 1987;59:2760-3.

106. Barnes C, D'Silva C, Jones JP, Lewis TJ. Lectin coated piezoelectric crystal biosensors. Sensor Actuators B7 1992:347-350.

107. Hillier AC, Ward MD. Scanning electrochemical mass sensitivity mapping of the quartz crystal microbalance in liquid media 1992;64:2539-54.

108. Fawcett NC, Evans JA, Chen LC, Drozda KA, Flowers N. A quartz crystal detector for DNA. Anal Lett 1988;21:1099-110.

109. Muramatsu H, Tamiya E, Suzuki M, Karube I. Quartz-crystal gelation detector for the determination of fibrinogen concentration., Anal Chim Acta 1989;217: 321-6.

110. Fengjiao H, Wenhong Z, Qing G, Lihua N, Shouzhuo Y. Rapid detection of Escherichia coliform using a series electrode piezoelectric crystal sensor. Anal Lett 1994;27:655-69

111. Davis KA, Leary TR. Continuous liquid-phase piezoelectrtc biosensor for kinetic immunoassays Anal Chem 1989;61:1227-30.

112. Ghouchian HO, Kamo N, Latex piezoelectric immunoassay: effect of interfacial properties. Anal Chim Acta 1995;300:99-105.

113. Ghouchian HO, Kamo N, Hosokawa T, Akitaya T. Improvement of latex piezoelectric immunoassay: Detection of rheumatoid factor. Talanta 1994;41:401-6.

114. Nivens DE, Chambers JQ, Anderson T.F, Long-term DC, on-line monitoring of microbial biofilms using a quartz crystal microbalance. Anal Chem 1993;65:65-9.

115. Ebersole RC, Foss RP, Ward MD. Piezoelectric cell growth sensor. Biotechnol 1991;9:450-4.

116. Ebersole RC, J.A. Miller, J.R. Moran, and M.D. Ward, Spontaneously formed functionally active avidin monolayers on metal surfaces: a strategy for immobilizing biological reagents and design of piezoelectric biosensors, J. Am. Chem. Soc., 1990;112:3239-3241.

117. Matsuda T, Kishida A, Ebato H, Okahata Y. Novel instrumentation monitoring in situ platelet adhesivity with a quartz crystal microbalance. ASAIO J 1992: 38:M171–M173.

118. Mao X, Yang L, Su XL, Li Y. A nanoparticle amplification based quartz crystal microbalance DNA sensor for detection of Escherichia coli O157:H7. Biosens Bioelectron 2006;21:1178-85.

119. Eun AJ, Huang L, Chew FT, Fong-Yau Li S, Wong SM. Detection of two orchid viruses using quartz crystal microbalance-based DNA biosensors. Phytopathology 2002;92:654-8.

120. Wang L, Wei Q, Wu C, Hu Z, Ji J and Wang P. The *Escherichia coli* O157:H7 DNA detection on a gold nanoparticle-enhanced piezoelectric biosensor, Chinese Science Bulletin 2008;53:1175-84.

121. Wu VC, Chen SH, Lin CS, Real-time detection of Escherichia coli O157:H7 sequences using a circulating-flow system of quartz crystal microbalance. Biosens Bioelectron 2007;22:2967-75.

122. Collings AF, Caruso F. Biosensors: recent advances. Rep Prog Phys 1997;60:1397-445.

123. Thompson M, Arthur CL, Dhaliwal GK. Liquid-phase piezoelectric and acoustic transmission studies of interfacial immunochemistry. Anal Chem 1986;58: 1206-9.

124. Dong S, Li J. Self-assembled monolayers of thiols on gold electrodes for bioelectrochemistry and biosensors. Bioelectrochem Bioenerg 1997;42:7-13.

125. Tecilla P, Dixon RP, Slobodkin G, Alavi DS, Waldeck DH, Hamilton AD. Hydrogen-bonding self-assembly of multichromophore structures. J Am Chem Soc 1990; 112:9408-15.

126. Chaki NK, Vijayamohanan K. Self-assembled monolayers as a tunable platform for biosensor applications. Biosens Bioelectron 2002;17:1-12.

127. Li XM, Husken J, Reinhoudt DN. Reactive self-assembled monolayers on flat and nanoparticle surfaces, and their applications in soft and scanning probe lithographic nanofabrication technologies. J Mater Chem 2004;14:2954-71.

128. Mannelli I, Minunni M, Tombelli S, Mascini M. Quartz crystal microbalance (QCM) affinity biosensor for genetically modified organisms (GMOs) detection. Biosens Bioelectron 2003;18:129-40.

129. Minunni M, Mannelli I, Spiriti MM, Tombelli S, Mascini M. Detection of highly repeated sequences in non-amplified genomic DNA by bulk acoustic wave (BAW) affinity biosensor. Anal Chim Acta 2004;526:19-25.

130. Minnuni M, Tombelli S, Fonti J, Spiriti MM, Mascini M, Bogani P, et al. Detection of fragmented genomic DNA by PCR-free piezoelectric sensing using a denaturation approach. J Am Chem Soc 2005;127:7966-7.

131. Karamollaoglua I, Oktem HA, Mutlu M. QCM-based DNA biosensor for detection of genetically modified organisms (GMOs). Biochem Engineer J 2009;44:142–50.

132. Kaewphinit T. The development of DNA piezoelectric biosensor for the detection of *Mycobacterium tuberculosis*. [Dissertation M.Sc. Biomedical Science]. Bangkok: Faculty of Graduated School, Srinakharinwirot University; 2007.

133. National Center for Biotechnology Information [online]. Retrieved September 1, 2008, from URL: http://www.ncbi.nlm.nih.gov/.

134. Basic Local Alignment Search Tool [online]. Retrieved September 1, 2008, from URL::http://blast.ncbi.nlm.gov/Blast.cgi.

135. Grandjean L, Martin L, Gilman RH, Valencia T, Herrera B, Quino W, et al. Tuberculosis diagnosis and multidrug resistance testing by direct sputum culture in selective broth without decontamination or centrifugation. J Clin Microbiol 2008;46:2339-44.

136. Nebcutter 2.0 [online]. Retrieved September 1, 2008, from URL: http://tools.neb.com.

137. Liang Z, Zhang J, Wang L, Song S, Fan C, Li G. A centrifugation-based method for preparation of gold nanoparticles and its Application in biodetection. Int J Mol Sci 2007;8:526-32.

138. Skladal P. Piezoelectric quartz crystal sensors applied for bioanalytical assays and characterization of affinity interaction. J Braz Chem Soc 2003;14 491-502.

139. Liu T, Tang J, Han M, Jiang L. Surface modification of nanogold particles in DNA detection with quartz crystal microbalance. Chin Sci Bull 2003;48:873-5.

140. Nie LB, Yang Y, Li S, He NY. Enhanced DNA detection based on the amplification of gold nanoparticles using quartz crystal microbalance. Nanotechnology 2007;18:305501.

141. Zhao HQ, Lin L, Li JR, Tang JA, Duan MX, Jiang L. DNA biosensor with high sensitivity amplified by gold nanoparticles. J Nanopart Res 2001;3:321-3.

142. Liu T, Tang J, Han M, Jiang L. A novel micrograviметric DNA sensor with high sensitivity. Biochem Biophys Res Commun 2003;304:98-100.

143. Wang LJ, Wei QS, Wu CS, Hu ZY, Ji J, Wang P. The *Escherichia coli* O157:H7 DNA detection on a gold nanoparticle-enhanced piezoelectric biosensor. Chin Sci Bull 2008;53:1175-84.

144. Chen SH, Chuang YC, Lu YC, Lin HC, Yang YL, Lin CS. A method of layer-by-layer gold nanoparticle hybridization in a quartz crystal microbalance DNA sensing system used to detect dengue virus. Nanotechnology 2009;20:215501

145. Gill P, Ghalami M, Ghaemi A, Mosavari N, Tehrani HA, Sadeghizadeh M. Nanodiagnostic Method for Colorimetric Detection of *Mycobacterium tuberculosis* 16S rRNA. Nano Bio Technology 2008;4:28-35.

146. Uludag Y, Li X, Coleman H, Efstathiou S, Cooper MA. Direct acoustic profiling of DNA hybridisation using HSV type 1 viral sequences. Analyst 2008;33:52-7.

147. Mac Sweeney MM, Bertolino C, Berney H, Sheehan M. Characterization and optimization of an optical DNA hybridization sensor for the detection of multi-drug resistant tuberculosis. Conf Proc IEEE Eng Med Biol Soc 2004;3:1960-3.

148. Liu Sf, Li Yf, Li J, Jiang L. Enhancement of DNA immobilization and hybridization on gold electrode modified by nanogold aggregates. Biosens Bioelectron 2005; 21:789-95.

149. Takahagi T, Tsutsui G, Huang S, Sakaue H, Shingubara S. Scanning electron microscope observation of heterogeneous three-dimensional nanoparticle arrays using DNA. Jpn J Appl Phys 2001;40:L521-3.

150. Nie B, Shortreed MR, Smith LM. Quantitative detection of individual cleaved DNA molecules on surfaces using gold nanoparticles and scanning electron microscope imaging. Anal Chem 2006;78:1528-34.

151. Xu X, Caswell KK, Tucker E, Kabisatpathy S, Brodhacker KL, Scrivens WA. Size and shape separation of gold nanoparticles with preparative gel electrophoresis. J Chromatography A 2007;1167:35-41.

152. Mo Z, Wang H, Liang Y, Liu F, Xue Y. Highly reproducible hybridization assay of zeptomole DNA based on adsorption of nanoparticle bioconjugate. Analyst 2005;130:1589-94.

153. Shchepinov MS, Case-Green SC, Southern EM. Steric factors influencing hybridisation of nucleic acids to oligonucleotide arrays. Nucleic Acids Res 1997;25:1155-61.

154. Kent L, McHugh TD, Billington O, Dale JW, Gillespie SH. Demonstration of homology between IS*6110* of *Mycobacterium tuberculosis* and DNAs of other *Mycobacterium* spp. J Clin Microbiol 1995;33:2290-3.

155. Cowan, S.T.; Mosher, L.; Diem, L.; Massey J.P.; Crawford, J.T. Variable-number tandem repeat typing of Mycobacterium tuberculosis isolates with low copy

numbers of IS6110 by using mycobacterial interspersed repetitive units. J Clin Microbiol 2002;40:1592-602.

APPENDICES

APPENDICES

Reagents

1 HEPES buffer

HEPES	11.9 g
NaCl	11.7 g
H_2O	950 mL

Adjust pH 7.5

H_2O (Deionization Distilled water) adjust volume to 1,000 mL

2 Immobilization buffer (for biotin-modified oligonucleotide probe)

NaCl	17.532 g
Na_2HPO_4	2.8392 g
EDTA	0.0372 g
H_2O	900 mL

Adjust pH 7.4

H_2O (Deionization Distilled water) adjust volume to 1000 mL

3. Immobilization buffer (for thiol-modified oligonucleotide probe)

KH_2PO_4	27.02 g
H_2O	150 mL

Adjust pH 3.8

H_2O (Deionization Distilled water) adjust volume to 200 mL

4. Ethanolamin HCl 10X

Ethanolamin HCl	0.0976 g
H_2O	90 mL

Adjust pH 8.0 HCl

H_2O (Deionization Distilled water) adjust volume to 100 mL

5. 1-ethyl-3(3-dimethylaminopropil) carbodiimide (EDC) solution

EDC	0.0200 g
Absolute ethanol	200 µL

6 *N*-hydroxysuccinimide (NHS) solution

NHS	0.0200 g
H_2O (Distilled water)	200 µL

CURRICULUM VITAE

CURRICULUM VITAE

Name: Thongchai Kaewphinit

Date of Birth: 23 December 1980

Place of Birth: Nakhonratchasima, Thailand

Marital Status: Married

Institutional Affiliation: Department of Biochemistry,
Faculty of Medicine,
Srinakharinwirot University,
Sukhumvit 23, Bangkok 10110, Thailand

E-mail Address: tkaewphinit@yahoo.com

Home Address: 229/11 Khonsawan, Khonsawan, Chaiyaphum 36140,Thailand

Education:

High School 1998
Khonsawan school, Chaiyaphum

B.Sc. (Physics) 2003
King Mongkut University of Technology Thonburi, Bangkok

M.Sc. (Biomedical Science) 2007
Srinakharinwirot University, Bangkok

Ph.D. (Molecular Biology) 2010
Srinakharinwirot University, Bangkok